Hepatitis C virus infection of human hepatocyte organoids

Dissertation

zur Erlangung des akademischen Grades eines
Doktors der Medizin (Dr. med.)
an der
Medizinischen Fakultät der Universität Hamburg

vorgelegt von

Robin Habermann
aus Hamburg

2025

Betreuer:in / Gutachter:in der Dissertation: Prof. Dr. Marcus Altfeld
Gutachter:in der Dissertation: Prof. Dr. Julian Schulze zur Wiesch

Vorsitz der Prüfungskommission: Prof. Dr. Julian Schulze zur Wiesch
Mitglied der Prüfungskommission: Prof. Dr. Maura Dandri-Petersen
Mitglied der Prüfungskommission: Prof. Dr. Sören Gersting

Datum der mündlichen Prüfung: 04.03.2026

Table of contents

1 Problem definition

The hepatitis C virus (HCV) is a viral pathogen that causes chronic infection of the liver in humans, which can ultimately lead to the development of chronic liver disease (CLD). CLD is associated with high levels of morbidity and mortality.

HCV exclusively infects humans and some higher primates and is therefore difficult to study in vivo. In vitro studies of HCV have long been limited to hepatoma cell lines, whose cancerous origin limits their usefulness for certain areas of research. Other types of tissue used to study HCV in vitro are either difficult to obtain, have a short life span in culture or are very distinct from human hepatocytes in vivo.

Hepatocyte organoids (HepOrgs) are a promising novel method of culturing primary human tissue with a hepatocyte phenotype in vitro (Hu et al. 2018). The organoids form three-dimensional structures in vitro and can be cultured for prolonged periods of time.

This thesis aimed to establish an in-vitro cell culture model for HCV infection in HepOrgs derived from human liver tissue. The hypothesis of this thesis was that HepOrgs can be infected with HCV in vitro.

2 Introduction

2.1 Hepatitis C virus

Hepatitis C is a viral disease caused by infection with the hepatitis C virus (HCV). The virus was identified in 1989 as the infectious agent causing the non-A, non-B hepatitis (NANBH) (Choo et al. 1989) and was subsequently renamed HCV. The existence of another hepatitis virus had first been suspected in the 1970s, when cases of hepatitis occurred in patients after the transfusion of blood products. These were confirmed to neither be caused by the at this point of time already identified hepatitis A or B viruses (Prince et al. 1974, Alter et al. 1975). Today, more then 30 years after its discovery, HCV is still a significant cause of morbidity and mortality around the globe and remains a major public health threat. As a part of its 2030 Agenda for sustainable development, the United Nations (UN) called for action to combat viral hepatitis (UN 2015). The World Health Organization (WHO) set out the ambitious goal of ending viral hepatitis as a public health threat by 2030, by reducing the number of new infections by 90% and the number of deaths by 65% compared to 2015 (WHO 2016). To keep these goals within reach, further advances in the study of viral hepatitis are urgently needed.

2.2 Epidemiology

The global prevalence of chronic viremic hepatitis C virus infection is 1.1%, corresponding to 71.1 million active infections in 2015 (Blach et al. 2017). There are several different viral genotypes, and their distribution varies globally with different genotypes being more prevalent in different parts of the world. Genotypes 1 and 4 are the most prevalent globally. The world's highest HCV prevalence in any country is observed in Egypt, with a prevalence of 6.3%, followed by countries of the former USSR (Blach et al. 2017). Only six countries, China, Pakistan, Nigeria, India, Egypt and Russia, account for more than half of all global infections.

The global prevalence of anti-HCV antibodies is 1.6% and thereby higher than the number of currently infected (Gower et al. 2014). This discrepancy between current infections and seroprevalence is caused by people that have cleared HCV infection, either spontaneously or due to treatment.

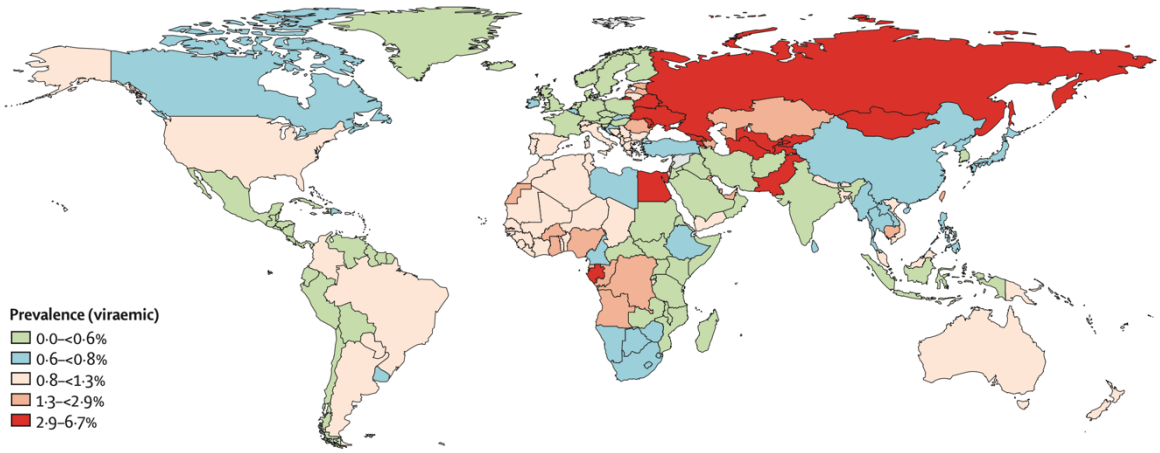

Figure 1: Global epidemiology of chronic HCV infection. Chronic viremic HCV infection is prevalent globally. The prevalence is highest in former member states of the USSR and Egypt. Adapted from Blach et al. (2017).

Viral hepatis causes a high global burden of disease. In contrast to many other infectious diseases, its burden of disease increased from 1990 to 2013. Deaths attributable to viral hepatitis ranked 7th leading cause of death globally in 2013, with 1.45 million deaths (Stanaway et al. 2016). Most of these were due to liver cirrhosis or hepatocellular carcinoma (HCC) resulting from chronic viral infection with the hepatitis B virus (HBV) or HCV. 48.4% of global mortality due to viral hepatitis were caused by HCV, which increased from 33.8% in 1990 (Stanaway et al. 2016). The number of disability adjusted life years (DALYs) caused by HCV, as a combined measure of morbidity and mortality, had more than doubled in 2013 compared to 1990.

The HCV related mortality of infected populations varies widely in different countries, depending substantially on the age structure of the infected cohorts. Countries with high historical rates of HCV transmission in the health care setting (e.g., Egypt and Turkey) have older HCV infected cohorts and therefore currently a higher burden of HCV related mortality than western European countries with younger HCV infected cohorts. The global number of new HCV infections is expected to decline in the future, but, due to aging patient cohorts, the HCV associated mortality will still increase, before it is projected to reach its peak around 2030 in many countries (Razavi et al. 2014).

2.3 Transmission

The hepatitis C virus is a blood borne pathogen and is transmitted by direct and invasive exposure to the blood of an infected person. Historically, the transmission

in the health care sector has played a large role, especially by the transfusion of blood products from HCV infected blood donors and the administration of drugs contaminated with the virus. Recipients of contaminated blood transfusions were the group of patients in whom HCV was first suspected as a novel pathogen in the 1970s. After blood transfusions, some patients developed hepatitis, which was not caused by the then already identified hepatitis A and B viruses (Prince et al. 1974, Alter et al. 1975). In addition to the transfusion of contaminated blood products, reusing of syringes or other invasive medical equipment historically led to the spread of HCV within the health care sector. In Egypt for example, the country with the highest HCV prevalence in the world, high historical rates of infection in the health care setting are well documented (Arafa et al. 2005). Past exposure to invasive medical procedures was the largest risk factor for HCV in Egypt, with a substantial proportion of cases attributable to intravenous schistosomiasis treatment in the 1960s and 1970s.

With the introduction of both blood donor and blood product screening for HCV and the use of single use syringes, the transmission in the health care setting is now markedly reduced. The risk of acquiring HCV via blood transfusion is now estimated to be about 1 in 2 million (Busch et al. 2019). In the health care sector, needle stick injuries remain a route for HCV transmission. Although the probability of viral transmission for needle stick injuries is rather low with 0.5% when the index patient is HCV infected (Jagger et al. 2002), occupational HCV infections are now more frequent in Germany than HBV infections (Nienhaus et al. 2012). This is due to the fact, that there is an effective vaccine against HBV.

Despite the many improvements in the health care sector regarding HCV transmission, hospitalization remains a risk factor for developing acute HCV infection (Martinez-Bauer et al. 2008). This indicates that nosocomial transmission of the virus has not been eliminated entirely.

The dominant route of HCV transmission nowadays is the use of contaminated needles in the setting of injection drug use (Murphy et al. 2000). Needle sharing between different persons leads to the transmission of HCV and other viral pathogens, such as human immunodeficiency virus (HIV), and causes high rates of chronic infection in people who inject drugs (PWID). As PWID often lack adequate access to health care, the morbidity caused by HCV in this population is especially high.

The risk of sexual transmission of HCV is very low. In a prospective study of 776 heterosexual couples discordant regarding their HCV status, not a single case of transmission occurred over 10 years, without the couples taking additional protective measures such as condom usage (Vandelli et al. 2004). Among men who have sex with men (MSM), the risk of sexual HCV transmission is higher, especially among men infected with HIV. These men show higher rates of acute symptomatic HCV infection than HIV uninfected MSM (Yaphe et al. 2012).
Vertical transmission of HCV from mother to newborn child is also possible, with a higher risk of transmission for mothers with higher levels of viraemia (Ohto et al. 1994). The risk of HCV transmission from mother to newborn is also markedly elevated if the mother is coinfected with HCV and HIV, although the transmission of both viruses to the newborns occurs independently from each other (Tovo et al. 1997).

2.4 Clinical manifestations and course of infection

In most infected patients, HCV is a chronic infection of the liver, which cannot be cleared by the host immune system. Yet, some of the people that are exposed to HCV and initially become infected with it, spontaneously clear it. About 25% of the patients acutely infected with HCV spontaneously clear infection with no remaining level of detectable viremia (Micallef et al. 2006). Higher rates of viral clearance are observed in patients with a favorable interleukin-28B (IL28B) genotype, female patients and those infected with HCV genotype 1 (Grebely et al. 2014).
The acute phase of infection with HCV is asymptomatic in most patients. If symptoms arise during acute infection, these may include flu-like symptoms, abdominal discomfort, anorexia and jaundice. Chronic infection with HCV is usually asymptomatic until complications from CLD arise that lead to clinical symptoms, such as jaundice or abdominal distension from ascites. Liver cirrhosis and hepatocellular carcinoma (HCC) are complications that can arise from chronic HCV infection, resulting in significant morbidity and mortality. Liver cirrhosis develops in 16% of patients after 20 years of chronic HCV infection and in 41% after 30 years of infection (Thein et al. 2008). Once cirrhosis is established, the annual risk for developing HCC is between 1% and 5% and the annual risk for hepatic decompensation is between 3% and 6%.

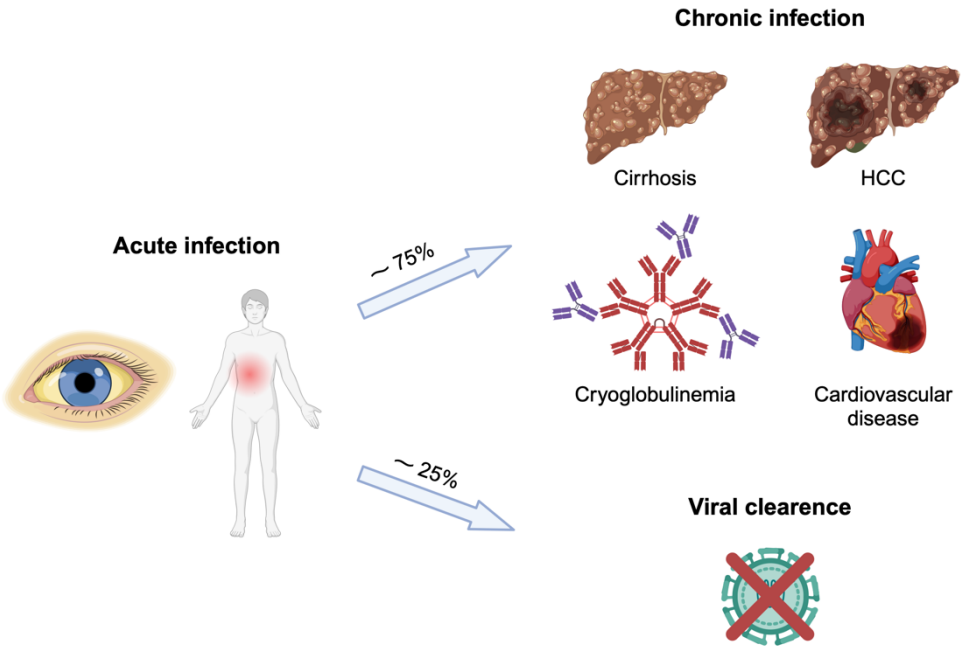

Figure 2: Overview of the clinical course of HCV infection. Acute HCV infection is asymptomatic in most patients. If symptoms arise, jaundice, right upper abdominal pain and nausea are the most frequent. Chronic infection can lead to cirrhosis and the development of hepatocellular carcinomas (HCC) and is associated with extrahepatic diseases such as cryoglobulinemic vasculitis and increased rates of cardiovascular disease. Created with BioRender.com.

Additional risk factors for developing clinically significant liver disease in the setting of chronic HCV infection are older age, high alcohol consumption and concurrent other chronic viral infections with HBV or HIV (Westbrook and Dusheiko 2014).

Chronic HCV infection is also associated with a range of extrahepatic manifestations. Between 40% and 60% of HCV infected patients develop mixed cryoglobulinemia, which may lead to vasculitis (Negro et al. 2015). Furthermore, HCV infected cohorts develop type 2 diabetes more frequently and have a higher cardiovascular morbidity and mortality than uninfected cohorts (Mehta et al. 2000).

2.5 Treatment and vaccination

Therapy of HCV had long consisted of interferon-based regimes, that showed high rates of treatment failure for some genotypes, while being associated many adverse reactions. The introduction of direct acting antivirals (DAA) a decade ago was a breakthrough in the treatment of chronic HCV infection. DAA directly target the non-structural viral proteins and can cure infection in almost all patients, whilst being very safe and well tolerable (Falade-Nwulia et al. 2017). However, many people infected with HCV are unaware of their infection and are therefore not treated for it. Additionally, high drug prices are a substantial barrier to access to the effective DAA

treatment in many parts of the world. With less than 2 million infected people starting treatment for HCV in 2016 (WHO 2018), only a small minority of the chronically infected had access to treatment.

A preventive vaccine could be an effective tool to reduce the burden of disease from HCV and possibly aid ending it as a public health threat. However, all attempts of developing an effective vaccine so far have proved futile. The latest candidate vaccine, an adenovirus vector based preventive HCV vaccine, failed in a large clinical trial in people at high risk of acquiring HCV infection, as the vaccine did not prevent chronic HCV infection (Page et al. 2021). Some of the barriers to vaccine development are the high genetic diversity of the virus, the lack of an effective animal model to test it and the incomplete understanding of what constitutes a protective immune responses to HCV (Bailey et al. 2019). The lack of progress in the development of an effective vaccine even led to prominent HCV researches arguing for the need of a controlled human infection model to aid the development of a vaccine (Liang et al. 2021).

2.6 Virology

HCV is a single strand ribonucleic acid (RNA) virus belonging to the family of the Flaviviridae and is part of the genus of Hepaciviridae. While other members of the Hepaciviridae have been discovered in a range of different species including mice, dogs and horses, HCV has a very narrow species tropism and can only infect humans and chimpanzees.

The viral genome is 9.6 kilobases long and encodes for one large polyprotein. HCV exhibits a high level of genetic diversity, and 8 different genotypes have been identified so far, with the most recent one discovered in India in 2018 (Borgia et al. 2018). The differences in nucleotide sequences between different genotypes are as big as 30-35%. NS5B, the viral RNA-dependent RNA polymerase, has a high error rate during replication, leading to mutations and the occurrence of different viral quasispecies within the same host, that vary in their nucleotide sequence.

The viral polyprotein encodes for ten different proteins, three structural and seven non-structural proteins. E1 and E2 are transmembrane glycoproteins and are a part of the virion membrane. The structural core protein forms the viral nucleocapsid. p7 and NS2 are important for virion assembly, while NS3, NS4A, NS4B, NS5A and NS5B are essential for viral replication.

HCV virions are spherical particles with a diameter ranging from 40 – 100 nm. They are closely associated with the host lipoprotein metabolism and the virions contain host apolipoproteins (apo) such as apoE, apoB and apoA-I (Catanese et al. 2013). The virions also contain large amounts of cholesteryl esters and its lipid composition therefore closely resembles that of very low density lipoprotein (VLDL) particles (Merz et al. 2011).

2.7 Cellular entry and viral life cycle

The viral entry into host hepatocytes is a process involving interactions with multiple different host proteins. This complex entry process is a major reason for the hepatocyte tropism of the virus. CD81 was the first host protein that was identified to be essential for viral entry into hepatocytes. It is a member of the transmembrane 4 family of proteins, also known as tetraspanins, and ubiquitously expressed in different tissues. The HCV envelope glycoprotein E2 binds the extracellular loop of CD81 (Pileri et al. 1998), leading to attachment of the virion to the host cell.

Soon after that discovery, the low-density lipoprotein receptor (LDLR) was found to also play a role in the viral entry process (Agnello et al. 1999). While the LDLR is not essential for the entry of the HCV virion into cells, its expression and physiological function increase viral replication within host cells (Albecka et al. 2012).

The scavenger receptor class b member 1 (SRB1) is also implicated in viral entry into hepatocytes. SRB1 is a high-density lipoprotein (HDL) receptor and mediates the transfer of cholesterol esters between cells and HDL particles. It is expressed at low levels in many different types of tissue but is highly expressed on hepatocytes. The viral glycoprotein E2 binds SRB1 on cells and this interaction is independent from the binding between E2 and CD81 (Scarselli et al. 2002). In addition to directly binding to E2, SRB1 also binds to lipoproteins that are a part of the HCV virion, such as apolipoprotein E (apoE). In fact, the first interaction between SRB1 and the HCV virion during cellular entry is meditated by its binding to apoE. The direct interaction between SRB1 and E2 likely plays a role during later steps of viral entry (Dao Thi et al. 2012). Furthermore, there is evidence that SRB1 plays a role in the cell-to-cell spread of HCV, independent of its ability to bind E2 or apoE (Zahid et al. 2013).

Another host cell factor implicated in viral entry are heparan sulfate proteoglycans (HSPGs). These cell surface proteoglycans also bind to the HCV envelope

glycoprotein E2 and contribute to the initial attachment of the virion to the host cell (Barth et al. 2003).

Claudin-1 is a tight junction protein that is implicated in viral entry into the host cells. Claudin-1 does not directly interact with the HCV virion but interacts with CD81 during the later stages of viral entry into the hepatocytes (Evans et al. 2007). Downregulation of claudin-1 on cells susceptible to HCV has been shown to inhibit HCV infection, indicating that the low expression of claudin-1 on extrahepatic tissues in humans might contribute to the hepatocyte tissue tropism of HCV.

Occludin, another tight junction protein, was later discovered to also be involved in viral entry of HCV into target cells. It is a defining factor for the narrow host tropism of HCV, as the human form of occludin is essential to facilitate HCV infection. Murine hepatocytes, that are not susceptible to HCV under physiological conditions, become susceptible to HCV pseudoparticle (HCVpp) infection when they are transfected with the human form of occludin (Ploss et al. 2009).

Genetically humanized mice whose hepatocytes stably express human CD81 and occludin are permissive to viral entry, indicating that these are the species tropism defining proteins for viral entry (Dorner et al. 2011). Although these genetically humanized mice are permissive to viral infection of hepatocytes, their innate and adaptive immune response rapidly clears infection. In contrast, genetically humanized mice that have additional knockouts in genes related to antiviral immunity, such as signal transducer and activator of transcription 1 (STAT1) or interferon regulatory factor 1 (IRF1), support persistent HCV infection, including the de novo production of infectious virions (Dorner et al. 2013).

The cholesterol uptake receptor Niemann-Pick C1–like 1 (NPC1L1) is another protein implicated in the viral entry of HCV into hepatocytes. The dependence of the HCV virion on NPC1L1 correlates with its cholesterol content, which indicates that the cholesterol content of the HCV virions also plays a role in viral entry (Sainz et al. 2012).

In 2011, the epidermal growth factor receptor (EGFR) and ephrin receptor A2 (EphA2) were identified as additional host proteins involved in the viral entry of HCV. Their role in viral entry is fulfilled by signaling via associated receptor tyrosine kinases (RTKs), which promotes the interaction of CD81 with claudin-1 that is essential for viral internalization (Lupberger et al. 2011). Activation of the EGFR in

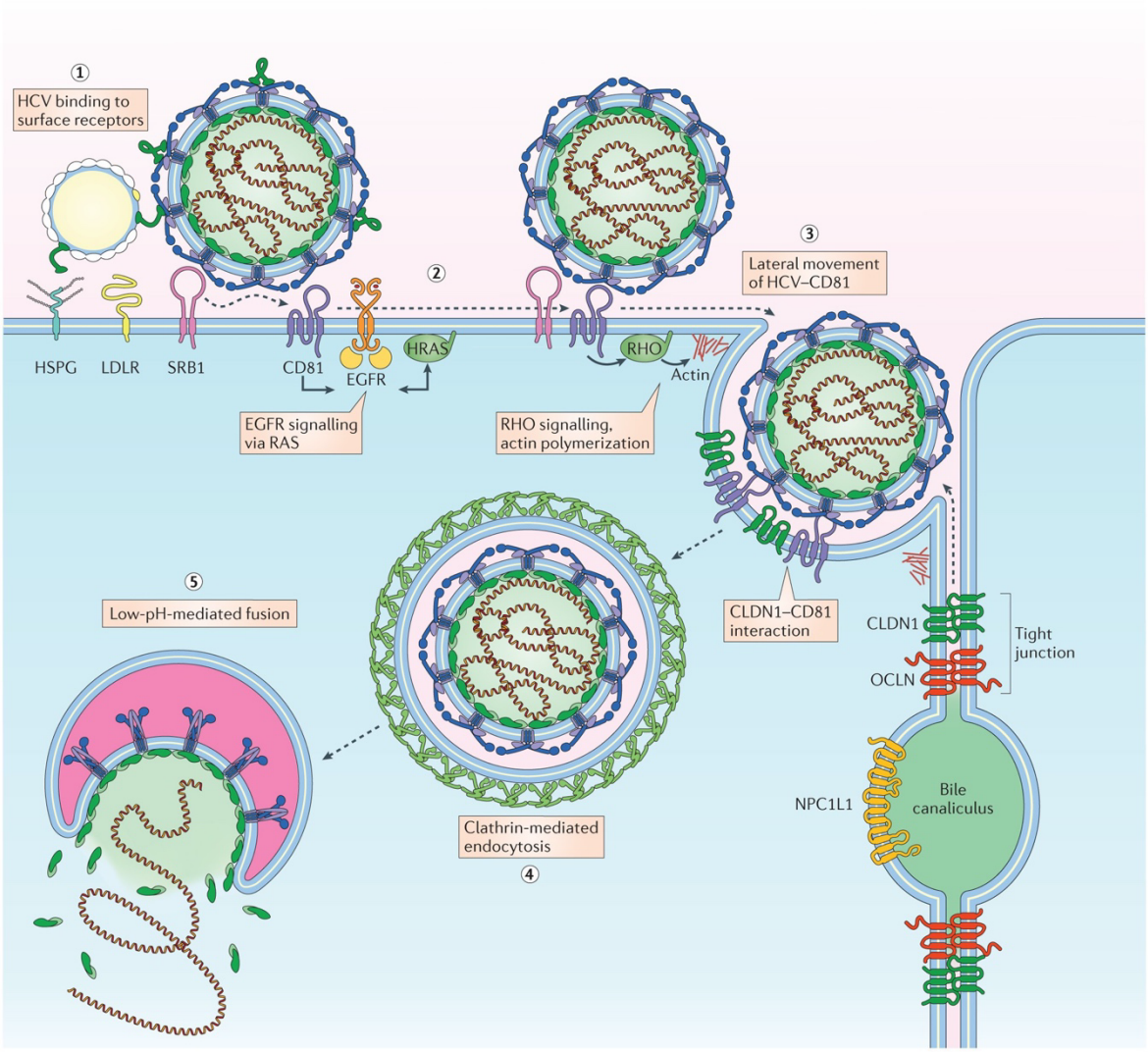

Figure 3: HCV attachment and entry into hepatocytes. HCV virions circulate in the bloodstream and eventually encounter the basolateral membrane of hepatocytes. Initial attachment is facilitated via interactions with HSPGs, the LDLR and SRB1 (1). Upon conformational changes of the viral glycoproteins, the virion binds to CD81 and activates signaling via the epidermal growth factor receptor (EGFR) (2). This signaling leads to the trafficking of the receptor virion complex towards the tight junctions (3). Upon interaction of CD81 and claudin-1, the virion is internalized via clathrin-mediated endocytosis (4). Upon contact with the low pH environment of endosomes, the viral membrane fuses with the endosomal membrane and the viral RNA is released into the cytosol (5). Adapted from Lindenbach and Rice (2013).

the setting of HCV internalization is mediated by interactions between the HCV virion and CD81.The receptor activation also leads to the endocytosis of the EGFR, which is a crucial process for HCV entry into the host cells (Diao et al. 2012).

These discoveries combined lead to an integrated model of HCV entry into hepatocytes in vivo (Lindenbach and Rice 2013, Gerold et al. 2020). HCV virions circulate in the blood of individuals invasively exposed to an inoculum containing HCV virions. Via circulation, the virions enter the space of Disse through the fenestrated endothelium of the hepatic sinusoids and encounter the basolateral

membrane of the host hepatocytes. There, they first attach to the surface of the hepatocytes by binding forces between the HCV glycoproteins E1 and E2 and apolipoproteins in the virion and HSPGs, the LDLR and SRB1 on the membrane of the hepatocytes. The virion then binds CD81 and the complex of CD81 and the virion is trafficked to the tight junctions. EGFR signaling promotes the formation of coreceptor complexes of CD81 and claudin-1. The virions are then internalized via clathrin-mediated endocytosis. The viral envelope then fuses with the endosomal membrane and the RNA is released into the cytosol. In the cytosol it is immediately translated into the viral polyprotein (Niepmann 2013).

2.8 In vitro study of HCV

2.8.1 Sub genomic replicon systems and HCV pseudoparticles

After the discovery of HCV in 1989, it took a few years to develop in vitro systems to study the virus. A first step towards developing physiological cell culture systems of the entire viral life cycle in vitro was the introduction of sub genomic replicon systems, enabling the study of viral replication in vitro. The genome of a genotype 1b virus sequence, lacking the sequence for the structural viral proteins, was successfully transfected into a human hepatoma cell line in 1999 (Lohmann et al. 1999). It replicated at high levels and viral protein expression became detectable within the cells. Sub genomic replicon systems for other viral genotypes, such as genotype 2a, followed soon after (Kato et al. 2003).

The study of viral entry into host cells has been advanced by developing HCV pseudoparticles (HCVpp) (Bartosch et al. 2003, Hsu et al. 2003). HCVpp are retroviral particles that bear HCV glycoproteins E1 and E2 on their surface. While the HCVpp systems allow studying the viral entry process independent of other stages of the viral life cycle, the close association of HCV with the lipoprotein metabolism cannot be depicted with this model, as the retroviral pseudoparticles do not resemble the lipid composition of HCV virions.

2.8.2 Cell culture systems of the entire viral life cycle

While the sub genomic replicon systems and HCVpp enabled the study of single steps of the viral life cycle at a time, a breakthrough in the study of HCV was the development of cell culture systems that support the entire viral life cycle and produce infectious viral particles in vitro. Using a chimeric virus consisting of

sequences from two different viral isolates of genotype 2a, J6 and JFH1, the entire viral life cycle could be depicted in vitro (Lindenbach et al. 2005). The chimeric virus was transfected into the human hepatoma cell line Huh 7.5 and produced infectious virions in cell culture (HCVcc), which could be used to infect naive Huh 7.5 cells. This was also feasible using the full-length genome of JFH1 in Huh 7 cells (Wakita et al. 2005). Infectious virus was produced by the Huh 7 cells, which could infect both naïve Huh 7 cells and a chimpanzee, although the resulting viremia in the chimpanzee was only transient.

Furthermore, the J6/JFH1 chimeric virus produced in cell culture can also infect chimpanzees and mice containing human liver grafts (Lindenbach et al. 2006). The virus recovered from these animals in turn is even more infectious than the original HCVcc, indicating there are differences between virions produced in cell culture and virions produced in vivo. In vivo produced HCV has a lower buoyant density than HCVcc, which correlates with the increased infectivity.

Another chimeric virus used in cell culture is Jc1. It consists of the sequences from two genotype 2a viruses, the structural sequence and a part of NS2A of J6 and the non-structural sequence of JFH1, but the sequence is different from the one previously described (Lindenbach et al. 2005). The infectious titers produced by Jc1 in vitro are 100 to 1000-fold higher than that of the parental JFH1, indicating that the structural proteins heavily influence the efficiency of infectious virus production in cell culture (Pietschmann et al. 2006).

The most widely used chimeric viruses for HCV research in vitro are based on sequences of the two genotype 2a isolates J6 and JFH1. J6 was isolated from the plasma of a chimpanzee infected with patient plasma (Yanagi et al. 1999) while JFH1 was directly isolated from the plasma of a 32-year-old male with fulminant acute hepatitis (Kato et al. 2001).

Some derivatives of the chimeric viruses frequently used in vitro are even more infectious than their parental strains. P100 was derived from Jc1 by serially passaging it in Huh 7.5 cells for 100 passages. During this long time in culture, it acquired adaptive mutations that increased its replicative fitness compared to Jc1 (Sheldon et al. 2014). Huh 7.5 cells infected with P100 contain more viral RNA and produce higher viral titers in the culture supernatant than Jc1 infected Huh 7.5 cells. In addition to the increased replicative fitness, P100 is less sensitive to interferon-α (INF-α) and DAA treatment (Perales et al. 2013, Sheldon et al. 2014).

2.8.3 In vitro permissive host cells

Human hepatoma cell lines, especially the Huh 7 cell line and its derivatives such as the Huh 7.5 cell line, were the first cellular model available for in vitro studies of productive HCV infection. These cell lines are still widely used in HCV research. The clonal Huh 7 cell line was isolated from the HCC of a 57-year-old male and the cells can be cultured in vitro for extended periods of time, whilst retaining a phenotype that resembles that of hepatocytes (Nakabayashi et al. 1982).

Its descendent, the Huh 7.5 cell line, is derived from Huh 7 cells that contained a sub genomic HCV replicon and were continuously treated with interferon alpha (IFN-α) (Blight et al. 2002). As a result from the prolonged IFN-α treatment, the RNA of the viral replicon was eliminated, and the cured cells were named Huh 7.5 cells. Upon transfection with a sub genomic HCV replicon, these Huh 7.5 cells show enhanced viral RNA replication in comparison to their parental Huh 7 cells (Blight et al. 2002).

Defects in genes related to the cellular antiviral response in the Huh 7.5 cell line are the cause for the higher viral replication rates (Sumpter et al. 2005). Huh 7.5 cells have a mutation in the retinoid acid inducible gene 1 (RIG-1), which is an intracellular sensor for double stranded RNA (dsRNA). During viral replication of HCV, dsRNA is formed as an intermediate of replication, which can be sensed by pattern recognition receptors (PRRs) such as RIG-1 or toll-like-receptor 3 (TLR3). Downstream signaling from these PRRs leads to the upregulation of the transcription of antiviral genes such as interferons. The mutation in the RIG-1 gene in Huh 7.5 cells results in a lack of downstream signaling from RIG-1 and therefore a lack of interferon regulatory factor 3 (IRF3) phosphorylation (Sumpter et al. 2005). Phosphorylated IRF3 translocates to the nucleus of the cell and activates transcription of antiviral genes and has been shown to suppress replication of sub genomic HCV replicons in vitro (Foy et al. 2003). Therefore, the mutation in the RIG-1 gene renders the Huh 7.5 cell line more susceptible to HCV infection than its parenteral Huh 7 cell line.

In addition to those cancer cell lines, primary human hepatocytes (PHH) are another in vitro system for the study of HCV. These cells are derived from primary human liver tissue and are therefore difficult to obtain. Compared to hepatoma cell lines, their lifetime in culture is very short and there can be considerable variations depending on the source and culturing conditions. PHH were infected with HCV in

vitro for the first time in 1998 (Fournier et al. 1998). Infections were performed with serum of chronically HCV infected patients. For about one out three patient serums used, there was evidence of viral replication in vitro, as the negative strand of HCV RNA could be detected. This indicated that at least a part of the viral life cycle could be performed in vitro in PHH.

Further research demonstrated that PHHs in vitro can also be infected with HCVcc produced in Huh 7 cells, whilst retaining key markers of hepatic differentiation (Podevin et al. 2010). The PHH infected with HCVcc produce infectious viral particles in vitro. These differ from those produced in Huh cells regarding their buoyant density, as had previously also been described in chimpanzees and mice with human liver grafts in vivo (Lindenbach et al. 2006). This indicates that PHH have a lipoprotein metabolism that functionally better resembles the in vivo conditions than Huh 7 cell line-based systems. In addition to PHH derived from adult human liver tissue, human hepatocytes derived from fetal liver tissue can also be infected with patient serum derived HCV (Lazaro et al. 2007).

Another cell type that is susceptible to HCV infection in vitro are cells derived from human pluripotent stem cells. These cells can be differentiated in vitro into hepatocyte-like cells (HLCs), which retain key features of mature hepatocytes, such as albumin and apoB expression. HLCs also express the known entry factors for HCV and support the entire viral life cycle, including the production of infectious virions (Roelandt et al. 2012, Schwartz et al. 2012).

In the presence of a JAK-STAT pathway inhibitor, which inhibits interferon signaling, viral replication is increased in HLCs compared to untreated cells (Schobel et al. 2018). In contrast, this effect is not observed in Huh 7 cells. This indicates that the reason for lower infection rates in HLCs than in Huh 7 cells might be a more intact innate immune response to viral infection, which limits infection in vitro in the absence of a JAK-STAT pathway inhibitor. Additionally, the lipoprotein metabolism of HLCs is more functional than that of Huh 7 cells in vitro (Schobel et al. 2018).

HLCs can be infected with both Jc1 and P100 in vitro, with the latter infecting the cells more efficiently and producing higher viral titers (Carpentier et al. 2020). In the absence of a JAK-STAT pathway inhibitor, the HLCs cleared infection with both Jc1 and P100 by the induction of a robust innate immune response, comparable to that observed in PHH. In the presence of the JAK-STAT pathway inhibitor ruxolitinib, chronic infection can be facilitated in HLCs.

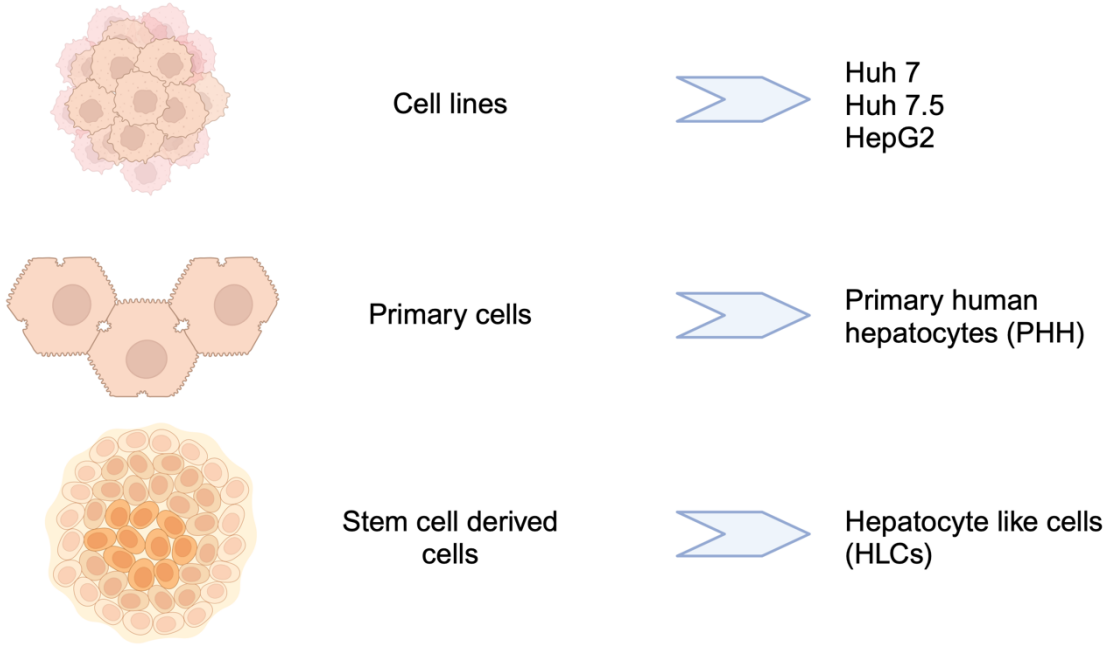

Figure 4: Overview of in vitro cell culture systems for HCV infection. Created with BioRender.com.

In addition to the two-dimensional models of HCV infection in vitro, three-dimensional systems of the Huh 7 and Huh 7.5 cell lines have been developed. Different approaches have been used to grow them in a three-dimensional culture system. One approach is using a rotating wall vessel (RWV), a mechanical construction whose fluid dynamics promote the aggregation of three-dimensional cellular structures. Huh 7 cells grown in an RWV form three-dimensional aggregates and possess a more differentiated and polarized phenotype than their two-dimensional counterparts. These three-dimensional Huh 7 cells are also susceptible to HCVcc infection in vitro (Sainz et al. 2009).

Another approach to culturing Huh 7 cells in a three-dimensional system is based on the use of Matrigel, which is a gel containing a mixture of proteins that resemble the composition of the extracellular matrix of many different tissues. It is produced by murine Engelbreth–Holm–Swarm sarcoma cells and enables cells to grow in a three-dimensional pattern (Kleinman and Martin 2005). Huh 7 cells grown in Matrigel form three-dimensional polarized structures, that form bile-canalicular-like structures and show a clearly polarized expression of the tight junction proteins claudin-1 and occludin (Molina-Jimenez et al. 2012). These Huh 7 cells grown in Matrigel can also be infected with HCVcc and produce virions of a lower buoyant density than Huh 7 cells grown as a monolayer. Additionally, Huh 7.5 cells can also

be grown as three-dimensional organoids in Matrigel, whilst showing no difference regarding the infection rates compared to cells grown in a monolayer (Baktash et al. 2018).
Taken together, there are quite a few different cell culture systems to study HCV infection in vitro, but each system has major limitations such as a short lifetime in culture (PHH) or a compromised immune response to infection (Huh 7.5 cell line).

2.9 Hepatocyte organoids

Ever since the development of the first in vitro cell culture systems for epithelial cells, these systems have been mostly limited to two-dimensional systems with the cells growing as a monolayer. These two-dimensional in vitro systems differ a lot from the physiological in vivo conditions, where cells arrange in three dimensions. Additionally, the two-dimensional epithelial cell cultures lack other cell types that interact with them in vivo, as they usually only contain one type of epithelial cell. With advances in stem cell research and the commercial availability of extracellular matrix (ECM)-rich hydrogels (e.g., Matrigel, BME2), it has become feasible to grow cells as three-dimensional organoids in vitro. These organoids consist of different organ specific cell types and grow in a defined, serum-free culture medium.
Organoids can be generated from stem cells in vitro. As a source of stem cells, either pluripotent stem cells (PSCs), both induced pluripotent stem cells (iPSCs) or embryonic stem cells (ESCs), or adult stem cells (aSCs) can be used. PSC derived organoids are generated by mimicking developmental processes, that occur during embryogenesis, in vitro (Clevers 2016).
Adult stem cell derived organoids are generated by imitating proliferation processes that physiologically occur during both tissue renewal and repair. The intestinal epithelium was the first tissue for which adult tissue derived stem cells could be used to generate three-dimensional organoids in vitro (Sato et al. 2009). These organoids exhibited a highly polarized, three-dimensional structure and proliferated in vitro.

The liver contains two different types of epithelial cells, hepatocytes, and bile duct epithelial cells (cholangiocytes). Hepatocytes fulfill the metabolic functions of the liver and produce plasma proteins such as albumin. Cholangiocytes on the other hand form the bile ducts, which transport the bile from the hepatocytes to the intestinal tract. Unlike other tissues that have a high rate of constant epithelial self-

renewal, such as the gastrointestinal tract, the healthy liver does not contain Lgr5 (Leucine rich repeat containing G protein-coupled receptor 5) expressing cells (Huch et al. 2013), which is a marker of proliferating stem cells (Barker et al. 2007). The ligands for Lgr5 are soluble R-spondins, which are secreted proteins that act as potent enhancers of the Wnt/β-catenin signaling pathway (de Lau et al. 2012). Binding of R-spondin to Lgr5 leads to enhancement of Wnt signaling (de Lau et al. 2011), which is crucial for proliferation and differentiation processes during tissue development.

Upon hepatic tissue injury however, Lgr5 is expressed on a group of cells near the bile ducts and these cells can proliferate and differentiate into both hepatocytes and cholangiocytes in vivo (Huch et al. 2013). In vitro, these Lgr5 expressing cells proliferate and form three-dimensional organoids when cultured in ECM-rich hydrogel in a specific medium that contains growth factors and R-spondin 1 (RSPO1). Differentiation of these organoids into a hepatocyte phenotype can be induced by inhibition of transforming growth factor beta (TGF-β) signaling, leading to an increased expression of hepatocyte markers such as albumin (Huch et al. 2013).

These ductal organoids have also been generated from human instead of murine liver tissue (Huch et al. 2015). In this system, the organoids originate exclusively from ductal epithelial cells, while hepatocytes form no organoids. These human organoids can even be transplanted into immunodeficient mice after liver injury, leading to the production of human albumin in vivo.

In addition to the Lgr5 expressing cells that occur close to the bile ducts upon hepatic injury and that can differentiate into cells with either a cholangiocyte or hepatocyte phenotype, the liver contains another cell population with stem cell characteristics. Near the central veins, there is a population of Wnt responsive proliferating hepatocytes. These cells express Axin2 as a marker of their response to Wnt signaling and are clearly distinct from the Lgr5 expressing cells near the bile ducts (Wang et al. 2015). They exhibit key characteristics of stem cells, with the ability to self-renew and differentiate. These cells contribute to hepatic self-renewal by proliferating and differentiating into functional hepatocytes in vivo.

Recent work by Hu et al. (2018) demonstrated, that hepatocyte organoids (HepOrgs) derived from both murine and human liver tissue can be grown in vitro

from mature hepatocytes. These HepOrgs have a morphology that is distinct from that of differentiated ductal organoids described previously (Huch et al. 2013, Huch et al. 2015). The levels of gene expression of hepatocyte specific genes in the HepOrgs are closer to those observed in primary human hepatocytes (PHH) than in the differentiated ductal organoids. HepOrgs can be kept in culture for multiple weeks whilst retaining key features of hepatocyte function, such as albumin secretion. Furthermore, they also partially resemble the functional anatomy of the liver with the formation of lumina within the organoids that resemble bile canaliculi. The plating efficiency of the organoids is increased for Axin2 expressing hepatocytes, indicating that these cells with stem cell characteristics proliferate better in vitro than Axin2 negative hepatocytes (Hu et al. 2018). Essential for the formation of organoids in vitro is Wnt pathway activation and the stimulation with growth factors, such as hepatocyte growth factor (HGF).

Murine hepatocyte organoids can also be generated in vitro using a different approach with the pro-inflammatory cytokine tumor necrosis factor α (TNF-α) as a crucial component of the culture medium (Peng et al. 2018). These hepatocyte organoids grown using the TNF-α containing medium also retain key features of adult hepatocytes, such as albumin secretion, low density lipoprotein (LDL) uptake and glycogen storage.

2.10 Aim of the study

Despite the introduction of highly effective treatment options for chronic HCV infection, the global morbidity and mortality caused by HCV is still very high. An effective vaccine that could reduce the global burden of disease in the future is not yet available. More research into viral pathogenesis and on interactions of virus-infected cells and immune cells is therefore needed, to aid vaccine development and better understand the pathogenesis of chronic liver disease in the setting of HCV infection. Established cell culture models of HCV infection in vitro, especially the widely used Huh 7 cell line and its derivatives, are not very well suited to study the immunological response to viral infection, as its immune response to viral infection is very dissimilar to that of hepatocytes. Three-dimensional hepatocyte organoid culture systems in vitro could possibly serve as a more physiological model for HCV infection. Hence, this study aimed to establish hepatitis C virus infection of adult human liver tissue derived hepatocyte organoids in vitro.

3 Materials and methods

3.1 Technical equipment

Table 1: List of technical equipment

Equipment	Supplier
BD LSRFortessa™ Cell Analyzer	Becton Dickinson, Franklin Lakes, NJ, USA
Carl Zeiss™ Axiovert 40C Mikroscope	Carl Zeiss, Oberkochen
Centrifuge Mega Star 1.6R	VWR International, Darmstadt
Centrifuge Micro Star 17R	VWR International, Darmstadt
EVOS M5000 Imaging System	Life Technologies Corporation, WA USA
Explorer™ Semi-Micro	OHAUS Europe, Nänikon, Switzerland
FlexCycler	Analytik Jena, Jena
FVL-2400N Combi-Spin	Biosan, Riga, Latvia
Heracell® 240i	Thermo Fisher Scientific, Waltham, MA USA
HERAsafe KS/KSP Classe II Biological Safety Cabinets	Thermo Fisher Scientific, Waltham, MA USA
LightCycler® 480 Instrument	Roche Diagnostics, Mannheim
Nanodrop 1000 Spectrophotometer	PEQLAB Biotechnologie, Erlangen
Orbital shaker 3005	GFL Gesellschaft für Labortechnik, Burgwedel
PCR UV^2 cabinet	Analytik Jena, Jena
PIPETBOY acu 2	INTEGRA Biosciences, Biebertal
Reax top vortexer	Heidolph Instruments, Schabach
TC20 Automated Cell Counter	Bio-Rad Laboratories, Feldkirchen
Thermomixer compact	Eppendorf, Hamburg
Water bath 1002	GFL Gesellschaft für Labortechnik, Burgwedel
StrataCooler	Agilent, Santa Clara, CA USA

3.2 Tissue culture equipment and plastics

Table 2: List of tissue culture equipment and plastics

Consumable	Supplier
adhesive tape for quantitative PCR	SARSTEDT, Nümbrecht
Biosphere® plus filter tips (2.5 µl, 10 µl, 100 µl 1000 µl)	SARSTEDT, Nümbrecht
Carbon Steel Safety Scalpel	B. Braun Melsungen, Melsungen
Cell Counting Slides for TC10™/TC20™	Bio-Rad laboratories, Feldkirchen
Cell culture flasks (75 cm^2, 175 cm^2)	SARSTEDT, Nümbrecht
Cell culture plates (6, 12, 24, 96 wells)	SARSTEDT, Nümbrecht

Centrifuge tubes CELLSTAR® (15 ml, 50 ml)	Greiner Bio-One, Kremsmünster, Austria
ClipTip™ Filtered Pipette Tips (20 µl, 50 µl, 200 µl, 300 µl)	Thermo Fisher Scientific, Waltham, MA USA
CryoPure tubes, 1.6 ml, Quickseal screw cap	SARSTEDT, Nümbrecht
Deckgläser 18 x 18 mm	Bernhard Schulz & Sohn, Hamburg
EASYstrainer 70 µm, for 50 mL tubes	Greiner Bio-One, Kremsmünster, Austria
Falcon® 5 ml Polystyrene Round-Bottom FACS tubes	Corning Inc., New York, NY USA
LightCycler® 480 Multiwell Plate	SARSTEDT, Nümbrecht
Menzel Gläser	Thermo Fisher Scientific, Waltham, MA USA
Multiply®-µStrip Pro PCR tubes, 0.2 ml,	SARSTEDT, Nümbrecht
Safe-Lock Tubes (1.5 ml, 2 ml)	Eppendorf, Hamburg
Serological pipettes (5 ml, 10 ml, 25 ml)	SARSTEDT, Nümbrecht
Syringe (5 ml, 10 ml)	B. Braun Melsungen, Melsungen
Tissue Culture Dish (100x20mm)	SARSTEDT, Nümbrecht
ultra-low attachment 24-well tissue culture plates	Corning Inc., New York, NY USA
Whatman® Puradisc 30 Syringe Filters	Whatman, GE Healthcare, Dassel

3.3 Reagents and kits

Table 3: List of reagents and kits

Reagents and Kits	Supplier
2-Propanol for molecular biology, =99.5%	Sigma Aldrich Chemie, Taufkirchen
A83-01	Tocris Bioscience, Bio-Techne, Wiesbaden
Advanced DMEM/F-12	Thermo Fisher Scientific, Waltham, MA USA
AlbuMAX™ II Lipid-Rich BSA	Gibco, Thermo Fisher Scientific, Waltham, MA USA
Ambion Single Cell-to-CT qPCR Kit	Invitrogen, Thermo Fisher Scientific, Waltham, MA USA
Anti-Mouse Ig, κ/Negative Control Compensation Particles Set	Becton Dickinson, Franklin Lakes, NJ, USA
Aqua ad injectabilia	B. Braun Melsungen AG, Melsungen
ArC™ Amine Reactive Compensation Bead Kit	Invitrogen, Thermo Fisher Scientific, Waltham, MA USA
B27 Supplement (50X) minus Vitamin A	Life Technologies, Thermo Fisher Scientific, Waltham, MA USA
BX-795 hydrochloride	Sigma Aldrich Chemie, Taufkirchen
Cell Recovery Solution	Corning, New York, NY USA
CHIR 99021	Bio-Techne, Wiesbaden

Chloroform	Th. Geyer, Renningen
Collagenase D	Sigma Aldrich Chemie, Taufkirchen
Cultrex Reduced Growth Factor Basement Membrane Extract, Type 2, Pathclear (BME2)	R&D Systems, Inc., Minneapolis, MN, USA
D-(−)-Fructose	Sigma Aldrich Chemie, Taufkirchen
Dexamethason	Sigma Aldrich Chemie, Taufkirchen
Dimethyl sulfoxide - 99.5%	Sigma Aldrich Chemie, Taufkirchen
DMEM, high glucose, GlutaMAX™ Supplement, pyruvate	Gibco, Thermo Fisher Scientific, Waltham, MA USA
DNAse I	Stemcell Technologies, Vancouver, Canada
DNase I (RNase-free) (2U/ul)	Invitrogen, Thermo Fisher Scientific, Waltham, MA USA
Dulbeco's Phosphate Buffered Saline	Sigma Aldrich Chemie, Taufkirchen
eBioscience™ IC Fixation Buffer	Invitrogen, Thermo Fisher Scientific, Waltham, MA USA
eBioscience™ Permeabilization Buffer (10X)	Invitrogen, Thermo Fisher Scientific, Waltham, MA USA
EBSS, calcium, magnesium, phenol red	Gibco, Thermo Fisher Scientific, Waltham, MA USA
EDTA	Promega, Walldorf
Ethanol absolute for analysis EMSURE®	Th. Geyer, Renningen
Fetal Bovine Serum	Capricorn Scientific, Ebsdorfergrund
Gastrin I human	Sigma Aldrich Chemie, Taufkirchen
GlutaMAX 100x (200mM)	Gibco, Thermo Fisher Scientific, Waltham, MA USA
Glycerol	Sigma Aldrich Chemie, Taufkirchen
GlycoBlue Coprecipitant	Life Technologies, Thermo Fisher Scientific, Waltham, MA USA
HEPES (1M)	Gibco, Thermo Fisher Scientific, Waltham, MA USA
Hoechst 34580	Sigma Aldrich Chemie, Taufkirchen
LIVE/DEAD™ Fixable Near-IR Dead Cell Stain Kit, for 633 or 635 nm excitation	Invitrogen, Thermo Fisher Scientific, Waltham, MA USA
N-Acetylcysteine	Sigma Aldrich Chemie, Taufkirchen
Nicotinamide	Sigma Aldrich Chemie, Taufkirchen
Oncostatin M	Pepro Tech, Hamburg
Paraformaldehyde	Sigma Aldrich Chemie, Taufkirchen
Penicillin-Streptomycin Solution stabilized (10.000 units penicillin and 10 mg streptomycin per ml)	Sigma Aldrich Chemie, Taufkirchen
qScript™ cDNA SuperMix	VWR International, Bruchsal

QuantiFast SYBR® Green PCR Kit	QIAGEN, Hilden
Recombinant Human EGF (500µg)	Pepro Tech EC, Hamburg
Recombinant Human FGF-10	Pepro Tech EC, Hamburg
Recombinant Human HGF (HEK293 derived)	Pepro Tech EC, Hamburg
Recombinant Human KGF (FGF-7)	Pepro Tech EC, Hamburg
Recombinant Human TGF-alpha	Pepro Tech EC, Hamburg
Recovery™ Cell Culture Freezing Medium	Gibco, Thermo Fisher Scientific, Waltham, MA USA
RNaseOUT™ Recombinant Ribonuclease Inhibitor	Invitrogen, Thermo Fisher Scientific, Waltham, MA USA
Ruxolitinib	Sellekchem, Selleck Chemicals, Berlin
Triton® X 100	Carl Roth, Karlsruhe
TRIzol	Life Technologies, Thermo Fisher Scientific, Waltham, MA USA
Trypan Blue solution, 0.4%	Sigma Aldrich Chemie, Taufkirchen
TrypLE™ Express Enzyme (1X), phenol red	Gibco, Thermo Fisher Scientific, Waltham, MA USA
TWEEN® 20	Sigma Aldrich Chemie, Taufkirchen
Y-27632	Stemcell Technologies, Vancouver, Canada

3.4 Antibodies

Table 4: Antibodies for flow cytometry

Antigen	Fluorophore	Clone	Host	Distributed by
anti-mouse IgG	PE	RMG1-1	rat	BioLegend, San Diego, CA USA
CD81	BV711	JS-81	mouse	Becton Dickinson, Franklin Lakes, NJ
EGFR	PE-Cy7	AY13	mouse	BioLegend, San Diego, CA USA
HCV Core Antigen	-	C7-50	mouse	Invitrogen, Thermo Fisher Scientific, Waltham, MA USA
SR-B1	APC	m1B9	mouse	BioLegend, San Diego, CA USA

Table 5: Antibodies for immunofluorescence

Antigen	Conjugate	Clone	Host	Distributed by
Immunofluorescence primary antibodies				
CD81	-	1.3.3.22	mouse	Invitrogen, Thermo Fisher Scientific, Waltham, MA USA
Claudin-1	-	polyclonal	rabbit	Invitrogen, Thermo Fisher Scientific, Waltham, MA USA
Occludin	-	polyclonal	rabbit	Invitrogen, Thermo Fisher Scientific, Waltham, MA USA
SR-B1	-	OTI1F3	mouse	Invitrogen, Thermo Fisher Scientific, Waltham, MA USA
Immunofluorescence secondary antibodies				
anti-mouse IgG	AF647	polyclonal	goat	Invitrogen, Thermo Fisher Scientific, Waltham, MA USA
anti-rabbit IgG	AF488	polyclonal	chicken	Invitrogen, Thermo Fisher Scientific, Waltham, MA USA

3.5 Oligonucleotide sequences

Table 6: List of oligonucleotide sequences used for RT-qPCR

Target	Forward Primer	Reverse Primer
CD81	TGTTCTTGAGCACTGAGGTGGTC	TGGTGGATGATGACGCCAAC
Claudin-1	GTGGAGGATTTACTCCTATGCCG	ATCAAGGCACGGGTTGCTT
GAPDH	CGGAGTCAACGGATTTGG	TGATGACAAGCTTCCCGTTC
Occludin	CCCTTTTAGGAGGTAGTGTAGGC	CCGTAGCCATAGCCATAACCA
SRB1	TCGCAGGCATTGGACAAACT	CTCCTTATCCTTTGAGCCCTTTT

3.6 Media and solutions

Table 7: List of solutions and buffers

Solutions and buffers	Composition
PBS-Tween (PBT)	0.1% (vol/vol) Tween 20 in PBS
Organoid washing buffer (OWB)	0.1% (vol/vol) Triton X-100 0.2% (wt/vol) bovine serum albumin (BSA)

	in PBS
Fructose-glycerol clearing solution	60% (vol/vol) glycerol 2.5 M fructose distilled water
PBS-BSA	1% BSA (wt/vol) in PBS
Paraformaldehyde (PFA)	4% (wt/vol) in PBS
Liver digestion solution	90% (vol/vol) EBSS 10% (vol/vol) DNAse I (stock 1mg/ml in PBS) 2.5 mg/ml Collagenase D
R-Spondin 1 conditioned medium	Homemade, produced in HEK293T-HA-Rspo1-Fc cells, as described in detail by Broutier et al. (2016)

Table 8: List of media

Medium	**Composition**
Advanced DMEM +++ (AD+++)	97% (vol/vol) Advanced DMEM/F-12 1% (vol/vol) GlutaMAX 1% (vol/vol) HEPES (1M) 1% (vol/vol) Penicillin-Streptomycin
DMEM10	89% (vol/vol) DMEM, high glucose, GlutaMAX™ Supplement, pyruvate 10% (vol/vol) fetal bovine serum (FBS) 1% (vol/vol) Penicillin-Streptomycin
Freezing medium	90% FBS, 10% DMSO
Hepatocyte organoid medium (HepM)	81% (vol/vol) AD+++ 15% (vol/vol) RSPO1 conditioned medium 2% (vol/vol) B27 Supplement minus Vitamin A 1.25 mM N-Acetylcysteine 50 ng/ml EGF 100 ng/ml fibroblast growth factor (FGF) 7 100 ng/ml FGF10 50 ng/ml HGF 20 ng/ml TGF-α 10 nM Gastrin 3 µM CHIR 99021 2 µM A83-01 10 mM Nicotinamide 10µM Y-27632
Wash medium	98% (vol/vol) DMEM (high glucose, GlutaMAX™ Supplement, pyruvate) 1% (vol/vol) FBS 1% (vol/vol) Penicillin-Streptomycin

3.7 Cell lines

Table 9: List of cell lines

Cell line	Description	Source
Huh 7.5	Immortal hepatocellular carcinoma cell line, derived from Huh 7 cell line	Charles M. Rice, Rockefeller University, NY

3.8 Biological samples

Table 10: Overview of biological samples

Tissue/Cells	Source
Human liver tissue	Karl J. Oldhafer, Asklepios Klinik Hamburg Barmbek
Primary human hepatocytes (PHH)	Florian W. Vondran, Medizinische Hochschule Hannover
HCV patient plasma	Julian Schulze zu Wiesch, Universitätsklinik Hamburg Eppendorf

Table 11: List of liver tissue donors

Donor	Diagnosis
1	Colorectal liver metastases (CRLM)
2	CRLM
3	CRLM
4	CRLM
5	CRLM
6	CRLM
7	CRLM
8	CRLM
9	Hepatic hemangioma
10	Liver metastasis (Ovarian carcinoma)
11	Hepatic hemangioma

3.9 Software

Table 12: List of software

Software	Manufacturer
FACSDiva™	Beckton Dickinson
FlowJo 10.7	Beckton Dickinson
GraphPad Prism 9	GraphPad Software
Mendeley	Elsevier

Microsoft Office	Microsoft
NIS Elements	Nikon
EndNote 20	Clarivate

3.10 Cell culture Huh 7.5 cell line

The Huh 7.5 cell line was cultured under standard cell culture conditions, in T75 flasks in DMEM10. For the time of culture, the cells were stored in an incubator at 37 °C, 5% CO_2. The cells were passaged twice weekly, depending on cell density as observed under a light microscope. For passaging, cells were dissociated from the flask using trypsin and counted using the TC20 automated cell counter. 2 x 10^6 cells were transferred to a new flask and supplemented with 10
ml fresh medium. Cells were only used for experiments until a maximum of passage 25. The cell line was tested for mycoplasma contamination, which was not the case.

3.11 Liver sample processing

The liver samples used for the generation of hepatocyte organoids were obtained from a large hospital with a focus on hepatic surgery in Hamburg, Germany. The tissue source were livers from patients, who underwent a partial hepatectomy for different medical reasons, most of them for the resection of liver metastases of epithelial carcinomas. The most frequent diagnosis in the patient cohort was liver metastasis from colorectal carcinoma. To remove the tumor, a part of the liver was resected, including the tumor and surrounding liver tissue. The surgeons then cut off some of the non-cancerous tissue from the resected tissue and provided us with tumor-free, healthy liver tissue for our research.

The liver samples were picked up shortly after surgery and processed directly afterwards. For the transport and until the beginning of the processing, the liver samples were stored at 4 °C. The use of human liver tissue for our research and the generation of hepatocyte organoids was approved by the Ärztekammer Hamburg (PV4898) and all donors provided written, informed consent. The liver processing protocols for the generation of hepatocyte organoids were adapted from previous work by Hu et al. (2018).

The liver samples were first weighed and then minced to small pieces in a petri dish with a scalpel and tweezers until the pieces were smaller than 2 mm in diameter. It was then transferred in 25 ml wash medium (4 °C) to a 50 ml falcon tube, where it

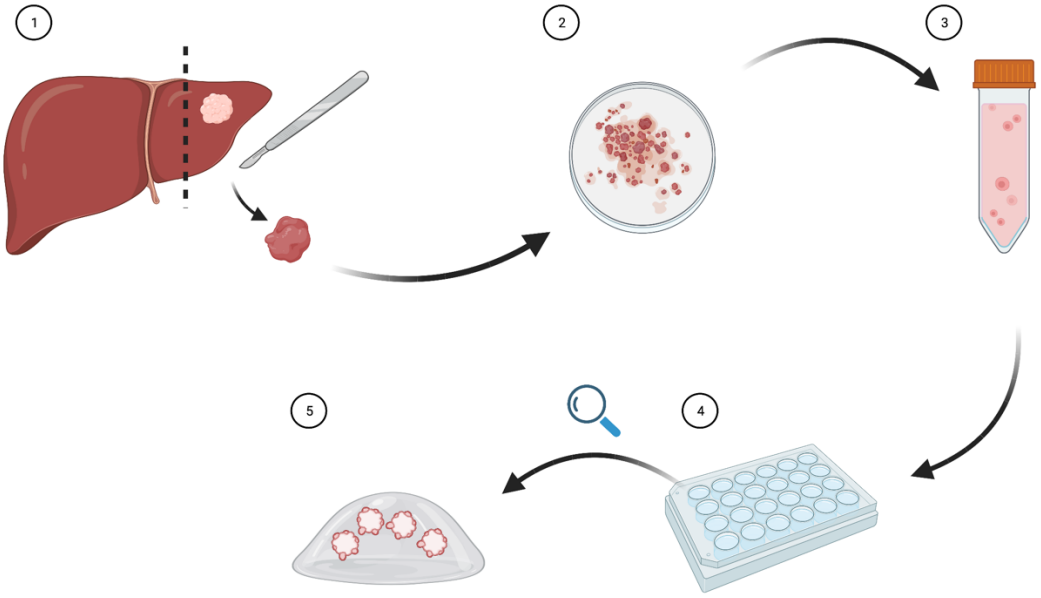

Figure 5: Generation of hepatocyte organoids from liver tissue. Surgically resected, tumor-free liver tissue (1) was minced to small pieces in a petri-dish (2) and then enzymatically digested to single cells (3). These cells were seeded in a droplet of BME2 and cultured in HepM in wells of a 24 well plate to grow as hepatocyte organoids (4+5). Created with BioRender.com.

was resuspended multiple times with a 25 ml serological pipette to wash off blood and fat from the liver tissue. The tissue settled for 10 minutes before approximately 20 ml of the supernatant were removed and replaced with 20 ml wash medium (4 °C). It was resuspended again multiple times before allowing it to settle again. After 10 minutes, the supernatant was removed completely. 5 ml sterile filtered liver digestion solution were added per gram of liver tissue and the suspension was mixed by resuspending.

The suspension was then incubated at 37 °C. After 15 - 20 minutes of incubation time, the suspension was checked for single cells. A drop of the suspension was examined under the light microscope to see whether the suspension already contained mostly single cells. If not, the incubation was resumed and the suspension was checked for single cells every 10 minutes, up to maximum total incubation time of 60 minutes. To stop the digestion process, 25 ml wash medium (4 °C) were added. The suspension was then passed through a sterile 70 µm cell strainer to filter out remaining larger tissue fragments. This was followed by a centrifugation step for 5 minutes at 300 x g at 4 °C. Next, the cells were washed twice in 10 ml wash medium, followed by another centrifugation step (5 minutes, 300 x g, 4 °C). Afterwards, the cell pellet was resuspended in AD+++ and the cells were counted.

For counting, 10 µl of the cell suspension were prediluted 1:10 in trypan blue solution before another 1:2 dilution in trypan blue. 10 µl of the diluted suspension were transferred to a counting slide and cells were counted using the TC20 automated cell counter. Cells were always counted in duplicate, and the mean was calculated. After counting and centrifugation, the cells were either frozen away or seeded directly. For freezing, up to 10 million cells were frozen away per cryo vial. The pellet was resuspended in 1 ml freezing medium (90% FBS, 10% DMSO) per cryovial for freezing. The vials were then transferred in a stratacooler to -80 °C, allowing them to cool down slowly. After 24 hours, the vials were transferred the liquid nitrogen tank and stored at < -160 °C until use.

3.12 Organoid culture

3.12.1 Organoid seeding and culture

The digested liver tissue was either seeded directly after processing or from cryopreserved vials, growing as hepatocyte organoids (HepOrgs) for the first time. When seeded from cryopreserved cells, the cells were first thawed at 37 °C and then cautiously added to 10 ml prewarmed (37 °C) AD+++. The cells were then counted in duplicate again, centrifuged (5 minutes, 300 x g, 4 °C), washed again in AD+++, before another centrifugation step. The cells were then transferred in 1 ml AD+++ (4 °C) to a 1.5 ml Eppendorf tube. From then onwards, the work was performed on ice, as the base membrane extract type 2 is only liquid at 4 °C and solidifies at temperatures above 15 °C. The tube was centrifuged on a desk centrifuge for one minute and the supernatant was discarded. 7.5 µl of hepatocyte organoid medium (HepM; 4 °C) and 22.5 µl BME2 (4 °C) were added for every 60.000 viable cells. The solution was resuspended carefully without adding any air bubbles. Droplets of 30 µl, containing 60.000 cells, were then seeded per well of a prewarmed (37 °C) 24 well plate. The plate was transferred to the incubator (37 °C, 5% CO_2) for 15 minutes for the droplets to solidify. When solid, 500 µl of prewarmed HepM (37 °C) were cautiously added to each well without damaging the gel droplet and the plates were transferred to the incubator. HepM was exchanged three times a week, removing the old HepM from each well and replacing it with 500 µl fresh HepM (37 °C).

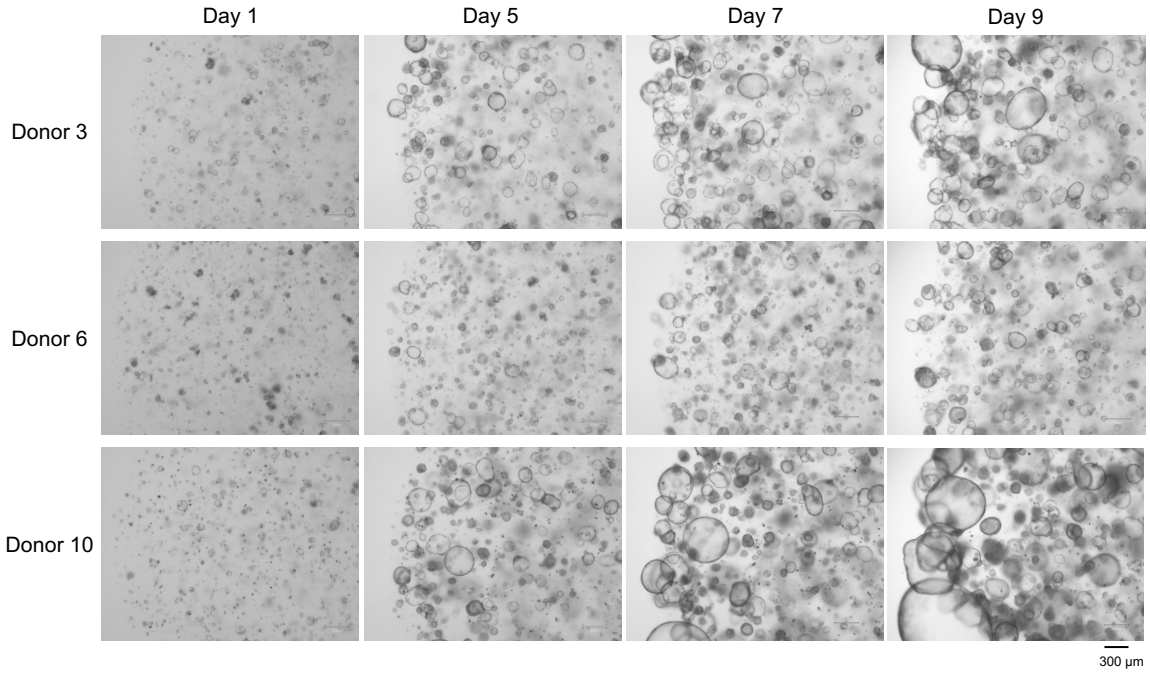

Figure 6: Growth of HepOrgs over time in light microscopy. The growth of organoids derived from the liver tissue of three exemplary donors is shown. The organoids were passaged at day 0 and organoid growth is shown over a period of nine days. In addition to the HepOrgs (small and dark), ductal-like organoids (large, more transparent, cystic) also grew within the cultures.

Fresh culture medium was prepared weekly and used for no longer than seven days. The organoids were kept in culture until they had sufficiently grown, as regularly checked via bright field microscopy. For the first passage after seeding the digested liver tissue (Passage 0; P.0) this took upwards of 20 days, until the organoids were large enough for either passaging or freezing them.

During the time in culture, the growth of larger, cystic organoids was observed within the HepOrg cultures (Figure 6). These organoids resembled the phenotype of ductal organoids. These ductal-like organoids grew in all HepOrg cultures derived from all donors used in this study.

3.12.2 Organoid harvesting, freezing and passaging

To passage or freeze the organoids, they needed to be retrieved from the ECM-rich hydrogel droplets. First, the medium was removed and discarded. Then 1 ml AD+++ (4 °C) was added to each well directly onto the gel droplet to dissolve it, as it is liquid at cold temperatures. The content of the well was resuspended multiple times and the tip of the pipette was used to scratch the bottom of the well to detach attached organoids. The suspension was then transferred to a 15 ml falcon tube, which was placed on ice. Up to 5 wells of identical conditions could be pooled in one 15 ml

falcon tube. The tube was filled up to 10 ml with AD+++ (4 °C) before a centrifugation step (5 minutes, 200 x g, 4 °C). After centrifugation, the supernatant, which included the liquid BME2, was discarded. The pellet was resuspended in 200 µl AD+++ and transferred to a 1.5 ml Eppendorf tube, which was placed on ice again. To mechanically dissociate the organoids, the suspension was resuspended fast, using different sizes of pipette tips. First 100 µl tips were used and then a 10 µl pipette tips. The suspension was resuspended about 100 times with each pipette tip.
The tube was then filled up with AD+++ to 1 ml and, after centrifugation and discarding the supernatant, the organoids were either reseeded or prepared for cryopreservation. For freezing, the organoids were resuspended in 0.5 ml Cell Recovery Solution per well of organoids and transferred to cryovials. These were placed in a stratacooler, placed at -80 °C for 24h and then moved to the liquid nitrogen tank and stored at less than -160 °C.
For reseeding, 7.5 µl HepM (4 °C) and 22.5 µl BME2 (4 °C) were added to the Eppendorf tube for every well of a 24 well that was subsequently seeded. The procedure is the same as described above for the seeding of the digested liver tissue. After passaging, +1 was added to the passage number, starting with passage 0 (P.0) for the organoids growing from the digested liver tissue. The organoids were passaged at a ratio of 1:4 every 7-14 days, depending on how dense they were growing as observed under the microscope. For experiments, no organoids higher than P.3 were used. During organoid culture, the medium was always exchanged three times per week and the plates were stored in incubators, at 37 °C, 5% CO_2.

3.13 Real time quantitative polymerase chain reaction (RT-qPCR)

3.13.1 Sample Harvest and RNA isolation

RNA isolation was performed using the TRIzol™ reagent and according to the manufacturers' instructions, with a few minor adaptations. For RNA isolation from the HepOrg samples, 500 µl TRizol were added to one well of organoids in a 24 well plate, after the HepM had been removed. The solution was resuspended multiple times until it was homogenous and no remnants of the organoids or gel droplets were visible. These 0.5 ml of TRIzol were then used for homogenizing multiple wells of the same condition, so a maximum of 4 wells were taken up per 0.5 ml TRIzol. For RNA extraction from the PHH, one cryovial was thawed, the cells were washed

and centrifuged and the cell pellet was homogenized in 0.5 ml TRIzol. After homogenization, the homogenate was transferred to a tube and stored at -80 °C until the RNA extraction was performed.

The samples were thawed on ice and after thawing 0.1 ml chloroform was added to each sample, before shaking by hand and incubating 2-3 minutes. This was followed by a centrifugation step (15 minutes, 12.000 x g, 4 °C). The upper, aqueous phase, which contained the RNA, was transferred to a new tube. 0.25 ml isopropanol and 2 µl Glycoblue were added to the samples, before manually shaking the tube and incubating for 20 minutes at - 20 °C. After that, the samples were centrifuged (10 minutes, 12.000 x g, 4 °C). After centrifugation, a blue pellet was clearly visible, and the supernatant was removed completely. The samples were then resuspended in 0.5 ml 75% Ethanol and briefly vortexed, before being centrifuged (5 minutes, 12.000 x g, 4 °C). The supernatant was removed entirely, and the samples were air dried at 50 °C for 5 minutes in a heat block. 25 µl RNA free water were added to the pellet for resuspension and the samples were incubated in a heat block at 55 °C for 10 minutes. A nanodrop spectrophotometer was subsequently used to determine the RNA yield. Total RNA content was measured, whilst the ratio of the absorbance at 260 nm to 280 nm was used to assess the purity of the RNA (Okamoto and Okabe 2000).

3.13.2 DNAse treatment

The RNA samples were first diluted to a concentration of 200 ng/µl. 25 µl were transferred to a new tube for DNAse (deoxyribonuclease) treatment. The DNAse master mix contained 0.67 µl water, 1 µl RNAse inhibitor 3.33 µl DNAse buffer and 3.33 µl DNAse (2 U/ml) for each sample. 8.3 µl of the master mix were added to the RNA and the samples were incubated in the heat block at 37 °C for 15 minutes. After that, 3.3 µl 25 mM EDTA were added to each sample. Then, the samples were flicked and spun down on a table centrifuge before being incubated at 65 °C for 10 minutes in the heat block. The samples were then either stored at -80 °C or directly transcribed to complementary desoxyribonucleic acid (cDNA).

3.13.3 cDNA transcription

For the cDNA transcription, 1 µg of RNA was used for each sample. The respective volume of the DNAse treated RNA sample was transferred to a PCR tube. 4 µl 5X

qScript cDNA SuperMix were added and the sample was filled up with PCR water to 20 µl. The samples were briefly vortexed and then spun down on a table centrifuge. They were then incubated in the thermocycler for 5 minutes at 25 °C, followed by 30 minutes at 42 °C and 5 minutes at 85 °C. For short term storage before performing the qPCR, the samples were stored at 4 °C, for longer storage at -20 °C.

3.13.4 RT-qPCR

The qPCR was performed in duplicates for each gene. The 10 µl reaction was performed in 96 well qPCR plate. 1 µl of the cDNA suspension and 5 µl 2X SYBR green master mix were used for every reaction. Forward and reverse primers were added at a final concentration of 200 nM each. The sample was then filled up to 10 µl with PCR water and the plate was briefly centrifuged using the short spin function, before starting the PCR. The PCR was performed on a Roche light cycler, using the following program: 50 °C for 10 minutes, 95 °C for 5 minutes, 40 cycles of 95 °C (10 seconds) followed by 60 °C (30 seconds) followed by a melting curve.

3.13.5 Analysis

The relative gene expression of the hepatocyte organoids compared to primary human hepatocytes was calculated by using the $_{\Delta\Delta}$CT method (Livak and Schmittgen 2001). The Ct values for each target gene and the reference gene, glyceraldehyde-3-phosphate dehydrogenase (GAPDH), were measured and the mean was calculated for the duplicates. The $_{\Delta}$CTE values were calculated by subtracting the Ct value of the reference gene from the Ct value of each target gene tested for the hepatocyte organoid samples. For the PHH used as reference, the same was done to calculate the $_{\Delta}$CTC values. The double delta Ct values were then calculated by subtracting the $_{\Delta}$CTC values from the $_{\Delta}$CTE for each gene tested. To calculate the fold expression relative to the PHH, $2^{-\Delta\Delta CT}$ was calculated for every gene.

3.14 Immunofluorescence

3.14.1 Sample harvest and staining

The protocol for the immunofluorescence imaging of three-dimensional organoids was adapted from previous protocols described in the literature (Dekkers et al. 2019). The protocol was developed specifically for the three-dimensional imaging of organoids and utilizes a homemade clearing agent that captures whole, undisrupted organoids and enables imaging them in their entirety.

First, the organoids were harvested from their extracellular matrix. The medium was removed, and every well was washed once with phosphate buffered saline (PBS) without disrupting the gel droplet. 1 ml cell recovery solution (4 °C) was added to each well of a 24 well plate. The plate was stored at 4 °C and shaken by hand every 15 minutes to promote dissolution of the gel droplet. When the droplet had dissolved completely and all organoids were floating in the suspension after 60 - 90 minutes, the organoids were transferred to 15 ml falcon tube. Both pipette tip and falcon tube were pre-coated with PBS-BSA to prevent them from sticking to them. Pre-coating was used for all steps until after fixation of the organoids.

The wells were then rinsed with 1 ml PBS-BSA to collect the remaining organoids. Multiple wells from the same donor and conditions could be pooled in one falcon. The falcon was filled up to 10 ml with PBS (4 °C) and centrifuged (3 minutes, 70 x g, 4 °C). The supernatant was carefully removed, and the organoids were resuspended in 1 ml 4% PFA, before being incubated for 45 minutes at 4 °C. Halfway through, they were gently resuspended. The tube was then filled up to 10 ml with PBT (4 °C) and centrifuged (5 minutes, 70 x g, 4 °C). After centrifugation, the supernatant was removed, and the organoids were resuspended in 200 µl OWB (4 °C). 200 µl of the suspension were then transferred to each FACS tube used for the staining and the samples were incubated for 15 minutes at 4 °C.

Next, the primary antibodies (2x concentration) in 200 µl OWB were added. For the secondary antibody only controls, 200 µl OWB were added instead. The samples were incubated overnight at 4 °C on a shaker at 60 revolutions per minute (r.p.m.). The next morning, 1 ml OWB was added to each tube, before allowing the organoids to settle at the bottom of the tube for 3 minutes. 1 ml OWB was carefully removed again without aspirating organoids, before adding another 1 ml OWB and incubating the samples for 2 hours on a shaker at 60 r.p.m..

This washing step was repeated two more times. Then again, 1 ml OWB was carefully removed (leaving 200 µl and the organoids in the tube) and the secondary antibodies were added in 200 µl OWB (2x concentration). The samples were incubated overnight at 4 °C on a shaker at 60 r.p.m.. The next day, the three washing steps with 2 hours incubation in between were performed again. After that, as much of the supernatant as possible was removed, without aspirating organoids. 50 µl of the fructose-glycerol clearing solution were added, using a P100 pipette tip with the end cut off, as the viscosity of the clearing solution was very high. The samples were incubated for 20 minutes before being transferred onto the prepared imaging slide. A 1 x 1 cm square was drawn on the imaging slide using a PAP pen, which creates a hydrophobic barrier. 2 layers of sticky tape were sticked next to the PAP pen line and 20 µl of the organoids in the clearing solution were transferred to each imaging slide, again using a P100 tip with the end cut off. A coverslip was carefully placed on top, and the fluid spread out slowly. The coverslip was then attached to the sticky tape. The slides were stored horizontally at 4 °C until imaging.

3.14.2 Image acquisition and analysis

The images were acquired on a Nikon A1 confocal microscope within a few days after slide preparation. A 40x water immersion objective was used for imaging. The laser power and gain (HV) were adjusted until the signal was optimal for image acquisition. For conditions that were intended for comparative analysis to other images, the acquisition settings were kept constant to ensure comparability. Nikon NIS elements was used for image acquisition and analysis. For comparative analysis, a look-up table (LUT) was applied, displaying a certain fluorescence range for each fluorochrome, to enhance signal visualization for each detection channel. For all conditions that were compared, the LUTs were kept identical. For the images of the entire three-dimensional HepOrgs merged into a two-dimensional projection, the software's denoise.ai function was used to enhance contrast. Then an entire z-stack of two-dimensional images that were acquired of one three-dimensional organoid were merged into a two-dimensional projection.

3.15 Flow cytometry

3.15.1 Cell harvest

The first step for the flow cytometry staining was the harvesting and preparation of single cells from the cultured cells. The Huh 7.5 cells were harvested using TrypLE express enzyme for cell dissociation from the culture plate and then transferred to a FACS tube or 96-well plate for staining. As only single cells can be acquired at the flow cytometer, the organoids first had to be dissociated to single cells. The hepatocyte organoids were harvested from the ECM-rich hydrogel and then transferred to a 15 ml falcon tube. A maximum of organoids from three different wells of the same condition were pooled in one tube. The tubes were filled up to 10 ml with AD+++ (4 °C) and centrifuged (5 minutes, 200 x g, 4 °C). The supernatant was removed and 300 µl TrypLE express enzyme (37 °C) were added to each tube. The organoids were then thoroughly resuspended 50 to 100 times using a 100 µl pipette. The tubes were transferred to a water bath (37 °C) to ensure optimal enzyme activity. Every five minutes, the suspension was resuspended 50 to 100 times to mechanically dissociate the organoids and aid the procession to single cells. After 15 to 20 minutes, a small volume of the suspension was transferred to well of a 24 well plate and checked under the microscope for whether the organoids had already been sufficiently dissociated to single cells. If yes, the tube was filled up with AD+++ (4 °C) to 10 ml and stored on ice to stop the digestion process. If not, the incubation and resuspension process was continued for up to 45 minutes in total, checking for single cells under the microscope every five minutes. The cells were then centrifuged (5 minutes, 600 x g, 4 °C) and, after removal of the supernatant, transferred in PBS to FACS tubes or wells of a 96 well plate for staining.

3.15.2 Staining

Flow cytometry staining was performed according to standard protocols. First, the FACS tubes or 96 well plate were centrifuged again (5 minutes, 600 x g). The supernatant was removed and the extracellular master mix was added to the respective sample. The extracellular master mix always contained the LIVE/DEAD™ Fixable Near-IR Dead Cell Stain Kit, which was used for discrimination of live and dead cells. This kit reacts with free amines and for cells

with damaged membranes yields a fluorescence signal a lot higher than for live cells with intact membranes, enabling discrimination of both groups. In addition to that, the extracellular master mix contained antibodies for surface staining of antigens. The cells were incubated in the dark for 20 minutes, before PBS was added for washing and another centrifugation step was performed. The cells were then fixed, using either 4% PFA for the samples where only a surface staining was performed or the eBioscience™ IC Fixation Buffer when an intracellular staining was performed. After 20 minutes of incubation (in the dark), PBS was added and the cells were centrifuged (5 minutes, 600 x g).

For the surface staining, the supernatant was removed and the cells were resuspended in PBS and stored at 4 °C in the dark until acquisition at the flow cytometer. For the intracellular staining, the cells were permeabilized for 20 minutes using the eBioscience™ Permeabilization Buffer. The cells were then again washed and centrifuged, before being incubated with the mouse anti-HCV core antibody, diluted in permeabilization buffer, for 30 minutes. Another washing and centrifugation step followed, before the cells were incubated with the anti-mouse IgG secondary antibody (PE), diluted in permeabilization buffer, for 30 minutes. After subsequent washing and centrifugation, the cells were resuspended in PBS and stored at 4 °C in the dark until acquisition at flow cytometer.

BD FACSDiva software was used for data acquisition on a BD LSR Fortessa cytometer. The acquisition rate was always kept constant during acquisition. All samples from one experiment were measured on the same application settings, if not within the same session. The application settings were always automatically adjusted to the daily performance checks, the BD Cytometer Setup and Tracking (CS&T) protocol, to ensure comparability. For the compensation, compensation beads were used.

3.15.3 Analysis

The data generated was always saved in the flow cytometry standard file format (.fcs) and analyzed using FlowJo software. First, the cells of interest were identified and discriminated from detritus by their respective pattern of forward scatter area (FSC-A) to sideward scatter area (SSC-A). Next, dead cells were excluded by gating on APC-Cy7 negative cells, as the LIVE/DEAD™ Fixable Near-IR marked all cells with damaged cell membranes. Single cells were then identified by plotting the

relation of forward scatter area to forward scatter height against each other, as aggregates of cells have a distinct relation of those parameters and could therefore be excluded. The expression of the proteins of interest for the respective experiments was assessed last. Controls, either fluorescence minus one (FMO) or negative controls, were used to set the gates accurately. For the FMOs, identical biological samples were used. Those were incubated with master mixes lacking one specific antibody each, which in comparison to each other indicate the fluorescence intensity signal threshold that is specific for an antibody. The negative controls were used for the infection readouts and a mock infected control was used to set the threshold for viral protein expression. All histograms and plots depicted show fluorescence intensity on the x-axis on a logarithmic scale. For the histograms, cell numbers are on the y-axis and are normalized to mode. For the plots, the scale for SSC-A is linear.

3.16 Virus production

The viral stocks used for infections were produced and kindly provided by Gabrielle Vieyres and Isabelle Reichert of the research group cell biology of RNA viruses at the Leibniz Institute for experimental virology.

The viral stocks of the HCV chimera Jc1 were produced by transient transfection of Huh 7.5 cells with in vitro transcribed RNA, using electroporation, as previously described in detail (Haid et al. 2010). One day post electroporation, the harvest of viral particles in the supernatant of the cells was begun and continued until three days after electroporation. Supernatants were pooled and filtered at 0.45 µm.

The P100 viral stock was amplified in Huh 7.5 cells from the original stock provided by Julie Sheldon (Sheldon et al. 2014). Huh 7.5 cells at 80% confluency were incubated with an aliquot of the P100 stock and the supernatant of the cells was harvested daily from days two to four post infection. All harvested supernatants were pooled, and the viral stock was aliquoted and stored at -80 °C until it was used for infection. To determine the viral titer of the produced virus for both Jc1 and P100, serial dilutions of the viral stock were titrated on Huh 7.5 cells and subsequent immunohistochemical staining for the NS5A protein was performed. Thereby the tissue culture infectious dose 50 (TCID50), as described by Lindenbach et al. (2005), was calculated. The TCID50 per ml of the viral stocks can be converted to

focus forming units (FFU) per ml by multiplying with 0.7 and was subsequently used to calculate the multiplicity of infection (MOI) for the incubations with cells.

3.17 HCV infection

3.17.1 Huh 7.5 cell line HCV infection

First, 2.5 * 10^5 Huh 7.5 were seeded per well of a 6 well plate. The cells were in culture already for at least one week before being used for infection. 2 ml DMEM10 were added to each well and the cells were incubated for 4 h (37 °C, 5% CO_2) for them to adhere to the plate. The virus stock was then thawed quickly at 37 °C. After removing the culture medium from the wells, the calculated amount virus stock was added to the wells to obtain the desired MOI. The MOI was calculated by dividing the titer of the viral stock (in FFU/ml) by the number of cells per well. The wells were then filled up with DMEM10 to 1 ml. For the mock infected controls, medium was used instead of the viral stock. The cells were then incubated with the virus for 4 to 12 hours, depending on the experiment. After the incubation time, the entire supernatant was removed and 2 ml fresh DMEM10 were added to each well. The cells were kept in culture for 72 hours, until they were harvested for flow cytometry staining.

3.17.2 Hepatocyte organoid HCV infection

For the infection experiments of the HepOrgs various modifications of the infection protocol were tested. The general principle of inoculation with the virus was always the same and is described here. The organoids were grown in culture prior to the inoculation with the virus until the wells were filled with many grown organoids but still had some space for further growth. First, two wells per donor were harvested, processed to single cells, and counted. All wells of the donor had been seeded at the same density and were presumed to contain the same number of cells. The cell number was used to calculate the volume of virus stock needed to obtain the desired MOI. For infection, the medium was removed from the wells and, after quickly thawing the virus stock, the calculated volume was added to each well. The wells were then filled up with HepM to 500 µl. After an incubation time ranging from 4 to 12 hours, depending on the experiment, the entire supernatant was removed and

500 µl fresh HepM were added to each well. For the mock infected controls, the corresponding amount of medium was used instead of the viral stock.

After 72 hours, the organoids were harvested for flow cytometry staining. For most experiments, the organoids were pre-treated with 10 µM ruxolitinib one day before infection and cultured with 10 µM ruxolitinib throughout the experiment until cell harvest. For one experiment, some organoids were pre-treated and then cultured with 1 µM BX-795. When organoids were inoculated with the virus in suspension instead of in their ECM-rich hydrogel droplets, they were first harvested from their matrix. Then, they were transferred to a falcon tube and incubated there in a suspension of virus stock and HepM for 4 hours. After the incubation time, the organoids were again seeded to the same number of wells they were retrieved from. For the infection of single cells, all the organoids from each donor were harvested from their ECM-rich hydrogel droplets and trypsinized, to obtain single cells. The cells were then counted and reseeded at the desired density. The calculated amount of viral stock was added to each well and the cells were incubated with the virus for 4 h. The supernatant was subsequently removed and 500 µl fresh HepM were added to each well. For some experiments, a modified version of the organoid medium without epidermal growth factor (EGF) was used from two days before infection onwards.

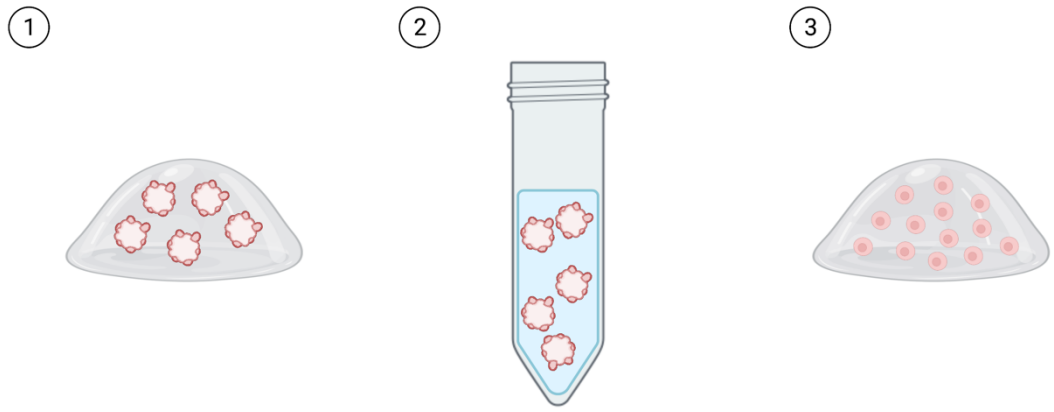

Figure 7: Overview of the organoid conditions used for inoculations with the virus. Three different conditions of the organoids were tested for inoculations with the virus. For the time of the inoculation with the virus, the organoids were either kept in their usual extracellular matrix (1), removed from the extracellular and kept in suspension (2) or processed to single cells and then reseeded to the ECM-rich hydrogel (3). Created with BioRender.com.

3.17.3 Plasma infection

For the infections with patient derived virus, 100 µl plasma were used per well for both the Huh 7.5 cell line and the HepOrgs. The viral load in the patient plasma used for infections ranged from 2.62 $x10^6$ to 1.35 $x10^7$ international units (IU) per ml. All plasma donors provided written, informed consent and the use of patient plasma was approved by the Ärztekammer Hamburg (WF-14-09).

3.18 Organoid medium modifications

For the experiments with the modifications of the HepM, the organoids were passaged before being cultured in the modified versions of the HepM for seven days. Modifications of the medium included supplementation of the HepM with dexamethasone (1 or 3 µM), dexamethasone (1 µM) plus oncostatin M (10 ng/ml) and HepM without EGF. For the conditions without EGF in the medium, the organoids were cultured in medium without EGF for either two, five or seven days. Before that, normal HepM was used for culture. After seven days in culture in the modified media, the organoids were harvested for flow cytometric analysis of protein expression.

3.19 Statistical analysis

Statistical analyses were performed using GraphPad Prism 9 software. Median and interquartile range (IQR) of all data are indicated in the charts. Comparisons within a group of matched samples were performed with a paired t test. The Mann-Whitney test was used for nonparametric comparisons between two independent groups.
Comparisons between multiple dependent groups were performed using the Friedmann test with post hoc Dunn's multiple comparisons test. In the charts, different numbers of asterisks indicate the level of statistical significance. * $P < 0.05$, ** $P < 0.01$, *** $P < 0.001$, **** $P < 0.0001$.

4 Results

4.1 Expression of CD81, claudin-1, occludin and SRB1 on hepatocyte organoids

The tetraspanin CD81, the tight junction proteins claudin-1 and occludin and SRB1 are known to be essential for infection of hepatocytes with HCV. The first step to establishing a hepatocyte organoid-based model of HCV infection was therefore to investigate the expression of these proteins on the HepOrgs using confocal immunofluorescence microscopy.

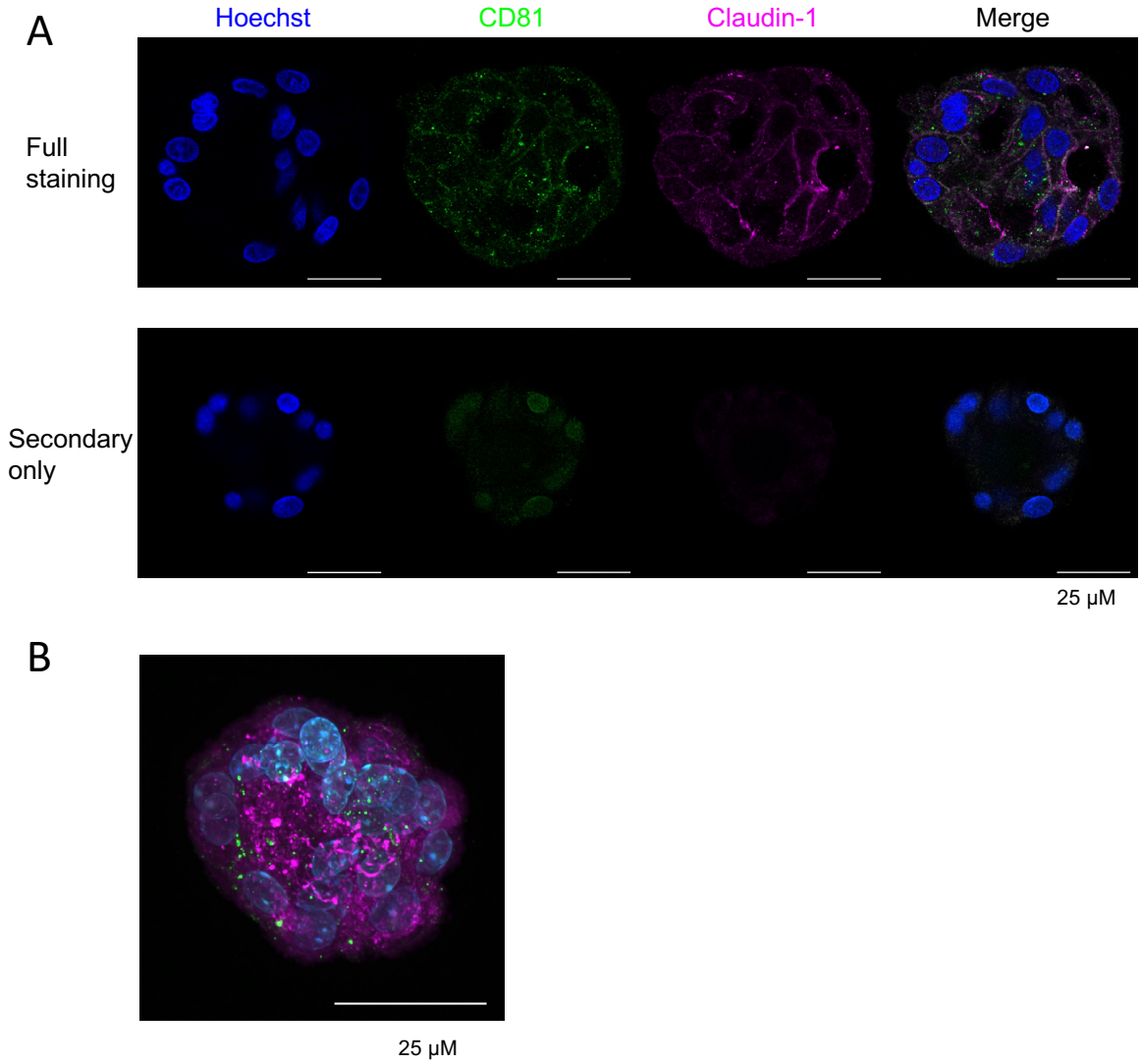

Figure 8: Expression of CD81 and claudin-1 on hepatocyte organoids. Representative immunofluorescence images of hepatocyte organoids. Staining for CD81 (green), claudin-1 (pink) and nuclei (Hoechst; blue). (A) Comparison between full antibody staining and secondary antibody only control of a two-dimensional slice of two HepOrgs. (B) One entire three-dimensional organoid projected in a two-dimensional image. The scale indicates 25 µm for A and B.

Both CD81 and claudin-1 were expressed on hepatocyte organoids (Figure 8A). The tetraspanin CD81 was mostly expressed on the cell membrane of the cells and was evenly distributed on the cell membranes throughout the entire organoid.

Claudin-1 was also expressed on the cell membrane of cells within the hepatocyte organoids. Unlike CD81, it showed a clearly polarized pattern of distribution throughout the organoid and its expression was concentrated towards the luminal side of the organoids, around the multiple lumina of the organoid depicted in figure 8A. This is also visible in figure 8B, which shows an entire organoid merged into a two-dimensional projection, where the expression of claudin-1 was concentrated on the luminal membranes of the organoid.

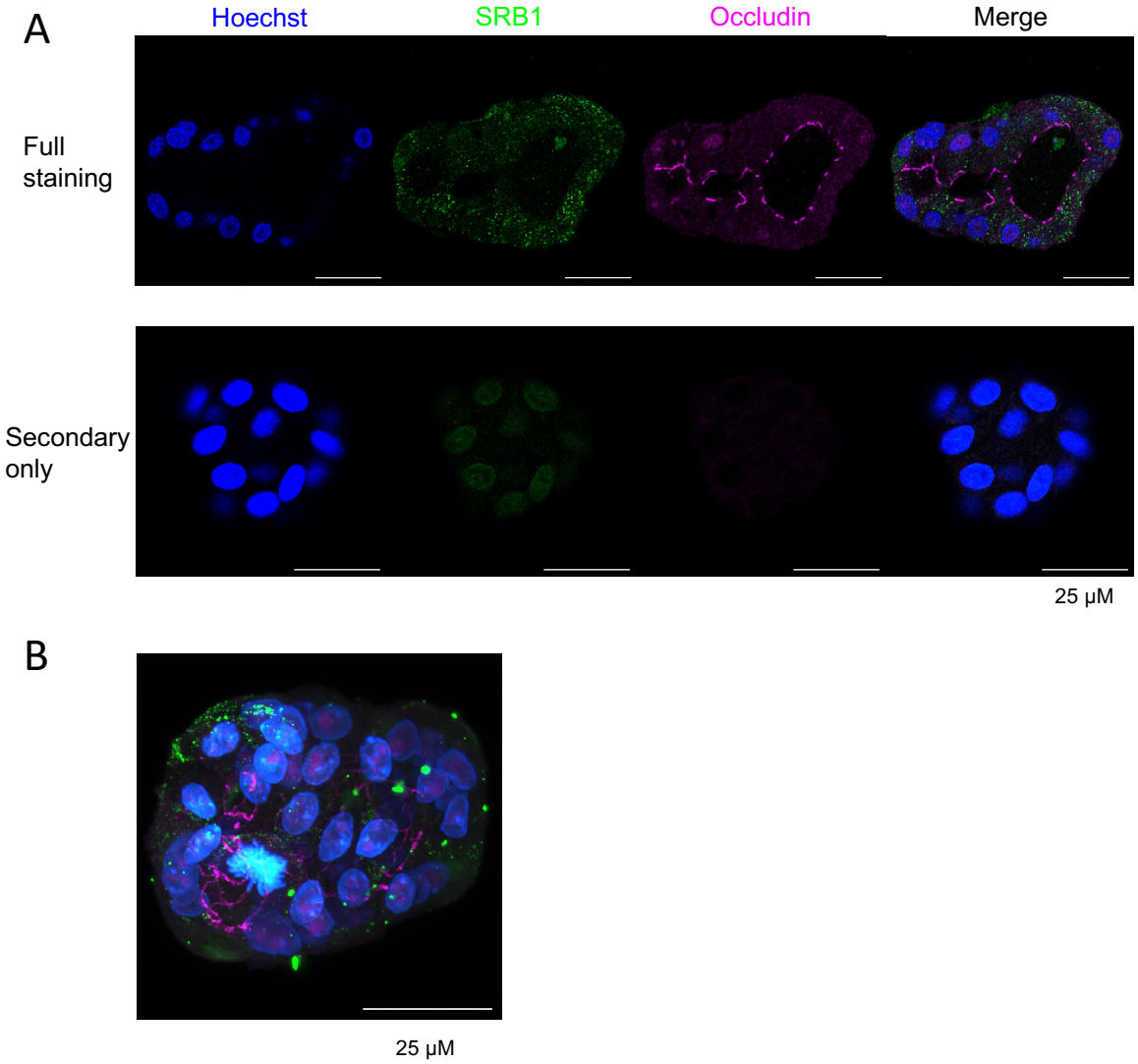

Figure 9: Expression of SRB1 and occludin on hepatocyte organoids. Representative immunofluorescence images of hepatocyte organoids. Staining for SRB1 (green), occludin (pink) and nuclei (Hoechst; blue). (A) Comparison between full antibody staining and secondary antibody only control of a two-dimensional slice of two HepOrgs. (B) One entire three-dimensional organoid projected in a two-dimensional image. The scale indicates 25 µm for A and B.

SRB1 is a cell surface high-density lipoprotein (HDL) receptor, which is essential for HCV entry into hepatocytes (Catanese et al. 2007). It is expressed at high levels in the human liver and is a receptor for HDL (Acton et al. 1996). The HepOrgs expressed SRB1 (Figure 9A). It was expressed throughout the entire organoid with no clear polarized pattern of expression. It was expressed on both the cell membranes and within the cytosol. As depicted in figure 9, occludin was expressed on the hepatocyte organoids as well. Unlike SRB1, it was expressed very unevenly on the cell membrane of the HepOrg cells. Its expression was almost exclusively limited to the cell membranes adjacent to the lumen of the organoid, where it showed a web-like pattern of expression spanning the entire lumen of the organoids (Figure 9B).

For all four proteins expressed on HepOrgs there was also detectable expression of the corresponding messenger RNA (mRNA) (Figure 10). The relative mRNA expression of claudin-1, CD81 and SRB1 in relation to the reference gene (GAPDH) was considerably lower than in the PHH. The relative gene expression of claudin-1 was 0.03 (median, IQR 0.024 - 0.091, n=7). The relative CD81 expression was a little bit higher with 0.077 (median, IQR 0.051 - 0.259, n=7). The relative SRB1 expression was similar to that of claudin-1, with a median relative expression of 0.078 (median, IQR 0.06 - 0.128, n=7). Unlike the other three genes investigated, the relative expression of occludin compared to PHH varied a lot for organoids derived from different donors. Its relative expression was a lot higher than the other three genes investigated with 2.049 (median, IQR 0.637 - 4.595, n=7) and for organoids derived from some donors even exceeded the relative expression compared to the PHH by up to six-fold.

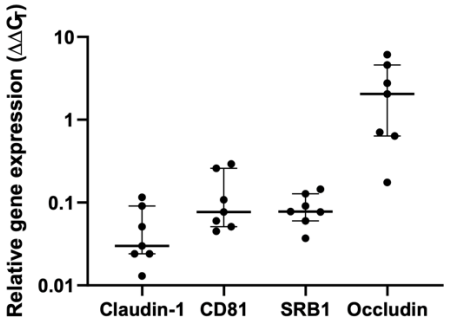

Figure 10: mRNA expression of HCV entry factors. Relative gene expression of claudin-1, CD81, SRB1 and occludin in HepOrgs (n = 7) compared to PHH (unmatched donor). Relative gene expression was calculated using the ΔΔCT method. Median and interquartile range are indicated.

Taken together, the data demonstrates that the essential entry factors for HCV were expressed on hepatocyte organoids. Furthermore, the HepOrgs were clearly

polarized, with the expression of tight junction proteins towards the lumen of the organoids.

4.2 HCV infection of Huh 7.5 cell line

There are multiple different readouts to assess infection of cells with HCV in vitro. HCV RNA can be detected by RT-qPCR and infectious virus production can be investigated by titrating the culture supernatant on permissive cell lines and determining the TCID50. Furthermore, viral proteins can be detected in infected cells by immunohistochemistry, immunofluorescence, or flow cytometry.

To establish a reliable flow cytometric readout for HCV infection in HepOrgs, infections and subsequent flow cytometric analysis were first performed with the Huh 7.5 cell line. The HCV core protein is a structural viral protein and forms the viral nucleocapsid. Detection of the HCV core protein by flow cytometry can be used to discriminate between HCV infected and uninfected cells, as it is only expressed in infected cells (Kang et al. 2014). For establishing the flow cytometry-based infection readout, the Huh 7.5 cells were incubated with P100 at a MOI of 1 for 4 hours. 72 hours after infection, the cells were harvested and stained for the expression of the HCV core protein.

The flow cytometry-based infection readout discriminated clearly between HCV infected and uninfected cells (Figure 11A). In the mock infected sample, the cells did not express the HCV core protein, while for the cells inoculated with the virus, there was a large population of cells expressing the HCV core protein. Furthermore, controls ensured that the signal obtained was HCV core protein specific, as the secondary antibody only control on infected cells did not show a positive signal (figure 11B). A condition of infected cells, that were not permeabilized for the antibody staining, showed a marked reduction the HCV core protein signal (Figure 11B). This indicated that most of the viral protein was located intracellular. A histogram comparing all infection and staining conditions (Figure 11C) demonstrates the large differences in HCV core protein signal among all different conditions. The infection rate in this system was very consistent, with a median infection rate of 83.9 % (IQR 83.3% – 84.33%, n = 5) 72 hours after inoculation of the cells with the virus (Figure 11D). This data indicated that flow cytometry can be used to clearly discriminate between HCV uninfected and infected cells.

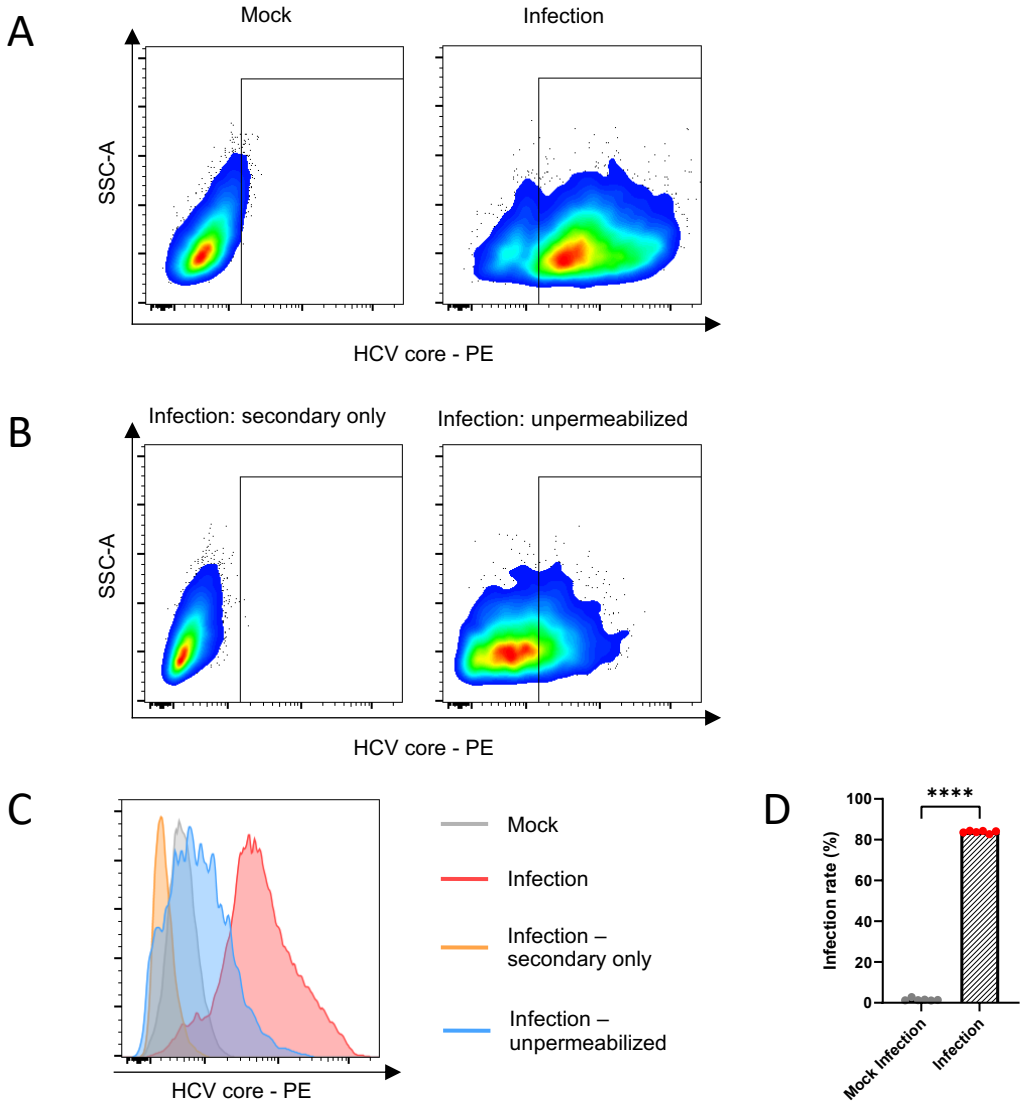

Figure 11: Flow cytometry staining for HCV core protein in Huh 7.5 cell line. (A) Comparison between mock infected condition and cells inoculated with HCV (infection). (B) Additional staining conditions for condition inoculated with the virus. Secondary antibody only control and an unpermeablized control, where cells were not permeabilized for intracellular staining. (C) Histogram showing direct comparison between all staining conditions from A and B. (D) Comparison of infection rates between infection condition and mock infected condition (n = 5). A paired t test was used for statistical analysis. **** $P \leq 0.0001$

Different strains of the hepatitis C virus are used for infection in cell culture systems. Jc1 is one of the most widely used viruses in cell culture and is a chimeric virus derived from sequences of two genotype 2a isolates. P100 is derived from Jc1 and was created by serial passaging for 100 passages in Huh 7.5 cells. It acquired adaptive mutations during passaging which led to an increased replicative fitness in cell culture. Both viruses were tested in the Huh 7.5 system with the flow cytometry readout to compare infection rates. Jc1 yielded low infection rates 72 hours after inoculation with the virus and the infection rate varied widely depending on the MOI

used for infection. It increased from 1.9% at an MOI of 0.1 to 28.2% at an MOI of 1 (Figure 12A). In contrast, P100 yielded higher infection rates, approaching 90% 72 hours after inoculation with the virus (Figure 12B). Unlike for Jc1, the infection rates did not differ considerably depending on the MOI used for infection, with an infection rate of 86.3% at an MOI of 0.1 and 88.4% at an MOI of 1. Due to the observed higher infectivity of P100 compared to Jc1 that had also been previously described (Perales et al. 2013, Sheldon et al. 2014), P100 was used for subsequent hepatocyte organoid infections.

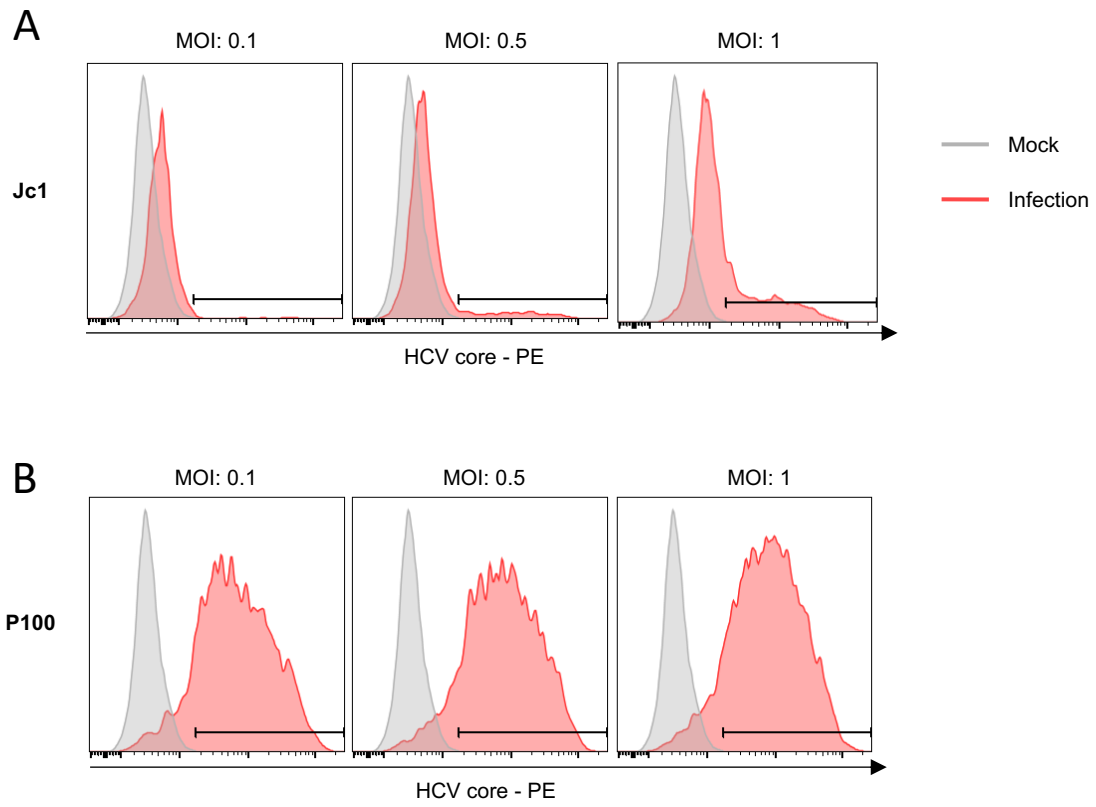

Figure 12: Comparison between Jc1 and P100 infection rates in Huh 7.5 cell line. HCV core protein expression was assessed 72h after inoculation with the virus via flow cytometry. (A) Histograms comparing the HCV core protein expression for different MOI used for infection with Jc1 (red) with the mock infected condition (grey). (B) Histograms comparing the HCV core protein expression for different MOI with the mock infected condition with P100 used for infection.

4.3 HCV infection of hepatocyte organoids

For the first infection of hepatocyte organoids, P100 was used at an MOI of 1 and all organoids were treated with 10µM ruxolitinib, beginning at the time of infection. Ruxolitinib inhibits JAK/STAT signaling and has been shown to enhance HCV infection in PHH (Tegtmeyer et al. 2021). The organoids were incubated with the

virus for 12 hours. HCV core protein expression was assessed 72 hours after the end of the incubation time with the virus.

There was no detectable HCV core protein expression in any of organoids derived from two different donors. There was no difference in the signal for the HCV core protein between the mock infected control and the organoids inoculated with the virus (Figure 13A). This was contrasted by the high infection rate observed in the Huh 7.5 cell line used as a positive control. 90.5% of the cells had detectable HCV core protein expression 72 hours after infection (Figure 13B).

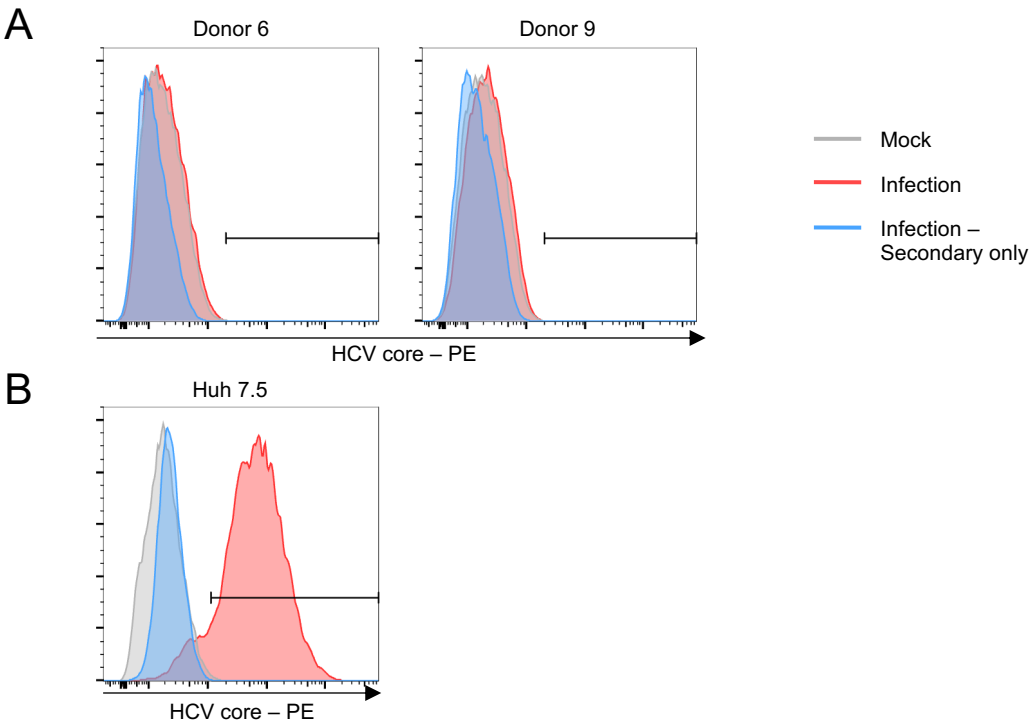

Figure 13: HCV infection of HepOrgs in comparison to Huh 7.5 cell line. HCV core protein expression was assessed 72 hours after inoculation of the organoids with the virus. (A) Histograms comparing the HCV core protein expression in organoids derived from two different donors. Comparison between the mock infection (grey), and the infection with full staining (red) and secondary antibody only control (blue). (B) Histogram of the Huh 7.5 cell line used as positive control for the infection.

To investigate, whether differences in the polarity and the extracellular matrix between the organoids and the Huh 7.5 cell line could explain the lack of detectable infection in the organoids, modifications in the infection conditions were tested. For the first experiment, the organoids were incubated with the virus embedded in their extracellular matrix, while the Huh 7.5 cells do not have an extracellular matrix when grown as a monolayer. This difference was addressed by removing the organoids from their extracellular matrix and putting them in suspension for the incubation with the virus. Another difference between the cells was the polarity of the organoids, as

the Huh 7.5 cells are not polarized when grown in a two-dimensional monolayer, as indicated by their inability to form tight junctions (Mee et al. 2008). This difference was experimentally addressed by enzymatically digesting the organoids to single cells or mechanically disrupting them to smaller organoids prior to the incubation with the virus. The organoids were pretreated with 10 µM ruxolitinib one day before infection and cultured with it until the cells were harvested for flow cytometry staining.

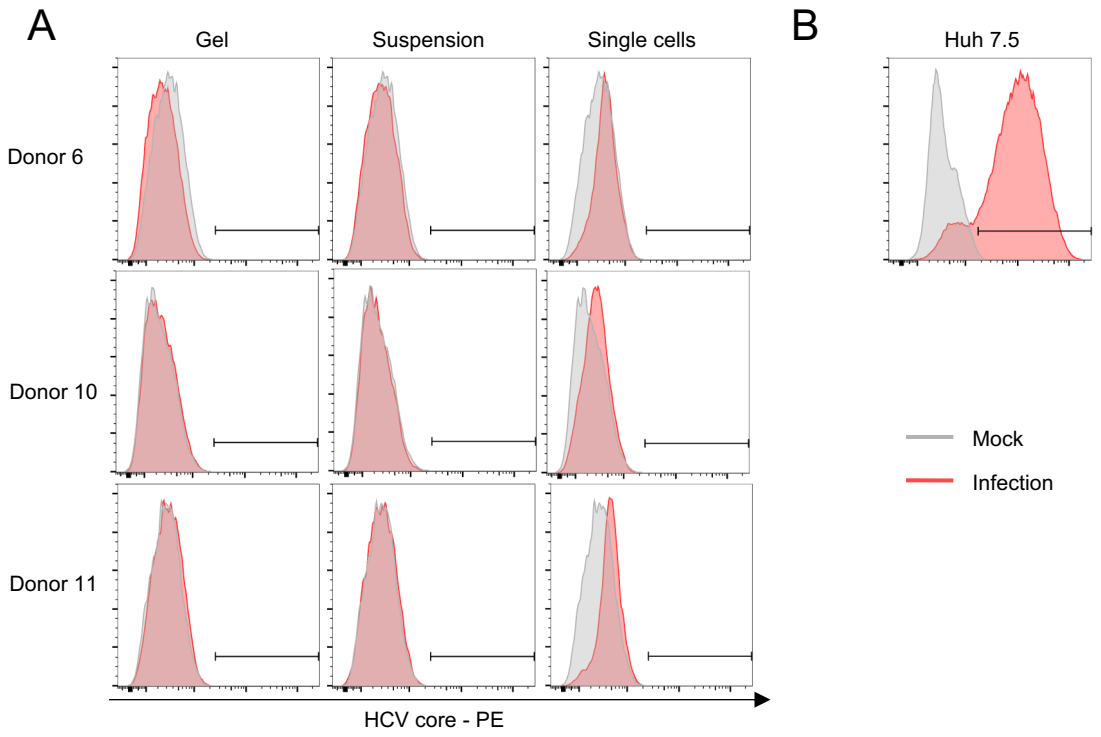

Figure 14: Comparison of different infection conditions for HepOrg HCV infection. HCV core protein expression was assessed 72 hours after inoculation with the virus. (A) Three different infection conditions were tested for HepOrgs derived from three different donors. The organoids were inoculated with the virus either embedded in extracellular matrix (gel), in suspension or as single cells embedded in extracellular matrix. Compared is the expression of HCV core protein between mock infected control (grey) and infection condition (red) for each condition tested. (B) Histogram of Huh 7.5 cell line HCV infection, which was used as positive control for HCV infection.

The organoids for the single cell condition were enzymatically digested to single cells prior to incubation with the virus and were embedded in ECM-rich hydrogel during the incubation. The organoids for the other two conditions were mechanically dissociated to smaller organoids prior to incubating them with the virus either embed in extracellular matrix (gel) or in suspension.

There was no detectable HCV core protein expression in any of the three infection conditions tested compared to the mock infected controls. This was observed for HepOrgs derived from all three different donors tested. In contrast, 87.3% of the

Huh 7.5 cells used as a positive control showed expression of the HCV core protein. Overall, the data presented in figure 14 indicated that neither the polarity nor their structure within the extracellular matrix were the reason for the absence of detectable HCV infection within the HepOrgs.

4.4 HCV receptor expression on HepOrgs and Huh 7.5 cell line

In addition to CD81, SRB1, claudin-1 and occludin, the EGFR is also known to play an important role for the cellular entry of HCV. In consideration of the lack of detectable HCV infection in the organoids compared to the Huh 7.5 cell line, flow cytometric analysis of the expression of three proteins implicated in the virion internalization, SRB1, CD81 and the EGFR, was compared between the Huh 7.5 cell line and HepOrgs.

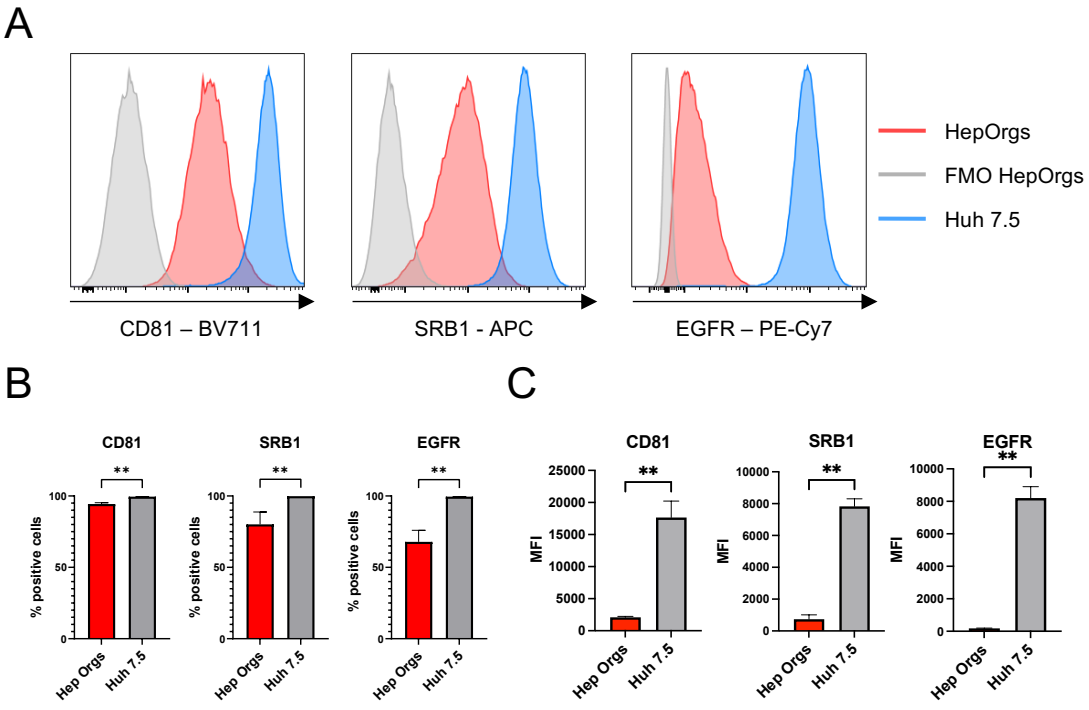

Figure 15: Comparison of expression of HCV entry factors on Huh 7.5 cell line and HepOrgs. The expression of CD81, SRB1 and the EGFR was compared between HepOrgs and the Huh 7.5 cell line using flow cytometry. (A) Histograms comparing the expression of the respective protein on HepOrgs (one exemplary donor shown; red) and the Huh 7.5 cell line (blue). FMO controls are shown for the HepOrgs as a reference (grey). (B) The percentage of cells expressing the respective protein is compared between HepOrgs and Huh 7.5 cell line (n = 5). (C) Comparison of the MFI between HepOrgs and Huh 7.5 cell line for the different proteins (n = 5) Mann-Whitney test was used for statistical analysis. ** $P \leq 0.01$.

The proportion of cells that expressed the EGFR, CD81 and SRB1 was significantly ($p < 0.01$) different between the HepOrgs and the Huh 7.5 cell line. Virtually all cells of the Huh 7.5 cell line expressed all three proteins on their cell membrane. For the

HepOrgs on the other hand, only 67.9% of the cells expressed the EGFR (median, IQR: 62.6% – 75.9%, n=5) and 80.1% % (median, IQR 71.5% - 88.8%, n=5) expressed the SRB1. The expression of CD81 was more widespread on the HepOrgs, with 94.4% (median, IQR: 86.95% - 95.3%, n=5) of the cells expressing the protein. The difference in protein expression between the HepOrgs and the Huh 7.5 cell line was even more substantial when considering the differences in median fluorescence intensities (MFIs) instead of the percentage of cells that expressed the proteins. The MFI gives a basic indication of the amount of protein expressed on a cell, with higher MFIs indicating more protein expression (Hogg et al. 2015).

The Huh 7.5 cell line expressed significantly more EGFR, CD81 and SRB1 than the hepatocyte organoids. The MFI for CD81 for the HepOrgs was 2084 (IQR 1413 – 2236, n = 5) compared to 17562 (IQR 16856 – 20215, n = 5) for the Huh 7.5 cell line. For SRB1 the MFI was 726 (median, IQR 553.5 – 1004, n = 5) for the HepOrgs compared to 7833 (median, IQR: 7565 – 8301, n = 5) for the Huh 7.5 cell line. The relative difference between the MFIs was largest for the EGFR, with an MFI of 172 (median, IQR 155.5 – 188.5, n = 5) for the HepOrgs compared to 8201 (median, IQR: 7831 – 8902, n = 5) for the Huh 7.5 cells.

These large differences in protein expression between HepOrgs and the Huh 7.5 cell line raised the question, whether the hepatocyte organoids might not express enough of those proteins to facilitate viral entry into the cells. Consequently, this led to the question, whether the expression of those proteins could be increased on the HepOrgs and whether they would then become susceptible to HCV infection in vitro.

4.5 Variations of the HepOrg culture medium

To alter the expression of these proteins on the organoids, different modifications of the culture medium were tested. Dexamethasone and oncostatin M (OSM) have been used to induce in vitro differentiation in murine fetal liver cells (Kamiya et al. 2001), human fetal hepatocyte organoids (Hu et al. 2018)) and murine hepatocyte organoids (Peng et al. 2018). The low expression of the EGFR on the HepOrgs raised the question, whether the high concentration of EGF in the HepM (50ng/ml) might lead to receptor internalization and degradation. This had been described in HeLa cells previously (Sigismund et al. 2008).

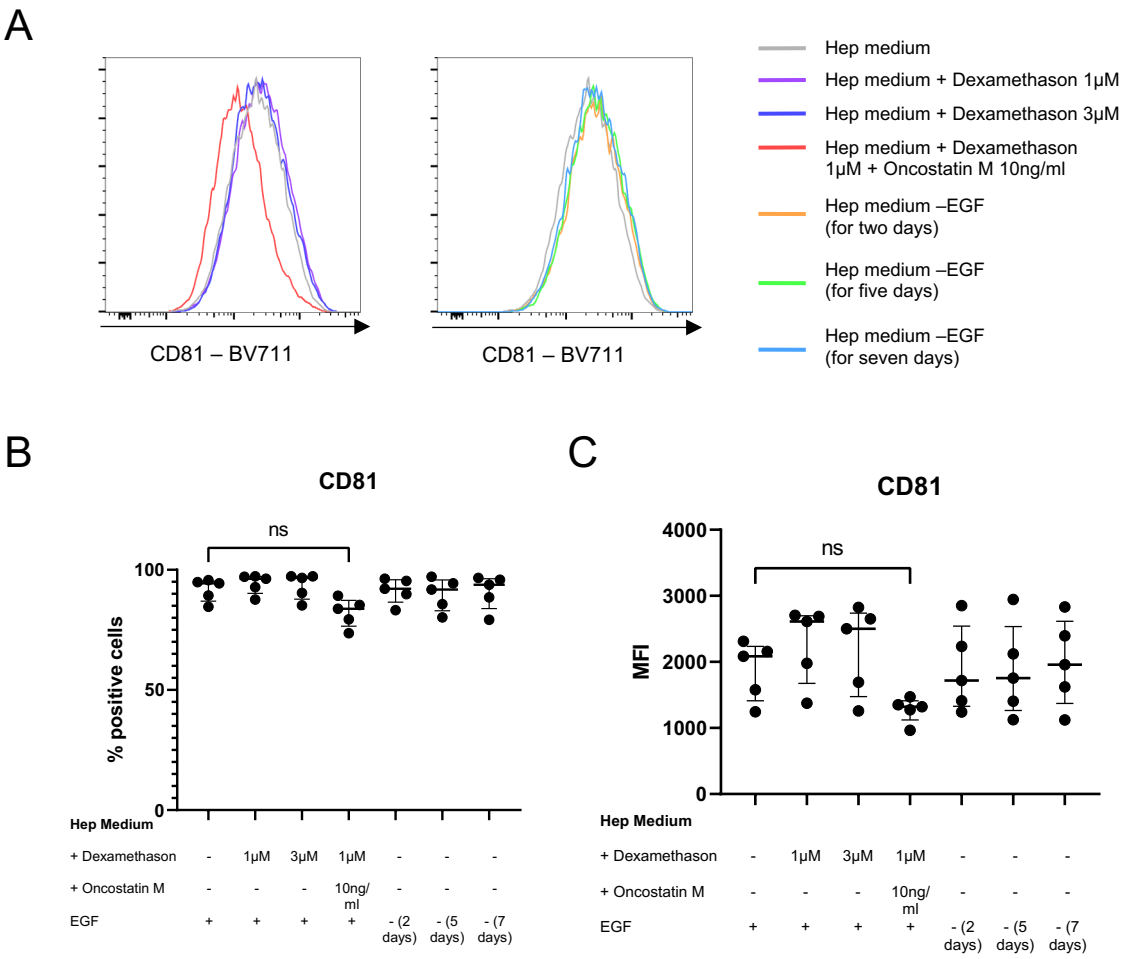

Figure 16: Expression of CD81 on HepOrgs for different modifications of culture medium. The organoids were cultured in the modified versions of the HepM for 7 days before the protein expression was assessed by flow cytometry. For the HepM without EGF condition, the organoids were cultured in the HepM without EGF for either 7, 5 or 2 days prior to the flow cytometry staining. (A) Histograms comparing the expression of CD81 among all conditions. (B) Comparison of relative frequencies of cells expressing CD81 in the culture for all conditions. The regular HepM is shown as a reference in the first column (Dexamethasone (-), oncostatin M (-), EGF (+)). (C) Comparison of the MFI for CD81 among all different conditions. n = 5 for all conditions.
Friedmann test and subsequent Dunn's multiple comparison test was used for statistical analysis.

The effect of six different modifications of the HepM on the expression of the EGFR, CD81 and SRB1 was investigated. The medium was supplemented with dexamethasone (1 µM or 3 µM) or dexamethasone (1 µM) and OSM (10 ng/ml), or HepM without EGF was used for two, five or seven days before assessing the protein expression on the organoids.

Neither of the modifications of the medium had any effect on the expression of CD81 on the HepOrgs (Figure 16). The proportion of CD81 expressing cells remained similar for all conditions tested (Figure 16B) and there were no significant changes in MFI compared to the standard HepM (Figure 16C).

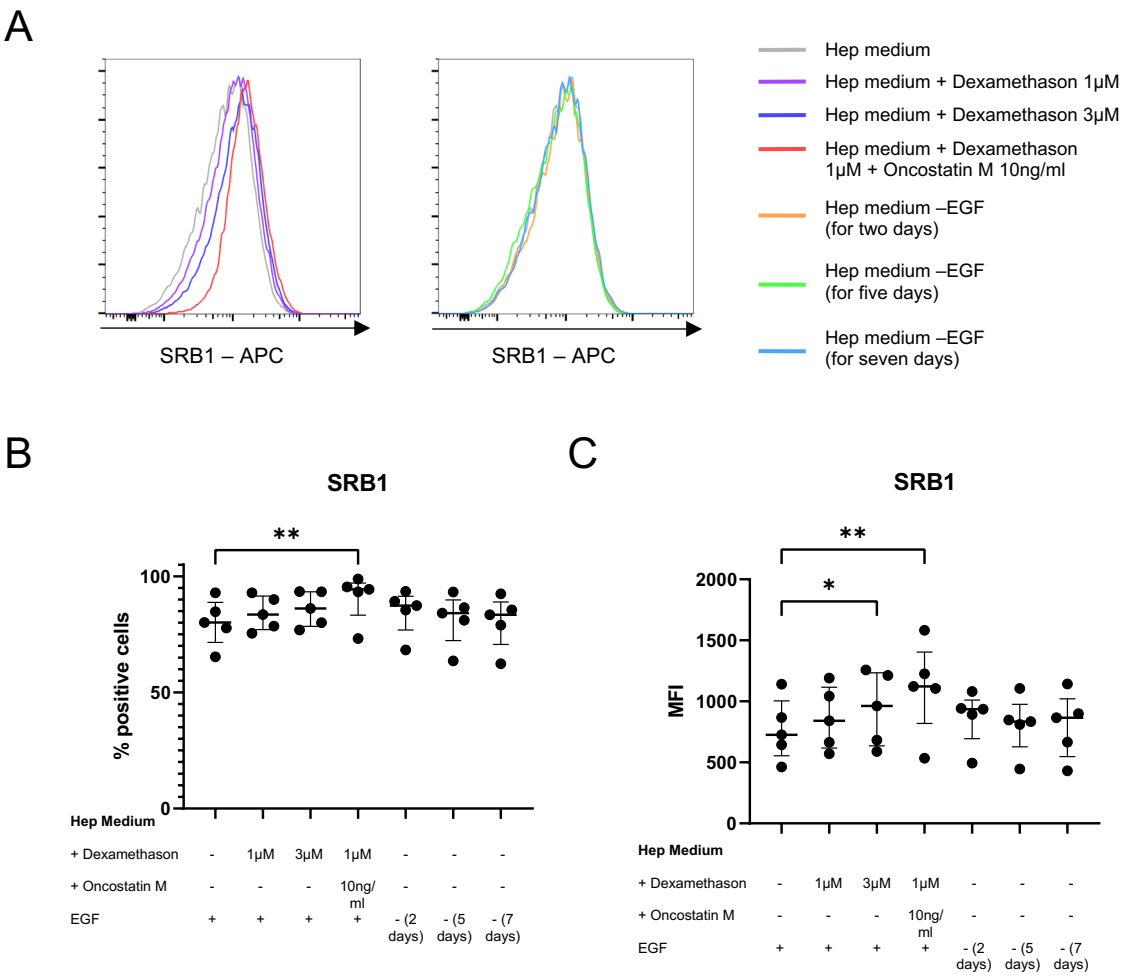

Figure 17: Expression of SRB1 on HepOrgs for different modifications of culture medium. The organoids were cultured in the modified versions of the HepM for 7 days before the protein expression was assessed by flow cytometry. For the HepM without EGF condition, the organoids were cultured in the HepM without EGF for either 7, 5 or 2 days prior to the flow cytometry staining. (A) Histograms comparing the expression of SRB1 among all conditions. (B) Comparison of relative frequencies of cells expressing SRB1 in the culture for all conditions. The regular HepM is shown as a reference in the first column (Dexamethasone (-), oncostatin M (-), EGF (+)). (C) Comparison of the MFI for SRB1 among all different conditions. n = 5 for all conditions.
Friedmann test and subsequent Dunn's multiple comparison test was used for statistical analysis. * $P \leq 0.05$, ** $P \leq 0.01$.

The expression of SRB1 on the other hand was influenced by modifications of the medium. The proportion of SRB1 expressing cells within the organoid culture was significantly upregulated, compared to the standard HepM, when supplemented with dexamethasone and OSM (Figure 17B). When cultured with standard HepM, 80.1% (median, IQR: 71.5 - 88.8%, n=5) of the cells expressed SRB1, compared to 94.4% (median, IQR: 83.3 – 97.1%, n=5) for the HepM supplemented with dexamethasone and OSM. The other modifications of the medium tested did not alter the proportion of SRB1 expressing cells in the organoid culture. The median fluorescence intensity increased as well for the medium supplemented with dexamethasone and OSM

compared to HepM. It increased from 726 (median, IQR: 553.5 - 1004, n=5) for the HepM to 1122 for the medium supplemented with dexamethasone and OSM (median, IQR: 819.5 - 1404, n=5). A significant increase in the MFI was also observed for the HepM supplemented with 3 µM dexamethasone with an MFI of 963 (median, IQR: 635.5 - 1235, n=5). All other modifications of the medium tested had no effect on the SRB1 expression on the HepOrgs (Figure 17C).

As hypothesized, the expression of the EGFR was influenced substantially by removing EGF from the medium. The proportion of EGFR expressing cells within the organoids increased significantly when the organoids were cultured without EGF in the medium for five or seven days (Figure 18B).

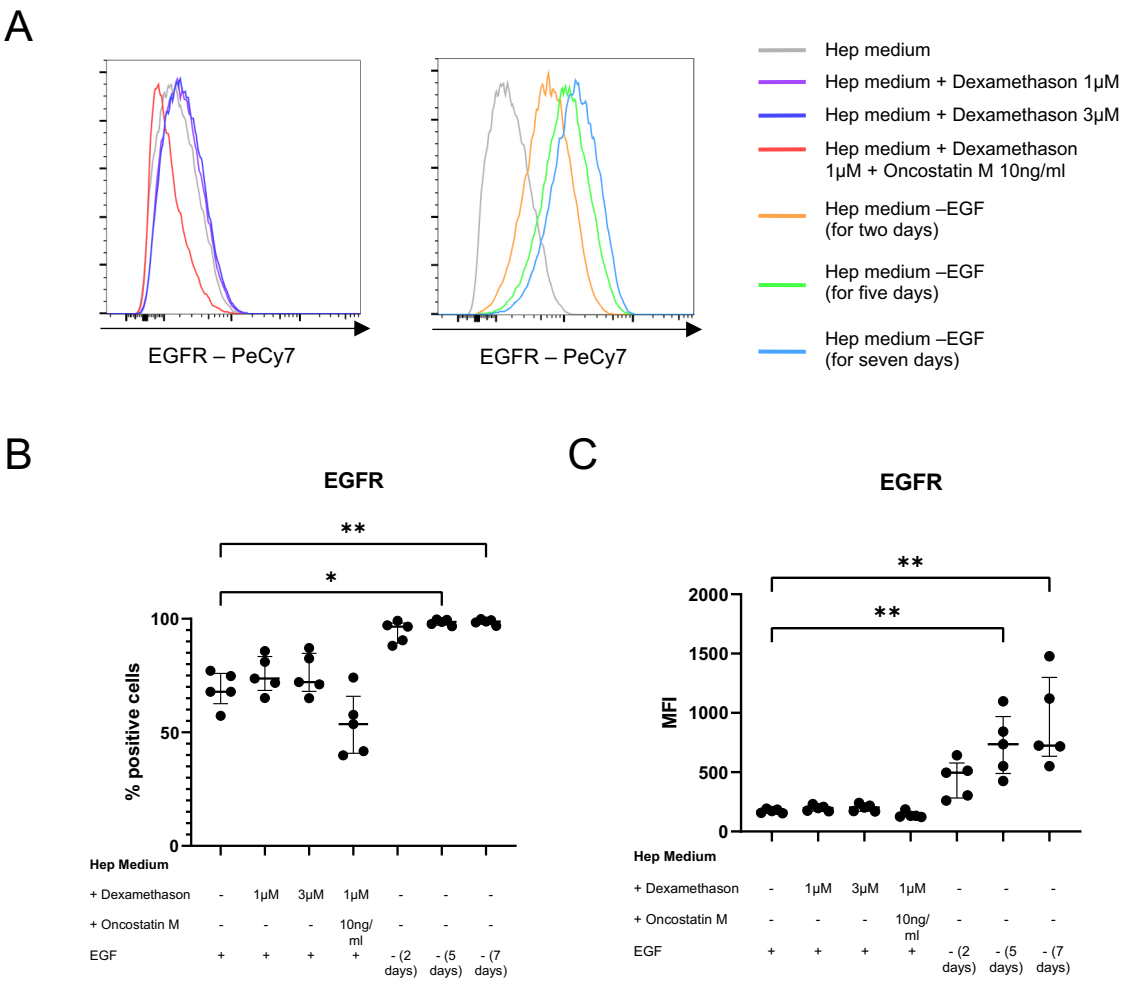

Figure 18: Expression of EGFR on HepOrgs for different modifications of culture medium. The organoids were cultured in the modified versions of the HepM for 7 days before the protein expression was assessed by flow cytometry. For the HepM without EGF condition, the organoids were cultured in the HepM without EGF for either 7, 5 or 2 days prior to the flow cytometry staining. (A) Histograms comparing the expression of EGFR among all conditions. (B) Comparison of relative frequencies of cells expressing EGFR in the culture for all conditions. The regular HepM is shown as a reference in the first column (Dexamethasone (-), oncostatin M (-), EGF (+)). (C) Comparison of the MFI for EGFR among all different conditions. n = 5 for all conditions.
Friedmann test and subsequent Dunn's multiple comparison test was used for statistical analysis. * $P \leq 0.05$, ** $P \leq 0.01$.

When cultured in HepM, 67.9% (median, IQR: 62.6 - 76%, n=5) of the cells expressed the EGFR, compared to 98.6% (median, IQR: 97.2 – 99.6%, n=5) and 98.8% (median, IQR: 97.7 – 99.7%, n=5) for the conditions cultured without EGF in the medium for five and seven days, respectively. The protein expression on the HepOrgs was also significantly increased, with an increase in the MFI for both conditions (Figure 18C). It increased from an MFI of 172 (median, IQR: 155.5 – 188.5, n=5) for the HepM to 736 (median, IQR: 488.5 – 969.5, n=5) for the condition without EGF for five days and 724 (median, IQR: 634 - 1299, n=5) for the condition without EGF in the medium for seven days. The supplementation of the medium with dexamethasone and OSM had no significant effect on EGFR expression on the cells.

In summary, the expression of CD81 was not increased by any of the modifications of the medium tested, while the supplementation of the medium with dexamethasone and OSM increased the expression of the SRB1 on the HepOrgs. The surface expression of the EGFR was increased considerably when the organoids were cultured in medium without EGF, with a higher expression of the EGFR for longer times in culture without EGF. Any of the modest increases observed for the expression of SRB1 and the EGFR still led to expression levels far lower than those observed in Huh 7.5 cells.

4.6 Modifications of HepOrg HCV infection

The low expression of the EGFR on the HepOrgs led to the hypothesis, that the downregulation of the EGFR on hepatocyte organoids caused by high concentrations of EGF in the medium might contribute to the lack of detectable HCV infection in HepOrgs. The infection protocol was therefore modified to test this hypothesis. The organoids were cultured in medium without EGF for from two days prior to infection onwards, to increase surface EGFR expression. The observed increase in EGFR expression was larger after more than two days of culture without EGF (Figure 18), but removal of EGF from the medium had previously been shown to dampen organoid proliferation (Hu et al. 2018). Therefore two days without EGF in the medium prior to the incubation with the virus was chosen. Furthermore, another pharmaceutical intervention was tested. The tank binding kinase 1 (TBK1) inhibitor BX-795 had previously been shown to enhance HCV infection in human fetal liver cells (HFLCs) in vitro, by dampening the cells innate immune response to infection (Catanese et al. 2013). It was therefore added to the culture one day prior

to incubation with the virus, to investigate whether it would facilitate infection of the HepOrgs used in this study. Additionally, a MOI of 2 instead of one was tested in organoids derived from one donor.

The modifications of the infection protocol did not lead to a detectable infection of the hepatocyte organoids. For organoids derived from two donors, that were incubated with the virus at an MOI of 1, neither the organoids treated with ruxolitinib nor those treated with BX-795 expressed the HCV core protein 72 hours after incubation with the virus.

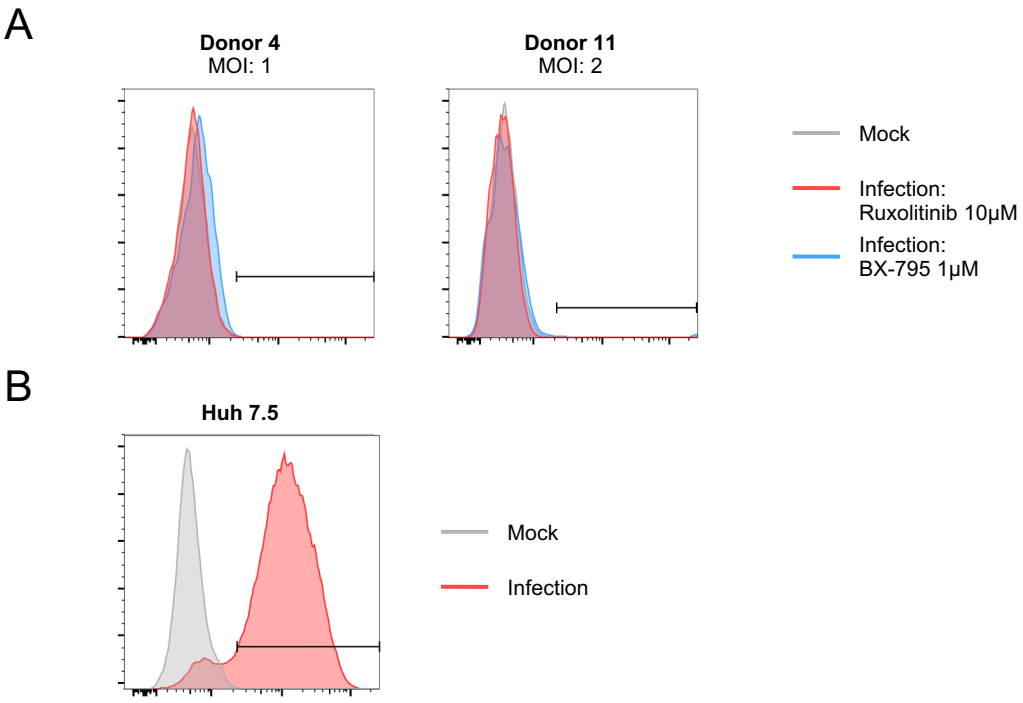

Figure 19: HepOrg HCV infection using modified infection protocol. The organoids were cultured in medium without EGF from two days before the infection onwards. HCV core protein expression was assessed 72 hours after inoculation with the virus. (A) HepOrgs were incubated with HCV at different MOI of 1 (n = 2, only one shown) or 2 (n = 1). Histograms show comparison between the mock infected condition (grey) and the infection conditions treated with 10 µM ruxolitinib (red) or BX-795 (blue). (B) Huh 7.5 cell line HCV infection as positive control.

This was also observed for organoids derived from one donor that were incubated with the virus at a higher MOI of 2 (Figure 19A). The lack of HCV core protein expression stood in contrast to the Huh 7.5 cell line used as positive control, where 90.7% of the cells expressed the HCV core protein after 72 hours (Figure 19B).

The lack of detectable HCV infection after modified infection protocols led to the conclusion that HepOrgs cultured as described (Hu et al. 2018), could not be infected with cell culture produced HCV (P100).

As an alternative to cell culture produced virus, plasma from HCV infected patients can be used to infect hepatocytes in vitro (Gondeau et al. 2014). To investigate whether the lack of infection in the HepOrgs might be caused by using cell culture produced and adapted virus, plasma from three different HCV infected individuals was used instead of P100. The organoids were cultured with HepM supplemented with dexamethasone and oncostatin M (1 µM and 10 ng/ml) for the week prior to incubation with the virus. Medium without EGF was used from two days before incubation with the virus onwards and all organoids were pretreated with 10 µM ruxolitinib.

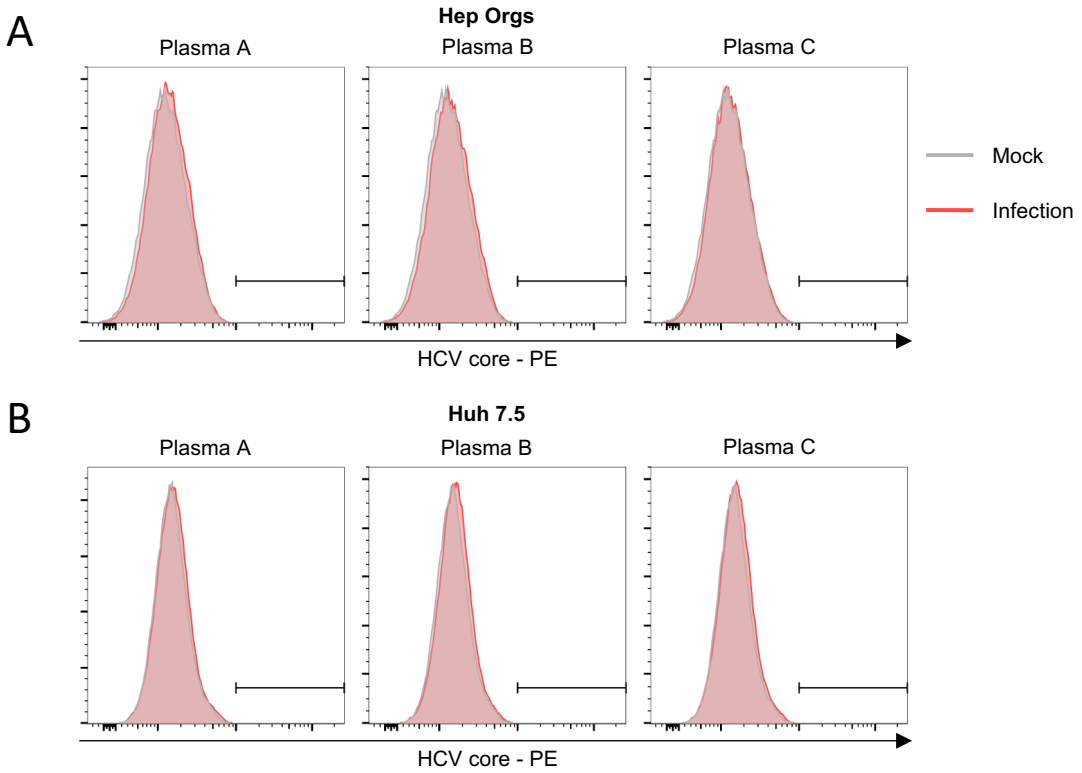

Figure 20: HepOrg and Huh 7.5 cell line infection with patient derived virus. HepOrgs and the Huh 7.5 cell line were incubated with plasma from three different patients infected with HCV. (A) Representative histograms for HepOrgs derived from one exemplary donor (n = 3) comparing the expression of HCV core protein between mock infected condition (grey) and the patient plasma condition (red). (B) Comparison between the HCV core protein expression for Huh 7.5 cells inoculated with mock virus (grey) and patient plasma (red) from three different patients.

Figure 20 shows that the use of patient derived virus instead of cell culture produced virus did not lead to a detectable infection of the organoids 72 hours after incubation with the virus. All organoids derived from the three donors tested did not express the HCV core protein after incubation with plasma derived from three different patients. In contrast to the previous experiments with cell culture derived virus, there was no detectable infection of the Huh 7.5 cells either.

Collectively, the data presented here indicates that hepatocyte organoids derived from adult human liver tissue and cultured as previously described (Hu et al. 2018) could not be infected with the hepatitis C virus.

5 Discussion

After the discovery of HCV as a hepatotropic virus in 1989, advances in the understanding of the novel pathogen were slowed down by a lack of available in vitro models and suitable in vivo models. The only available in vivo model in chimpanzees was very laborious and costly and has since been stopped for ethical concerns. The introduction of in vitro infection models of HCV in the Huh 7 cell line was a breakthrough in HCV research which has helped our understanding of the virus significantly and ultimately also aided the development of effective antiviral therapies. Since then, other in vitro models for the study of HCV have been introduced with PHH and HLCs also being used in HCV research. All the different cell types that are used for in vitro infection with HCV have advantages and disadvantages and are not equally suitable for every field of research. The Huh 7.5 cell line for example is highly susceptible to HCVcc infection in vitro, but its defects in genes related to innate immunity result in an immune response to infection that is very dissimilar to that of mature hepatocytes (Tegtmeyer et al. 2021). Therefore, the Huh 7.5 cell line is not very well suited for investigating immunological questions, for which the cells' innate immune response to viral infection would need to be intact. Hepatocyte organoids are a novel method of culturing patient derived primary cells in vitro in a three-dimensional structure (Hu et al. 2018). The organoids can be kept in culture for several weeks, which is longer than PHH whose functional life span in vitro is very limited (Gomez-Lechon et al. 2014). As HCV is a chronic infection in vivo it would be interesting to develop an in vitro model based on primary adult liver tissue that could be infected with HCV for extended periods of time in vitro. This study therefore investigated whether hepatocyte organoids could be infected with HCV.

5.1 Hepatocyte organoids express essential proteins for viral cell entry

Several proteins have been identified to be essential for the entry of the HCV virion into host cells. The tight junction proteins occludin and claudin-1, the tetraspanin CD81 and the scavenger receptor SRB1 are all implicated in the entry process of HCV into host cells. In this study, the expression of these proteins in HepOrgs was investigated as a first step to assess whether the HepOrgs could be infected with HCV. HepOrgs did in fact express all four proteins investigated, as was observed

by immunofluorescence microscopy of entire three-dimensional organoids. As a control to ensure that the immunofluorescence signal obtained was specific for the respective proteins and not caused by the secondary antibodies directly, secondary antibody only controls were used and compared to the full staining with primary and secondary antibodies. The direct comparison clearly demonstrated that the signals in the immunofluorescence images were not caused by the secondary antibodies directly and are therefore specific for the respective proteins.

Both occludin and claudin-1 exhibited a polarized pattern of expression within the organoids, with both proteins being expressed on the cell membranes towards the lumen of the organoid. This polarized pattern of expression is comparable to that observed in hepatocytes in vivo, where claudin-1 and occludin are expressed on the apical cell membrane (Mensa et al. 2011).

The lumina of the HepOrgs would in this case resemble bile canaliculi in vivo, which are formed by the apical cell membrane of hepatocytes. The formation of bile canaliculi in HepOrgs has been described previously, with the expression of the canalicular transporter protein ATP binding cassette subfamily C member 2 (MRP2) towards the lumen of HepOrgs (Hu et al. 2018). Furthermore, this polarized pattern of occludin and claudin-1 expression has also previously been described in Huh 7 cells when those are grown as three-dimensional spheroids (Molina-Jimenez et al. 2012). The expression pattern of claudin-1 and occludin within the HepOrgs was therefore comparable both to the physiological in vivo conditions and established three-dimensional in vitro infection models of HCV infection. CD81 and SRB1 were expressed within the organoids as well, but their pattern of expression was not as polarized as for the tight junction proteins.

In addition to the immunofluorescence analysis of protein expression within the hepatocyte organoids, gene expression of the respective proteins was assessed and compared to PHH. As was to be expected for proteins that were expressed in the organoids, the mRNA of the respective genes was also detected, giving evidence of transcription of the genes within the HepOrgs. The relative mRNA expression levels were considerably lower for claudin-1, SRB1 and CD81 in the organoids compared to PHH. This indicated that these genes were transcribed at lower levels in HepOrgs than in PHH, which could also result in lower levels of protein expression. In contrast, the relative occludin expression was even higher in HepOrgs derived from some donors than in the PHH used as a comparison.

However, the expression of occludin varied a lot more among organoids derived from different donors than for the other genes investigated. The reason for this variability remained unclear and increasing the sample size would be necessary to verify these results.

5.2 Flow cytometry can be used to identify HCV infected cells in the Huh 7.5 cell line

Different methods are used to investigate whether cells in vitro are infected with HCV. Among the most widely used methods are RT-PCR, immunofluorescence and TCID50 titrations. RT-PCR is used to detect viral RNA, while immunofluorescence is used to detect the expression of viral proteins within host cells. TCID50 titrations of the culture supernatant detect infectious virions in the supernatant. In addition to those methods, flow cytometry analysis after staining for viral proteins can also be used to assess cells for viral infection with HCV (Kang et al. 2014). It offers the advantage, that the fraction of infected cells can easily be determined, and large numbers of cells can be assessed in relatively short periods of time. Furthermore, the expression of multiple other proteins can be investigated at the same time on the same cells, which would enable for instance investigating the impact of HCV infection on the expression of immune cell ligands on infected cells.

To establish a flow cytometry based readout that could be used for assessing HCV infection the HepOrgs, it was tested using the Huh 7.5 cell line, which is highly susceptible to HCV infection in vitro (Wakita 2019). In this study, the flow cytometry-based readout for HCV infection in the Huh 7.5 cell line in fact allowed to clearly discriminate between HCV infected and uninfected cells. Expression of the HCV core protein was assessed using a primary anti-HCV core protein antibody and a secondary antibody labeled with a fluorochrome. The mock infected control indicated the level of background fluorescence in uninfected Huh 7.5 cells and was used as a comparison to the conditions that were inoculated with the virus. The fluorescence signal obtained for the HCV core protein was core protein specific, as a secondary antibody only control ensured it was not caused directly by the secondary antibody. An unpermeabilized control, where the cells were not permeabilized prior to incubation with the antibodies, was used to ensure that the signal obtained was caused by intracellular expression of the viral protein. The marked reduction in the fluorescence signal intensity observed for the

unpermeablized control proved that in fact most of the HCV core antigen was expressed intracellular, as was to be expected for a viral protein that is translated in the cytosol of the host cell.

The infection rates of two different HCV strains, Jc1 and P100, were compared in the Huh 7.5 system. P100 yielded infection rates that were a lot higher than for Jc1, even when added to the cells at a lower MOI than Jc1. This is likely a manifestation of the higher infectivity and reproductive fitness of P100 that has been described before (Perales et al. 2013, Sheldon et al. 2014).

5.3 Hepatocyte organoids cannot be infected with HCV

To investigate whether the hepatocyte organoids could be infected with HCV, the virus was added to the supernatant of grown organoids embedded in their extracellular matrix. 72 hours after the incubation with the virus, there was no detectable expression of the HCV core protein within the organoids, as the protein signal for the organoids incubated with the virus did not differ from the mock infected controls in flow cytometric analysis. This indicated that the organoids were not infected with HCV. The Huh 7.5 cell line was used as a positive control for infection and incubated with the same batch of virus as the organoids. The infection observed in the Huh 7.5 cells proves that the lack of detectable infection in the organoids was not caused by a lack of viable infectious virus in the viral stock used for the inoculation of the cells. Therefore, the lack of detectable infection observed in the organoids compared to the Huh 7.5 cells could either be caused by inherent differences between the cells or by differences in the inoculation conditions of the cells with the virus.

These differences during the incubation with the virus are due to disparities in the cell culturing conditions between the HepOrgs and the Huh 7.5 cell line. The Huh 7.5 cells grow in a two-dimensional monolayer and, unlike the organoids, are not embedded in extracellular matrix in vitro. In contrast to the organoids, the Huh 7.5 cell line is less polarized when grown as a monolayer, as they do not form tight junctions (Mee et al. 2008). Cellular polarity had previously been shown to play a role in HCV infection in vitro, with infection rates differing at different levels of polarization. In the human liver cancer cell line HepG2 transfected with CD81 (HepG2-CD81), reducing cellular polarity, and disrupting tight junction integrity

increased HCV entry into the cells (Mee et al. 2009). Decreases in susceptibility to HCV infection, with the increasing polarization during the time in cell culture, have also been observed in PHH (Gondeau et al. 2014). For the PHH, trypsinization of the polarized cells, which was used as a method of disrupting polarization, recovered the permissiveness to HCV infection.

Therefore, modifications of the organoid incubation with the virus were tested in this study, to investigate whether the lack of infection might be caused by either the extracellular matrix or the high level of polarization of the HepOrgs. To test this hypothesis, the organoids were removed from their extracellular matrix and put in suspension for the incubation with the virus or were trypsinized to single cells before incubation with the virus. Both modifications of the infection conditions had no effect on the level of HCV core protein expression within the organoids after 72 hours, as there was no detectable HCV core protein expression in any of the organoids derived from any of the different donors that were tested. This indicated that the lack of detectable HCV infection was neither caused by their extracellular matrix nor by their high level of polarization.

In fact, Huh 7 and Huh 7.5 cells can also be infected with HCV in vitro when cultured as three-dimensional polarized spheroids whose structure is similar to that of the HepOrgs (Molina-Jimenez et al. 2012, Baktash et al. 2018). Therefore, the lack of HCV infection within the organoids was likely caused by inherent differences between the organoid cells and susceptible cells such as the Huh 7.5 cell line and not just by differences in the cell culturing conditions between those cells.

5.4 Hepatocyte organoids express key proteins implicated in viral entry at lower levels than the Huh 7.5 cell line

While the hepatocyte organoids expressed key proteins, that are essential for viral entry of HCV into host cells, they might not have expressed enough of the proteins to allow viral entry into the cells and facilitate infection. Therefore, the expression of key proteins that are important for viral entry into cells was compared between the Huh 7.5 cell line and the HepOrgs.

The HepOrgs expressed considerably less SRB1, EGFR and CD81 than the Huh 7.5 cell line. While expression of all three proteins was universal in the Huh 7.5 cell line, not all cells within the organoids expressed these proteins and the level of protein expression was strikingly lower than in the Huh 7.5 cell line. The lack of any

SRB1, EGFR or CD81 expression on some of the organoid cells indicated that the cultures contained a heterogenous cell population. All three proteins are expressed on mature hepatocytes, therefore the lack of expression on some cells indicated either dedifferentiation in vitro or the presence of different cell types within the culture.

Sufficient protein expression of entry receptors on host cells is essential for cells to be susceptible to HCV infection in vitro. A relationship between the susceptibility to HCV infection and the amount of protein expression on the target cells has been clearly described for CD81 before. HepG2 cells only become susceptible to HCV infection when transfected with CD81 (Zhang et al. 2004). In the Huh 7 cell line, variations of susceptibly to HCV infection have been observed among different subclones with varying levels of CD81 expression (Akazawa et al. 2007). Susceptibility to infection in clones with little CD81 expression could be rescued by transfecting them with CD81. Silencing of CD81 expression using siRNA in clones with high levels of CD81 expression led to lower levels of infection. In contrast, variations in the level of SRB1 expression in the different clones did not have an impact on susceptibility to HCV infection. Similarly Koutsoudakis et al. (2007) described a minimal threshold of CD81 expression on Huh 7.5 cells that was necessary to allow HCV infection. A relatively high level of CD81 expression was a key factor to allow productive infection of host cells with HCV.

It is therefore tempting to speculate, that the markedly lower levels of CD81 expression on the HepOrgs compared to the Huh 7.5 cell line might be a reason for why the organoids could not be infected with HCV. To test this hypothesis, the organoids could be transfected with CD81 to investigate whether higher levels of CD81 expression render them susceptible to infection.

5.5 Expression of SRB1 and EGFR is increased on HepOrgs using modified culture medium

Due to the low levels of expression of key proteins that are important for viral entry into host cells on the hepatocyte organoids, this study investigated whether modifications of the culture medium could increase the expression of CD81, SRB1 and EGFR. While none of the modifications tested influenced the expression of CD81 on the HepOrgs, the expression of SRB1 and EGFR was altered by modifications of the medium. SRB1 expression on the organoids was increased

when the culture medium was supplemented with dexamethasone and OSM. OSM in combination with dexamethasone had previously been shown to increase the expression of markers of hepatic differentiation in murine and human fetal hepatocytes in vitro (Kamiya et al. 2001, Chinnici et al. 2015). This increase in SRB1 expression upon stimulation of the organoids with dexamethasone and OSM could therefore be a manifestation of an increase in hepatic differentiation of the organoids, as SRB1 is expressed at high levels hepatocytes. Still, the increase in SRB1 expression observed in the organoid cultures supplemented with dexamethasone and OSM was only very modest compared to the organoids cultured under standard conditions. The level of SRB1 expression remained much lower than in the Huh 7.5 cell line.

EGFR expression on the organoids was increased upon removal of its ligand, EGF, from the culture medium. It was expressed at higher levels the longer the organoids were cultured in medium that did not contain EGF.

The low expression of EGFR on the HepOrgs using standard culture medium was therefore caused by the high concentrations of EGF in the culture medium. Downregulation of the EGFR in cells cultured with high concentrations of EGF in the medium had been described before (Sigismund et al. 2008). When cells were cultured with high concentrations of EGF in the medium, the EGFR was more likely to be degraded as opposed to recycled upon receptor internalization, which decreased the EGFR expression. The concentration of EGF in the HepM in this study was even considerably higher than the highest concentration used by Sigismund et al. (2008). This study demonstrated that the high concentrations of EGF in the HepOrg culture medium led to a marked downregulation of the EGFR cell surface of the organoids. This downregulation was then reversed by removing EGF from the medium, which consequently led to an increase in the surface EGFR expression on the organoids.

Despite the effect the removal of EGF from the medium had on the EGFR expression on the organoids, its removal from the medium also has an impact on organoid growth. This was not investigated in this study, but previous research has highlighted the importance of EGF for hepatocyte organoid generation (Hu et al. 2018). Organoid proliferation was reduced in the absence of EGF in the culture

medium and fewer organoids were formed for the same number of cells initially seeded.

5.6 Hepatocyte organoids cannot be infected with HCV using patient derived virus

Instead of using cell culture derived HCV, such as P100 or Jc1, patient derived virus can also be used for in vitro infections (Fournier et al. 1998). In this study, the use of patient plasma from chronically infected patients instead of cell culture produced P100 did not lead to a detectable infection of the hepatocyte organoids. In contrast to previous experiments where cell culture derived P100 was used, the patient plasma derived HCV could not infect the Huh 7.5 cells either. This lack of infection in the Huh 7.5 cell line using patient plasma illustrates one challenging aspect of in vitro infections with HCV. Until now, JFH1 remains the only viral isolate directly from a patient that can infect Huh 7 cells and its descendants in vitro without further adaptive mutations (Wakita 2019). This indicates that, although the Huh 7 cell lines and its descendant are highly susceptible to infections with chimeric viruses that are adapted to their host cells in the laboratory, they cannot easily be infected with the broad spectrum of genetically diverse viruses that occur in vivo. Due to the lack of detectable viral infection in the Huh 7.5 cell line using patient plasma, there was no positive control that proved the infectivity of the plasma. Therefore, despite high levels of viraemia measured in the patient plasma, it is not certain, that the patient plasma contained infectious HCV virions.

In addition to the incubation with patient plasma, other variations of the infection conditions for the HepOrgs using P100 did not result in a detectable level of HCV infection within the organoids. Neither using a modified culture medium to increase EGFR and SRB1 expression nor the use of BX-795, as an alternative to ruxolitinib to inhibit the organoids' immune response to infection, led to a detectable level of HCV infection of the HepOrgs.

5.7 Strengths and limitations

This study investigated whether hepatocyte organoids derived from adult human liver tissue could be infected with HCV. It has several strengths and limitations that are important to take into consideration when interpreting the findings of this study.

To assess whether the organoid cells were infected with HCV, a flow cytometry readout for HCV infection was established. It was validated using the Huh 7.5 cell line as a reliable model of in vitro HCV infection. Detection of the HCV core antigen using flow cytometry allowed to clearly discriminate between HCV infected and uninfected cell populations in the Huh 7.5 cell line. This is in accordance with the previous use of flow cytometry to detect HCV infection within cells (Kang et al. 2014). The use of the Huh 7.5 cell line as positive control for all infection experiments with the hepatocyte organoids ensured that the virus used was viable for infection. The lack of detectable HCV core protein expression within any of the organoids incubated with HCV in this study led to the conclusion that there was no robust infection of any of the HepOrgs.
Additional RT-qPCR analysis of the organoids, as a very sensitive method for detecting viral RNA, would further allow to exclude that the organoids were infected with HCV at very low levels. As only flow cytometry was used to assess the cells for viral infection in this study, it cannot be excluded that the organoids were infected with HCV at very low levels and the cells expressed only very little to no viral protein. In this case, the flow cytometry readout might not be sensitive enough to detect the infection.

The hepatocyte organoids are a novel method of culturing adult human liver tissue derived cells in vitro for extended time periods and in a three-dimensional structure. In this study, one recurrent issue arose during the culture of the hepatocyte organoids in vitro. Within the culture of the hepatocyte organoids, growth of larger, cystic, ductal-like organoids was observed in addition to the smaller HepOrgs, as can be observed in figure 6. The ductal-like organoids could easily be identified during the regular observation of the organoid cultures with a bright field microscope, as their morphology is clearly distinct from that of HepOrgs. Ductal-like organoid growth within cultures of hepatocyte organoids has been described previously for organoids derived from fetal liver tissue (Hendriks et al. 2021). Yet the extent of ductal-like organoid growth within the organoid cultures in this study seemed to be a lot larger. Compared to single ductal-like organoids depicted in their cultures, the ductal-like organoids appeared to grow faster than the HepOrgs in some of the organoid cultures used in this study. In some cultures, those ductal-like organoids constituted the majority of the organoids. There was some donor-to-donor

variation regarding the extent of the ductal-like organoid growth within the cultures, with some growing less and others more. Yet, ductal-like organoids grew in all organoid cultures derived from all different donors that were used during this study. The extent of ductal-like organoid growth increased with the passage number, therefore only organoid cultures up to passage 3 were used for all experiments. Additionally, donors with lower proportions of ductal-like organoids within the HepOrg cultures were used for the experiments.

Hendriks et al. (2021) described two methods to reduce the growth of ductal-like organoids within the hepatocyte organoid cultures. The first was to remove visible biliary structures during preparation of the tissue samples before organoid culture, as a preventive measure. For ductal-like organoids that grew within an organoid culture, manual removal was recommended as a method to keep the hepatocyte organoid culture pure. For the liver tissue that was obtained from surgery in this study, it proved impossible to visually identify any biliary structures within the sample during tissue preparation, therefore those structures could not be removed from the samples. Additionally, manually picking and removing ductal-like organoids from the culture seemed futile, as the cultures contained too many ductal-like organoids for this method to be feasible.
Due to the narrow tissue tropism of HCV focused on human hepatocytes, the substantial growth of ductal-like organoids within the cultures was problematic, as these might not be susceptible to HCV infection. Further characterizations of the organoid cultures would be needed to investigate the differences in gene and protein expression between the HepOrgs and the ductal-like organoids growing in the same cultures.

Hepatocyte organoids derived from adult human liver tissue in vitro are a method that is not yet widely available and is used in few laboratories only. Extensive characterizations of the organoids were performed and published by Hu et al. (2018). The organoid cultures in this study were established and maintained as described in that publication, but the phenotype of the organoids could still differ. No extensive characterization of the phenotype of the HepOrgs used in this study were performed, such as investigating the protein expression of hepatocyte markers or single-cell transcriptomic analysis. Therefore, it is unknown whether the phenotype

of the organoids used in this study resembles the phenotype of human adult hepatocytes as closely as was described previously. Not all reagents used in this study were identical to those used by Hu et al. (2018). This is especially critical for RSPO1, which was homemade in both cases and produced in HEK293T-HA-Rspo1-Fc cells as described previously (Broutier et al. 2016). This production of RSPO1 in a cell line might lead to differences in the concentration of RSPO1 in the HepOrg culture medium, as the concentration of RSPO1 in the supernatant of the HEK293T-HA-Rspo1-Fc cells was not measured during this study. RSPO1 is a critical component of the culture medium for the HepOrgs. When it is removed from the medium, barely any HepOrgs form at all (Hu et al. 2018). Slight variations in concentration in the medium might therefore ultimately influence the proliferation and the phenotype of the organoids. Due to the lack of measurements of the RSPO1 concentration in the HepOrg medium used in this study, it is possible that the concentration varied from the RSPO1 concentration in the HepOrg medium used by Hu et al. (2018), even though the same protocols were used for the RSPO1 production.

This lack of established and standardized protocols and reagents in the organoid field is a key reason why directly comparing results from different studies is often difficult (Marsee et al. 2021). Different approaches for generating and culturing organoids with a hepatocyte phenotype and a lack of a consistent nomenclature further aggravate this issue.

In contrast to previous studies on organoids with a hepatocyte phenotype, Hu et al. (2018) used no specific differentiation medium to increase the differentiation of the HepOrgs generated from adult liver tissue. Previous studies on organoids with a hepatocyte phenotype, that were derived from ductal epithelial cells (Huch et al. 2015, Broutier et al. 2016), used expansion medium for the generation and expansion of the organoids, followed by a differentiation medium to induce a phenotype that resembles that of mature hepatocytes more closely. Still, Hu et al. (2018) described higher levels of hepatocyte marker expression using the novel culturing conditions compared to the expansion and subsequent hepatic differentiation of ductal epithelial organoids. In this study, no differentiation medium was used to induce hepatic differentiation of the organoids. Yet, extensive growth of ductal-like organoids was observed within the HepOrg cultures during this study.

Therefore, it would be interesting to investigate whether the use of hepatic differentiation medium could increase HepOrg differentiation of the cultures and reduce the growth of ductal-like organoids within the cultures.

Different studies have described different methods to generate organoids with a hepatic phenotype from adult liver tissue in vitro (Huch et al. 2015, Hu et al. 2018, Peng et al. 2018). These organoids vary regarding their culturing conditions and organoid phenotype and, as this study only generated hepatocyte organoids as described by one publication, no generalized conclusions can be drawn on whether hepatocyte organoids generated using different culturing conditions can be infected with HCV. Interestingly, organoids derived from ductal epithelial cells and differentiated towards a hepatocyte phenotype have already successfully been infected with HBV in vitro (De Crignis et al. 2021). Therefore, it would be interesting to investigate whether those organoids are also permissive to HCV infection.

5.8 Outlook

The objective of this thesis was to establish a novel in vitro cell culture model for HCV infection using hepatocyte organoids. Collectively, the data presented showed that the hepatocyte organoids generated in this study could not be infected with HCV.

This work demonstrated, that HepOrgs expressed key proteins that are essential for viral entry into host cells, but the level of protein expression was markedly lower than in a cell line that is susceptible to HCV infection in vitro.

Previous studies have demonstrated that a critical threshold for CD81 expression is needed on cells to be susceptible to HCV infection in vitro (Akazawa et al. 2007, Koutsoudakis et al. 2007). In conjunction with the observation that HepOrgs expressed CD81 at distinctly reduced levels compared to the susceptible Huh 7.5 cell line, it is tempting to speculate that low expression levels CD81 on the HepOrgs could contribute to the lack of detectable HCV infection in the organoids.

Still, the data presented in this study does not allow to draw a definitive conclusion for why the HepOrgs could not be infected with HCV. A lower level of CD81 is only one of many differences between the HepOrgs and the Huh 7.5 cell line, therefore there could also be other reasons for the lack of infection in the organoids.

It remains unclear, which step of the viral life cycle could not be performed within the hepatocyte organoids.

One important factor that limits HCV infection in vitro in both PHH and HLCs is the upregulation of interferon stimulated genes (ISGs) activating antiviral defense mechanisms (Carpentier et al. 2020, Tegtmeyer et al. 2021). Treatment with a JAK-STAT pathway inhibitor increased infection rates and the duration of infection in both systems. The HepOrgs in this study were also treated with ruxolitinib, a JAK-STAT pathway inhibitor, therefore it is unlikely that the infection was solely prevented by the upregulation of antiviral genes. Still, it would be interesting to characterize HepOrgs in regard of their expression of antiviral genes and observe whether there are changes in gene expression upon incubation with the virus.

Primary human hepatocytes are susceptible to HCV infection in vitro. As the hepatocyte organoids were generated from primary human adult liver tissue, the same liver tissue could also be used for the culture and subsequent infection of PHH in vitro. A direct comparison of PHH and HepOrgs generated from the same liver tissue could lead to a better understanding for why the HepOrgs could not be infected with HCV in vitro. Furthermore, a step-by-step approach examining the organoids susceptibility to HCV infection at different time points after the beginning of culture in organoids specific medium could provide critical insights into possible dedifferentiation processes within the organoids, that might prevent HCV infection in vitro.

Despite the existence of very effective drugs that can cure almost any patient of their HCV infection, hundreds of thousands of people are still dying each year as a consequence of liver disease arising from chronic HCV infection (Stanaway et al. 2016). In the absence of an effective prophylactic vaccine and with many millions of people chronically infected with HCV around the globe, the global burden of disease caused by HCV will remain high in the foreseeable future. The development of novel, more physiological in vitro models of HCV infection could be critical to further ameliorate our understanding of the virus and lead to advances in the understanding of the pathophysiology of liver disease caused by HCV. Whether further improvements in culturing hepatocyte organoids in vitro may render them a suitable model for HCV infection, remains to be elucidated.

6 Abstract

Chronic HCV infection is one of leading causes of chronic liver disease globally and results in hundreds of thousands of deaths each year. Despite the introduction of efficient antiviral drugs a decade ago, global morbidity and mortality caused by HCV will remain high for the foreseeable future.

Cell culture models, based on cell lines or primary cells, are the mainstay of HCV research. Hepatocyte organoids are a novel cell culture technique that allows to grow hepatocytes in a three-dimensional system for extended periods of time in vitro. The major aim of this thesis was to test, whether hepatocyte organoids could provide a suitable in vitro model of HCV infection. During this study, hepatocyte organoids were generated from healthy adult liver tissue and kept in culture for multiple weeks. The hepatocyte organoids were not susceptible to HCV infection in vitro. Key proteins that are necessary for viral entry into host cells were expressed at markedly lower levels in hepatocyte organoids than in a cell line susceptible to HCV infection. This study highlights key obstacles of working with hepatocyte organoids, with variances in organoid phenotype and the growth of ductal-like organoids within the hepatocyte organoid cultures.

6.1 Zusammenfassung

Eine chronische HCV-Infektion ist eine der häufigsten Ursache für chronische Lebererkrankungen weltweit und führt zu hunderttausenden Todesfällen jährlich. Trotz der Verfügbarkeit effektiver antiviraler Therapien seit etwa 10 Jahren, wird die von HCV verursachte Morbidität und Mortalität in der nahen Zukunft weiter hoch bleiben.

Zellkulturmodelle, basierend auf Zelllinien oder humanen Primärzellen, sind ein Eckpfeiler der HCV-Forschung. Hepatozyten Organoide sind eine neue Zellkultur Methodik, welche es erlaubt, Hepatozyten für längere Zeiträume in einer dreidimensionalen Kultur in vitro zu kultivieren. Das Ziel dieser Arbeit war es zu testen, ob Hepatozyten Organoide ein mögliches in vitro Modell für HCV-Infektion darstellen. In dieser Studie wurden Hepatozyten Organoide generiert und über mehrere Wochen in Kultur gehalten. Die Hepatozyten Organoide waren nicht empfänglich für eine Infektion mit HCV in vitro. Proteine, welche essenziell für den Eintritt von HCV in Zellen sind waren auf den Organoiden deutlich weniger exprimiert als auf einer Zelllinie, die empfänglich für HCV ist. Diese Arbeit hebt

wichtige Hürden der Arbeit mit Hepatozyten Organoiden hervor, mit Varianzen im Phänotyp der Organoide sowie dem Wachstum von Organoiden mit einem biliären Phänotyp innerhalb der Kulturen.

7 References

Acton, S., A. Rigotti, K. T. Landschulz, S. Xu, H. H. Hobbs and M. Krieger (1996). "Identification of scavenger receptor SR-BI as a high density lipoprotein receptor." Science **271**(5248): 518-520.

Agnello, V., G. Abel, M. Elfahal, G. B. Knight and Q. X. Zhang (1999). "Hepatitis C virus and other flaviviridae viruses enter cells via low density lipoprotein receptor." Proc Natl Acad Sci U S A **96**(22): 12766-12771.

Akazawa, D., T. Date, K. Morikawa, A. Murayama, M. Miyamoto, M. Kaga, H. Barth, T. F. Baumert, J. Dubuisson and T. Wakita (2007). "CD81 expression is important for the permissiveness of Huh7 cell clones for heterogeneous hepatitis C virus infection." J Virol **81**(10): 5036-5045.

Albecka, A., S. Belouzard, A. Op de Beeck, V. Descamps, L. Goueslain, J. Bertrand-Michel, F. Terce, G. Duverlie, Y. Rouille and J. Dubuisson (2012). "Role of low-density lipoprotein receptor in the hepatitis C virus life cycle." Hepatology **55**(4): 998-1007.

Alter, H. J., P. V. Holland, A. G. Morrow, R. H. Purcell, S. M. Feinstone and Y. Moritsugu (1975). "Clinical and serological analysis of transfusion-associated hepatitis." Lancet **2**(7940): 838-841.

Arafa, N., M. El Hoseiny, C. Rekacewicz, I. Bakr, S. El-Kafrawy, M. El Daly, S. Aoun, D. Marzouk, M. K. Mohamed and A. Fontanet (2005). "Changing pattern of hepatitis C virus spread in rural areas of Egypt." J Hepatol **43**(3): 418-424.

Bailey, J. R., E. Barnes and A. L. Cox (2019). "Approaches, Progress, and Challenges to Hepatitis C Vaccine Development." Gastroenterology **156**(2): 418-430.

Baktash, Y., A. Madhav, K. E. Coller and G. Randall (2018). "Single Particle Imaging of Polarized Hepatoma Organoids upon Hepatitis C Virus Infection Reveals an Ordered and Sequential Entry Process." Cell Host Microbe **23**(3): 382-394 e385.

Barker, N., J. H. van Es, J. Kuipers, P. Kujala, M. van den Born, M. Cozijnsen, A. Haegebarth, J. Korving, H. Begthel, P. J. Peters and H. Clevers (2007). "Identification of stem cells in small intestine and colon by marker gene Lgr5." Nature **449**(7165): 1003-1007.

Barth, H., C. Schafer, M. I. Adah, F. Zhang, R. J. Linhardt, H. Toyoda, A. Kinoshita-Toyoda, T. Toida, T. H. Van Kuppevelt, E. Depla, F. Von Weizsacker, H. E. Blum and T. F. Baumert (2003). "Cellular binding of hepatitis C virus envelope glycoprotein E2 requires cell surface heparan sulfate." J Biol Chem **278**(42): 41003-41012.

Bartosch, B., J. Dubuisson and F. L. Cosset (2003). "Infectious hepatitis C virus pseudo-particles containing functional E1-E2 envelope protein complexes." J Exp Med **197**(5): 633-642.

Blach, S., S. Zeuzem, M. Manns, I. Altraif, A.-S. Duberg, D. H. Muljono, I. Waked, S. M. Alavian, M.-H. Lee, F. Negro, F. Abaalkhail, A. Abdou, M. Abdulla, A. A. Rached, I. Aho, U. Akarca, I. Al Ghazzawi, S. Al Kaabi, F. Al Lawati, K. Al Namaani, Y. Al Serkal, S. A. Al-Busafi, L. Al-Dabal, S. Aleman, A. S. Alghamdi, A. A. Aljumah, H. E. Al-Romaihi, M. I.

Andersson, V. Arendt, P. Arkkila, A. M. Assiri, O. Baatarkhuu, A. Bane, Z. Ben-Ari, C. Bergin, F. Bessone, F. Bihl, A. R. Bizri, M. Blachier, A. J. Blasco, C. E. B. Mello, P. Bruggmann, C. R. Brunton, F. Calinas, H. L. Y. Chan, A. Chaudhry, H. Cheinquer, C.-J. Chen, R.-N. Chien, M. S. Choi, P. B. Christensen, W.-L. Chuang, V. Chulanov, L. Cisneros, M. R. Clausen, M. E. Cramp, A. Craxi, E. A. Croes, O. Dalgard, J. R. Daruich, V. de Ledinghen, G. J. Dore, M. H. El-Sayed, G. Ergör, G. Esmat, C. Estes, K. Falconer, E. Farag, M. L. G. Ferraz, P. R. Ferreira, R. Flisiak, S. Frankova, I. Gamkrelidze, E. Gane, J. García-Samaniego, A. G. Khan, I. Gountas, A. Goldis, M. Gottfredsson, J. Grebely, M. Gschwantler, M. G. Pessôa, J. Gunter, B. Hajarizadeh, O. Hajelssedig, S. Hamid, W. Hamoudi, A. Hatzakis, S. M. Himatt, H. Hofer, I. Hrstic, Y.-T. Hui, B. Hunyady, R. Idilman, W. Jafri, R. Jahis, N. Z. Janjua, P. Jarčuška, A. Jeruma, J. G. Jonasson, Y. Kamel, J.-H. Kao, S. Kaymakoglu, D. Kershenobich, J. Khamis, Y. S. Kim, L. Kondili, Z. Koutoubi, M. Krajden, H. Krarup, M.-s. Lai, W. Laleman, W.-c. Lao, D. Lavanchy, P. Lázaro, H. Leleu, O. Lesi, L. A. Lesmana, M. Li, V. Liakina, Y.-S. Lim, B. Luksic, A. Mahomed, M. Maimets, M. Makara, A. O. Malu, R. T. Marinho, P. Marotta, S. Mauss, M. S. Memon, M. C. M. Correa, N. Mendez-Sanchez, S. Merat, A. M. Metwally, R. Mohamed, C. Moreno, F. H. Mourad, B. Müllhaupt, K. Murphy, H. Nde, R. Njouom, D. Nonkovic, S. Norris, S. Obekpa, S. Oguche, S. Olafsson, M. Oltman, O. Omede, C. Omuemu, O. Opare-Sem, A. L. H. Øvrehus, S. Owusu-Ofori, T. S. Oyunsuren, G. Papatheodoridis, K. Pasini, K. M. Peltekian, R. O. Phillips, N. Pimenov, H. Poustchi, N. Prabdial-Sing, H. Qureshi, A. Ramji, D. Razavi-Shearer, K. Razavi-Shearer, B. Redae, H. W. Reesink, E. Ridruejo, S. Robbins, L. R. Roberts, S. K. Roberts, W. M. Rosenberg, F. Roudot-Thoraval, S. D. Ryder, R. Safadi, O. Sagalova, R. Salupere, F. M. Sanai, J. F. S. Avila, V. Saraswat, R. Sarmento-Castro, C. Sarrazin, J. D. Schmelzer, I. Schréter, C. Seguin-Devaux, S. R. Shah, A. I. Sharara, M. Sharma, A. Shevaldin, G. E. Shiha, W. Sievert, M. Sonderup, K. Souliotis, D. Speiciene, J. Sperl, P. Stärkel, R. E. Stauber, C. Stedman, D. Struck, T.-H. Su, V. Sypsa, S.-S. Tan, J. Tanaka, A. J. Thompson, I. Tolmane, K. Tomasiewicz, J. Valantinas, P. Van Damme, A. J. van der Meer, I. van Thiel, H. Van Vlierberghe, A. Vince, W. Vogel, H. Wedemeyer, N. Weis, V. W. S. Wong, C. Yaghi, A. Yosry, M.-f. Yuen, E. Yunihastuti, A. Yusuf, E. Zuckerman and H. Razavi (2017). "Global prevalence and genotype distribution of hepatitis C virus infection in 2015: a modelling study." The Lancet Gastroenterology & Hepatology **2**(3): 161-176.

Blight, K. J., J. A. McKeating and C. M. Rice (2002). "Highly permissive cell lines for subgenomic and genomic hepatitis C virus RNA replication." J Virol **76**(24): 13001-13014.

Borgia, S. M., C. Hedskog, B. Parhy, R. H. Hyland, L. M. Stamm, D. M. Brainard, M. G. Subramanian, J. G. McHutchison, H. Mo, E. Svarovskaia and S. D. Shafran (2018). "Identification of a Novel Hepatitis C Virus Genotype From Punjab, India: Expanding Classification of Hepatitis C Virus Into 8 Genotypes." J Infect Dis **218**(11): 1722-1729.

Broutier, L., A. Andersson-Rolf, C. J. Hindley, S. F. Boj, H. Clevers, B. K. Koo and M. Huch (2016). "Culture and establishment of self-renewing human and mouse adult liver and pancreas 3D organoids and their genetic manipulation." Nat Protoc **11**(9): 1724-1743.

Busch, M. P., E. M. Bloch and S. Kleinman (2019). "Prevention of transfusion-transmitted infections." Blood **133**(17): 1854-1864.

Carpentier, A., J. Sheldon, F. W. R. Vondran, R. J. Brown and T. Pietschmann (2020). "Efficient acute and chronic infection of stem cell-derived hepatocytes by hepatitis C virus." Gut **69**(9): 1659-1666.

Catanese, M. T., R. Graziani, T. von Hahn, M. Moreau, T. Huby, G. Paonessa, C. Santini, A. Luzzago, C. M. Rice, R. Cortese, A. Vitelli and A. Nicosia (2007). "High-avidity monoclonal antibodies against the human scavenger class B type I receptor efficiently block hepatitis C virus infection in the presence of high-density lipoprotein." J Virol **81**(15): 8063-8071.

Catanese, M. T., K. Uryu, M. Kopp, T. J. Edwards, L. Andrus, W. J. Rice, M. Silvestry, R. J. Kuhn and C. M. Rice (2013). "Ultrastructural analysis of hepatitis C virus particles." Proc Natl Acad Sci U S A **110**(23): 9505-9510.

Chinnici, C. M., F. Timoneri, G. Amico, G. Pietrosi, G. Vizzini, M. Spada, D. Pagano, B. Gridelli and P. G. Conaldi (2015). "Characterization of Liver-Specific Functions of Human Fetal Hepatocytes in Culture." Cell Transplant **24**(6): 1139-1153.

Choo, Q. L., G. Kuo, A. J. Weiner, L. R. Overby, D. W. Bradley and M. Houghton (1989). "Isolation of a cDNA clone derived from a blood-borne non-A, non-B viral hepatitis genome." Science **244**(4902): 359-362.

Clevers, H. (2016). "Modeling Development and Disease with Organoids." Cell **165**(7): 1586-1597.

Dao Thi, V. L., C. Granier, M. B. Zeisel, M. Guerin, J. Mancip, O. Granio, F. Penin, D. Lavillette, R. Bartenschlager, T. F. Baumert, F. L. Cosset and M. Dreux (2012). "Characterization of hepatitis C virus particle subpopulations reveals multiple usage of the scavenger receptor BI for entry steps." J Biol Chem **287**(37): 31242-31257.

De Crignis, E., T. Hossain, S. Romal, F. Carofiglio, P. Moulos, M. M. Khalid, S. Rao, A. Bazrafshan, M. M. Verstegen, F. Pourfarzad, C. Koutsothanassis, H. Gehart, T. W. Kan, R. J. Palstra, C. Boucher, I. J. JN, M. Huch, S. F. Boj, R. Vries, H. Clevers, L. J. van der Laan, P. Hatzis and T. Mahmoudi (2021). "Application of human liver organoids as a patient-derived primary model for HBV infection and related hepatocellular carcinoma." Elife **10**.

de Lau, W., N. Barker, T. Y. Low, B. K. Koo, V. S. Li, H. Teunissen, P. Kujala, A. Haegebarth, P. J. Peters, M. van de Wetering, D. E. Stange, J. E. van Es, D. Guardavaccaro, R. B. Schasfoort, Y. Mohri, K. Nishimori, S. Mohammed, A. J. Heck and H. Clevers (2011). "Lgr5 homologues associate with Wnt receptors and mediate R-spondin signalling." Nature **476**(7360): 293-297.

de Lau, W. B., B. Snel and H. C. Clevers (2012). "The R-spondin protein family." Genome Biol **13**(3): 242.

Dekkers, J. F., M. Alieva, L. M. Wellens, H. C. R. Ariese, P. R. Jamieson, A. M. Vonk, G. D. Amatngalim, H. Hu, K. C. Oost, H. J. G. Snippert, J. M. Beekman, E. J. Wehrens, J. E. Visvader, H. Clevers and A. C. Rios (2019). "High-resolution 3D imaging of fixed and cleared organoids." Nat Protoc **14**(6): 1756-1771.

Diao, J., H. Pantua, H. Ngu, L. Komuves, L. Diehl, G. Schaefer and S. B. Kapadia (2012). "Hepatitis C virus induces epidermal growth factor receptor activation via CD81 binding for viral internalization and entry." J Virol **86**(20): 10935-10949.

Dorner, M., J. A. Horwitz, B. M. Donovan, R. N. Labitt, W. C. Budell, T. Friling, A. Vogt, M. T. Catanese, T. Satoh, T. Kawai, S. Akira, M. Law, C. M. Rice and A. Ploss (2013). "Completion of the entire hepatitis C virus life cycle in genetically humanized mice." Nature **501**(7466): 237-241.

Dorner, M., J. A. Horwitz, J. B. Robbins, W. T. Barry, Q. Feng, K. Mu, C. T. Jones, J. W. Schoggins, M. T. Catanese, D. R. Burton, M. Law, C. M. Rice and A. Ploss (2011). "A genetically humanized mouse model for hepatitis C virus infection." Nature **474**(7350): 208-211.

Evans, M. J., T. von Hahn, D. M. Tscherne, A. J. Syder, M. Panis, B. Wolk, T. Hatziioannou, J. A. McKeating, P. D. Bieniasz and C. M. Rice (2007). "Claudin-1 is a hepatitis C virus co-receptor required for a late step in entry." Nature **446**(7137): 801-805.

Falade-Nwulia, O., C. Suarez-Cuervo, D. R. Nelson, M. W. Fried, J. B. Segal and M. S. Sulkowski (2017). "Oral Direct-Acting Agent Therapy for Hepatitis C Virus Infection: A Systematic Review." Ann Intern Med **166**(9): 637-648.

Fournier, C., C. Sureau, J. Coste, J. Ducos, G. Pageaux, D. Larrey, J. Domergue and P. Maurel (1998). "In vitro infection of adult normal human hepatocytes in primary culture by hepatitis C virus." J Gen Virol **79 (Pt 10)**: 2367-2374.

Foy, E., K. Li, C. Wang, R. Sumpter, Jr., M. Ikeda, S. M. Lemon and M. Gale, Jr. (2003). "Regulation of interferon regulatory factor-3 by the hepatitis C virus serine protease." Science **300**(5622): 1145-1148.

Gerold, G., R. Moeller and T. Pietschmann (2020). "Hepatitis C Virus Entry: Protein Interactions and Fusion Determinants Governing Productive Hepatocyte Invasion." Cold Spring Harb Perspect Med **10**(2).

Gomez-Lechon, M. J., L. Tolosa, I. Conde and M. T. Donato (2014). "Competency of different cell models to predict human hepatotoxic drugs." Expert Opin Drug Metab Toxicol **10**(11): 1553-1568.

Gondeau, C., P. Briolotti, F. Razafy, C. Duret, P. A. Rubbo, F. Helle, T. Reme, M. P. Ripault, J. Ducos, J. M. Fabre, J. Ramos, E. I. Pecheur, D. Larrey, P. Maurel and M. Daujat-Chavanieu (2014). "In vitro infection of primary human hepatocytes by HCV-positive sera: insights on a highly relevant model." Gut **63**(9): 1490-1500.

Gower, E., C. Estes, S. Blach, K. Razavi-Shearer and H. Razavi (2014). "Global epidemiology and genotype distribution of the hepatitis C virus infection." J Hepatol **61**(1 Suppl): S45-57.

Grebely, J., K. Page, R. Sacks-Davis, M. S. van der Loeff, T. M. Rice, J. Bruneau, M. D. Morris, B. Hajarizadeh, J. Amin, A. L. Cox, A. Y. Kim, B. H. McGovern, J. Schinkel, J. George, N. H. Shoukry, G. M. Lauer, L. Maher, A. R. Lloyd, M. Hellard, G. J. Dore, M. Prins and C. S. G. In (2014). "The effects of female sex, viral genotype, and IL28B genotype on spontaneous clearance of acute hepatitis C virus infection." Hepatology **59**(1): 109-120.

Haid, S., M. P. Windisch, R. Bartenschlager and T. Pietschmann (2010). "Mouse-specific residues of claudin-1 limit hepatitis C virus genotype 2a infection in a human hepatocyte cell line." J Virol **84**(2): 964-975.

Hendriks, D., B. Artegiani, H. Hu, S. Chuva de Sousa Lopes and H. Clevers (2021). "Establishment of human fetal hepatocyte organoids and CRISPR-Cas9-based gene knockin and knockout in organoid cultures from human liver." Nat Protoc **16**(1): 182-217.

Hogg, K., J. Thomas, D. Ashford, J. Cartwright, R. Coldwell, D. J. Weston, J. Pillmoor, D. Surry and P. O'Toole (2015). "Quantification of proteins by flow cytometry: Quantification of human hepatic transporter P-gp and OATP1B1 using flow cytometry and mass spectrometry." Methods **82**: 38-46.

Hsu, M., J. Zhang, M. Flint, C. Logvinoff, C. Cheng-Mayer, C. M. Rice and J. A. McKeating (2003). "Hepatitis C virus glycoproteins mediate pH-dependent cell entry of pseudotyped retroviral particles." Proc Natl Acad Sci U S A **100**(12): 7271-7276.

Hu, H., H. Gehart, B. Artegiani, L. O.-I. C, F. Dekkers, O. Basak, J. van Es, S. M. Chuva de Sousa Lopes, H. Begthel, J. Korving, M. van den Born, C. Zou, C. Quirk, L. Chiriboga, C. M. Rice, S. Ma, A. Rios, P. J. Peters, Y. P. de Jong and H. Clevers (2018). "Long-Term Expansion of Functional Mouse and Human Hepatocytes as 3D Organoids." Cell **175**(6): 1591-1606 e1519.

Huch, M., C. Dorrell, S. F. Boj, J. H. van Es, V. S. Li, M. van de Wetering, T. Sato, K. Hamer, N. Sasaki, M. J. Finegold, A. Haft, R. G. Vries, M. Grompe and H. Clevers (2013). "In vitro expansion of single Lgr5+ liver stem cells induced by Wnt-driven regeneration." Nature **494**(7436): 247-250.

Huch, M., H. Gehart, R. van Boxtel, K. Hamer, F. Blokzijl, M. M. Verstegen, E. Ellis, M. van Wenum, S. A. Fuchs, J. de Ligt, M. van de Wetering, N. Sasaki, S. J. Boers, H. Kemperman, J. de Jonge, J. N. Ijzermans, E. E. Nieuwenhuis, R. Hoekstra, S. Strom, R. R. Vries, L. J. van der Laan, E. Cuppen and H. Clevers (2015). "Long-term culture of genome-stable bipotent stem cells from adult human liver." Cell **160**(1-2): 299-312.

Jagger, J., V. Puro and G. De Carli (2002). "Occupational transmission of hepatitis C virus." JAMA **288**(12): 1469; author reply 1469-1471.

Kamiya, A., T. Kinoshita and A. Miyajima (2001). "Oncostatin M and hepatocyte growth factor induce hepatic maturation via distinct signaling pathways." FEBS Lett **492**(1-2): 90-94.

Kang, W., P. S. Sung, S. H. Park, S. Yoon, D. Y. Chang, S. Kim, K. H. Han, J. K. Kim, B. Rehermann, Y. J. Chwae and E. C. Shin (2014). "Hepatitis C virus attenuates interferon-induced major histocompatibility complex class I expression and decreases CD8+ T cell effector functions." Gastroenterology **146**(5): 1351-1360 e1351-1354.

Kato, T., T. Date, M. Miyamoto, A. Furusaka, K. Tokushige, M. Mizokami and T. Wakita (2003). "Efficient replication of the genotype 2a hepatitis C virus subgenomic replicon." Gastroenterology **125**(6): 1808-1817.

Kato, T., A. Furusaka, M. Miyamoto, T. Date, K. Yasui, J. Hiramoto, K. Nagayama, T. Tanaka and T. Wakita (2001). "Sequence analysis of hepatitis C virus isolated from a fulminant hepatitis patient." J Med Virol **64**(3): 334-339.

Kleinman, H. K. and G. R. Martin (2005). "Matrigel: basement membrane matrix with biological activity." Semin Cancer Biol **15**(5): 378-386.

Koutsoudakis, G., E. Herrmann, S. Kallis, R. Bartenschlager and T. Pietschmann (2007). "The level of CD81 cell surface expression is a key determinant for productive entry of hepatitis C virus into host cells." J Virol **81**(2): 588-598.

Lazaro, C. A., M. Chang, W. Tang, J. Campbell, D. G. Sullivan, D. R. Gretch, L. Corey, R. W. Coombs and N. Fausto (2007). "Hepatitis C virus replication in transfected and serum-infected cultured human fetal hepatocytes." Am J Pathol **170**(2): 478-489.

Liang, T. J., J. J. Feld, A. L. Cox and C. M. Rice (2021). "Controlled Human Infection Model - Fast Track to HCV Vaccine?" N Engl J Med **385**(13): 1235-1240.

Lindenbach, B. D., M. J. Evans, A. J. Syder, B. Wolk, T. L. Tellinghuisen, C. C. Liu, T. Maruyama, R. O. Hynes, D. R. Burton, J. A. McKeating and C. M. Rice (2005). "Complete replication of hepatitis C virus in cell culture." Science **309**(5734): 623-626.

Lindenbach, B. D., P. Meuleman, A. Ploss, T. Vanwolleghem, A. J. Syder, J. A. McKeating, R. E. Lanford, S. M. Feinstone, M. E. Major, G. Leroux-Roels and C. M. Rice (2006). "Cell culture-grown hepatitis C virus is infectious in vivo and can be recultured in vitro." Proc Natl Acad Sci U S A **103**(10): 3805-3809.

Lindenbach, B. D. and C. M. Rice (2013). "The ins and outs of hepatitis C virus entry and assembly." Nat Rev Microbiol **11**(10): 688-700.

Livak, K. J. and T. D. Schmittgen (2001). "Analysis of relative gene expression data using real-time quantitative PCR and the 2(-Delta Delta C(T)) Method." Methods **25**(4): 402-408.

Lohmann, V., F. Korner, J. Koch, U. Herian, L. Theilmann and R. Bartenschlager (1999). "Replication of subgenomic hepatitis C virus RNAs in a hepatoma cell line." Science **285**(5424): 110-113.

Lupberger, J., M. B. Zeisel, F. Xiao, C. Thumann, I. Fofana, L. Zona, C. Davis, C. J. Mee, M. Turek, S. Gorke, C. Royer, B. Fischer, M. N. Zahid, D. Lavillette, J. Fresquet, F. L. Cosset, S. M. Rothenberg, T. Pietschmann, A. H. Patel, P. Pessaux, M. Doffoel, W. Raffelsberger, O. Poch, J. A. McKeating, L. Brino and T. F. Baumert (2011). "EGFR and EphA2 are host factors for hepatitis C virus entry and possible targets for antiviral therapy." Nat Med **17**(5): 589-595.

Marsee, A., F. J. M. Roos, M. M. A. Verstegen, H. P. B. O. Consortium, H. Gehart, E. de Koning, F. Lemaigre, S. J. Forbes, W. C. Peng, M. Huch, T. Takebe, L. Vallier, H. Clevers, L. J. W. van der Laan and B. Spee (2021). "Building consensus on definition and nomenclature of hepatic, pancreatic, and biliary organoids." Cell Stem Cell **28**(5): 816-832.

Martinez-Bauer, E., X. Forns, M. Armelles, R. Planas, R. Sola, M. Vergara, S. Fabregas, R. Vega, J. Salmeron, M. Diago, J. M. Sanchez-Tapias, M. Bruguera and H. C. V. S. G. Spanish Acute (2008). "Hospital admission is a relevant source of hepatitis C virus acquisition in Spain." J Hepatol **48**(1): 20-27.

Mee, C. J., J. Grove, H. J. Harris, K. Hu, P. Balfe and J. A. McKeating (2008). "Effect of cell polarization on hepatitis C virus entry." J Virol **82**(1): 461-470.

Mee, C. J., H. J. Harris, M. J. Farquhar, G. Wilson, G. Reynolds, C. Davis, I. S. C. van, P. Balfe and J. A. McKeating (2009). "Polarization restricts hepatitis C virus entry into HepG2 hepatoma cells." J Virol **83**(12): 6211-6221.

Mehta, S. H., F. L. Brancati, M. S. Sulkowski, S. A. Strathdee, M. Szklo and D. L. Thomas (2000). "Prevalence of type 2 diabetes mellitus among persons with hepatitis C virus infection in the United States." Ann Intern Med **133**(8): 592-599.

Mensa, L., G. Crespo, M. J. Gastinger, J. Kabat, S. Perez-del-Pulgar, R. Miquel, S. U. Emerson, R. H. Purcell and X. Forns (2011). "Hepatitis C virus receptors claudin-1 and occludin after liver transplantation and influence on early viral kinetics." Hepatology **53**(5): 1436-1445.

Merz, A., G. Long, M. S. Hiet, B. Brugger, P. Chlanda, P. Andre, F. Wieland, J. Krijnse-Locker and R. Bartenschlager (2011). "Biochemical and morphological properties of hepatitis C virus particles and determination of their lipidome." J Biol Chem **286**(4): 3018-3032.

Micallef, J. M., J. M. Kaldor and G. J. Dore (2006). "Spontaneous viral clearance following acute hepatitis C infection: a systematic review of longitudinal studies." J Viral Hepat **13**(1): 34-41.

Molina-Jimenez, F., I. Benedicto, V. L. Dao Thi, V. Gondar, D. Lavillette, J. J. Marin, O. Briz, R. Moreno-Otero, R. Aldabe, T. F. Baumert, F. L. Cosset, M. Lopez-Cabrera and P. L. Majano (2012). "Matrigel-embedded 3D culture of Huh-7 cells as a hepatocyte-like polarized system to study hepatitis C virus cycle." Virology **425**(1): 31-39.

Murphy, E. L., S. M. Bryzman, S. A. Glynn, D. I. Ameti, R. A. Thomson, A. E. Williams, C. C. Nass, H. E. Ownby, G. B. Schreiber, F. Kong, K. R. Neal and G. J. Nemo (2000). "Risk factors for hepatitis C virus infection in United States blood donors. NHLBI Retrovirus Epidemiology Donor Study (REDS)." Hepatology **31**(3): 756-762.

Nakabayashi, H., K. Taketa, K. Miyano, T. Yamane and J. Sato (1982). "Growth of human hepatoma cells lines with differentiated functions in chemically defined medium." Cancer Res **42**(9): 3858-3863.

Negro, F., D. Forton, A. Craxi, M. S. Sulkowski, J. J. Feld and M. P. Manns (2015). "Extrahepatic morbidity and mortality of chronic hepatitis C." Gastroenterology **149**(6): 1345-1360.

Nienhaus, A., C. Kesavachandran, D. Wendeler, F. Haamann and M. Dulon (2012). "Infectious diseases in healthcare workers - an analysis of the standardised data set of a German compensation board." J Occup Med Toxicol **7**(1): 8.

Niepmann, M. (2013). "Hepatitis C virus RNA translation." Curr Top Microbiol Immunol **369**: 143-166.

Ohto, H., S. Terazawa, N. Sasaki, N. Sasaki, K. Hino, C. Ishiwata, M. Kako, N. Ujiie, C. Endo, A. Matsui and et al. (1994). "Transmission of hepatitis C virus from mothers to infants. The Vertical Transmission of Hepatitis C Virus Collaborative Study Group." N Engl J Med **330**(11): 744-750.

Okamoto, T. and S. Okabe (2000). "Ultraviolet absorbance at 260 and 280 nm in RNA measurement is dependent on measurement solution." Int J Mol Med **5**(6): 657-659.

Page, K., M. T. Melia, R. T. Veenhuis, M. Winter, K. E. Rousseau, G. Massaccesi, W. O. Osburn, M. Forman, E. Thomas, K. Thornton, K. Wagner, V. Vassilev, L. Lin, P. J. Lum, L. C. Giudice, E. Stein, A. Asher, S. Chang, R. Gorman, M. G. Ghany, T. J. Liang, M. R. Wierzbicki, E. Scarselli, A. Nicosia, A. Folgori, S. Capone and A. L. Cox (2021). "Randomized Trial of a Vaccine Regimen to Prevent Chronic HCV Infection." N Engl J Med **384**(6): 541-549.

Peng, W. C., C. Y. Logan, M. Fish, T. Anbarchian, F. Aguisanda, A. Alvarez-Varela, P. Wu, Y. Jin, J. Zhu, B. Li, M. Grompe, B. Wang and R. Nusse (2018). "Inflammatory Cytokine TNFalpha Promotes the Long-Term Expansion of Primary Hepatocytes in 3D Culture." Cell **175**(6): 1607-1619 e1615.

Perales, C., N. M. Beach, I. Gallego, M. E. Soria, J. Quer, J. I. Esteban, C. Rice, E. Domingo and J. Sheldon (2013). "Response of hepatitis C virus to long-term passage in the presence of alpha interferon: multiple mutations and a common phenotype." J Virol **87**(13): 7593-7607.

Pietschmann, T., A. Kaul, G. Koutsoudakis, A. Shavinskaya, S. Kallis, E. Steinmann, K. Abid, F. Negro, M. Dreux, F. L. Cosset and R. Bartenschlager (2006). "Construction and characterization of infectious intragenotypic and intergenotypic hepatitis C virus chimeras." Proc Natl Acad Sci U S A **103**(19): 7408-7413.

Pileri, P., Y. Uematsu, S. Campagnoli, G. Galli, F. Falugi, R. Petracca, A. J. Weiner, M. Houghton, D. Rosa, G. Grandi and S. Abrignani (1998). "Binding of hepatitis C virus to CD81." Science **282**(5390): 938-941.

Ploss, A., M. J. Evans, V. A. Gaysinskaya, M. Panis, H. You, Y. P. de Jong and C. M. Rice (2009). "Human occludin is a hepatitis C virus entry factor required for infection of mouse cells." Nature **457**(7231): 882-886.

Podevin, P., A. Carpentier, V. Pene, L. Aoudjehane, M. Carriere, S. Zaidi, C. Hernandez, V. Calle, J. F. Meritet, O. Scatton, M. Dreux, F. L. Cosset, T. Wakita, R. Bartenschlager, S. Demignot, F. Conti, A. R. Rosenberg and Y. Calmus (2010). "Production of infectious hepatitis C virus in primary cultures of human adult hepatocytes." Gastroenterology **139**(4): 1355-1364.

Prince, A. M., B. Brotman, G. F. Grady, W. J. Kuhns, C. Hazzi, R. W. Levine and S. J. Millian (1974). "Long-incubation post-transfusion hepatitis without serological evidence of exposure to hepatitis-B virus." Lancet **2**(7875): 241-246.

Razavi, H., I. Waked, C. Sarrazin, R. P. Myers, R. Idilman, F. Calinas, W. Vogel, M. C. Mendes Correa, C. Hezode, P. Lazaro, U. Akarca, S. Aleman, I. Balik, T. Berg, F. Bihl, M. Bilodeau, A. J. Blasco, C. E. Brandao Mello, P. Bruggmann, M. Buti, J. L. Calleja, H. Cheinquer, P. B. Christensen, M. Clausen, H. S. Coelho, M. E. Cramp, G. J. Dore, W. Doss, A. S. Duberg, M. H. El-Sayed, G. Ergor, G. Esmat, K. Falconer, J. Felix, M. L. Ferraz, P. R. Ferreira, S. Frankova, J. Garcia-Samaniego, J. Gerstoft, J. A. Giria, F. L. Goncales, Jr., E. Gower, M. Gschwantler, M. Guimaraes Pessoa, S. J. Hindman, H. Hofer, P. Husa, M. Kaberg, K. D. Kaita, A. Kautz, S. Kaymakoglu, M. Krajden, H. Krarup, W. Laleman, D. Lavanchy, R. T. Marinho, P. Marotta, S. Mauss, C. Moreno, K. Murphy, F. Negro, V. Nemecek, N. Ormeci, A. L. Ovrehus, J. Parkes, K. Pasini, K. M. Peltekian, A. Ramji, N. Reis, S. K. Roberts, W. M. Rosenberg, F. Roudot-Thoraval, S. D. Ryder, R. Sarmento-Castro, D. Semela, M. Sherman, G. E. Shiha, W. Sievert, J. Sperl, P. Starkel, R. E. Stauber, A. J. Thompson, P. Urbanek, P. Van Damme, I. van Thiel, H. Van Vlierberghe, D. Vandijck, H. Wedemeyer, N. Weis, J. Wiegand, A. Yosry, A. Zekry, M. Cornberg, B. Mullhaupt and C. Estes (2014). "The present and future disease burden of hepatitis C virus (HCV) infection with today's treatment paradigm." J Viral Hepat **21 Suppl 1**: 34-59.

Roelandt, P., S. Obeid, J. Paeshuyse, J. Vanhove, A. Van Lommel, Y. Nahmias, F. Nevens, J. Neyts and C. M. Verfaillie (2012). "Human pluripotent stem cell-derived hepatocytes support complete replication of hepatitis C virus." J Hepatol **57**(2): 246-251.

Sainz, B., Jr., N. Barretto, D. N. Martin, N. Hiraga, M. Imamura, S. Hussain, K. A. Marsh, X. Yu, K. Chayama, W. A. Alrefai and S. L. Uprichard (2012). "Identification of the Niemann-Pick C1-like 1 cholesterol absorption receptor as a new hepatitis C virus entry factor." Nat Med **18**(2): 281-285.

Sainz, B., Jr., V. TenCate and S. L. Uprichard (2009). "Three-dimensional Huh7 cell culture system for the study of Hepatitis C virus infection." Virol J **6**: 103.

Sato, T., R. G. Vries, H. J. Snippert, M. van de Wetering, N. Barker, D. E. Stange, J. H. van Es, A. Abo, P. Kujala, P. J. Peters and H. Clevers (2009). "Single Lgr5 stem cells build crypt-villus structures in vitro without a mesenchymal niche." Nature **459**(7244): 262-265.

Scarselli, E., H. Ansuini, R. Cerino, R. M. Roccasecca, S. Acali, G. Filocamo, C. Traboni, A. Nicosia, R. Cortese and A. Vitelli (2002). "The human scavenger receptor class B type I is a novel candidate receptor for the hepatitis C virus." EMBO J **21**(19): 5017-5025.

Schobel, A., K. Rosch and E. Herker (2018). "Functional innate immunity restricts Hepatitis C Virus infection in induced pluripotent stem cell-derived hepatocytes." Sci Rep **8**(1): 3893.

Schwartz, R. E., K. Trehan, L. Andrus, T. P. Sheahan, A. Ploss, S. A. Duncan, C. M. Rice and S. N. Bhatia (2012). "Modeling hepatitis C virus infection using human induced pluripotent stem cells." Proc Natl Acad Sci U S A **109**(7): 2544-2548.

Sheldon, J., N. M. Beach, E. Moreno, I. Gallego, D. Pineiro, E. Martinez-Salas, J. Gregori, J. Quer, J. I. Esteban, C. M. Rice, E. Domingo and C. Perales (2014). "Increased replicative fitness can lead to decreased drug sensitivity of hepatitis C virus." J Virol **88**(20): 12098-12111.

Sigismund, S., E. Argenzio, D. Tosoni, E. Cavallaro, S. Polo and P. P. Di Fiore (2008). "Clathrin-mediated internalization is essential for sustained EGFR signaling but dispensable for degradation." Dev Cell **15**(2): 209-219.

Stanaway, J. D., A. D. Flaxman, M. Naghavi, C. Fitzmaurice, T. Vos, I. Abubakar, L. J. Abu-Raddad, R. Assadi, N. Bhala, B. Cowie, M. H. Forouzanfour, J. Groeger, K. M. Hanafiah, K. H. Jacobsen, S. L. James, J. MacLachlan, R. Malekzadeh, N. K. Martin, A. A. Mokdad, A. H. Mokdad, C. J. L. Murray, D. Plass, S. Rana, D. B. Rein, J. H. Richardus, J. Sanabria, M. Saylan, S. Shahraz, S. So, V. V. Vlassov, E. Weiderpass, S. T. Wiersma, M. Younis, C. Yu, M. El Sayed Zaki and G. S. Cooke (2016). "The global burden of viral hepatitis from 1990 to 2013: findings from the Global Burden of Disease Study 2013." The Lancet **388**(10049): 1081-1088.

Sumpter, R., Jr., Y. M. Loo, E. Foy, K. Li, M. Yoneyama, T. Fujita, S. M. Lemon and M. Gale, Jr. (2005). "Regulating intracellular antiviral defense and permissiveness to hepatitis C virus RNA replication through a cellular RNA helicase, RIG-I." J Virol **79**(5): 2689-2699.

Tegtmeyer, B., G. Vieyres, D. Todt, C. Lauber, C. Ginkel, M. Engelmann, M. Herrmann, C. K. Pfaller, F. W. R. Vondran, R. Broering, E. Vafadarnejad, A. E. Saliba, C. Puff, W. Baumgartner, C. Miskey, Z. Ivics, E. Steinmann, T. Pietschmann and R. J. P. Brown (2021). "Initial HCV infection of adult hepatocytes triggers a temporally structured transcriptional program containing diverse pro- and anti-viral elements." J Virol **95**(10): e00245-00221.

Thein, H. H., Q. Yi, G. J. Dore and M. D. Krahn (2008). "Estimation of stage-specific fibrosis progression rates in chronic hepatitis C virus infection: a meta-analysis and meta-regression." Hepatology **48**(2): 418-431.

Tovo, P. A., E. Palomba, G. Ferraris, N. Principi, E. Ruga, P. Dallacasa and A. Maccabruni (1997). "Increased risk of maternal-infant hepatitis C virus transmission for women coinfected with human immunodeficiency virus type 1. Italian Study Group for HCV Infection in Children." Clin Infect Dis **25**(5): 1121-1124.

UN. (2015). "Transforming our world: the 2030 Agenda for Sustainable Development." Retrieved 04.02.22 [Online on the internet], from https://www.un.org/ga/search/view_doc.asp?symbol=A/RES/70/1&Lang=E.

Vandelli, C., F. Renzo, L. Romano, S. Tisminetzky, M. De Palma, T. Stroffolini, E. Ventura and A. Zanetti (2004). "Lack of evidence of sexual transmission of hepatitis C among monogamous couples: results of a 10-year prospective follow-up study." Am J Gastroenterol **99**(5): 855-859.

Wakita, T. (2019). "Cell Culture Systems of HCV Using JFH-1 and Other Strains." Cold Spring Harb Perspect Med **9**(11).

Wakita, T., T. Pietschmann, T. Kato, T. Date, M. Miyamoto, Z. Zhao, K. Murthy, A. Habermann, H. G. Krausslich, M. Mizokami, R. Bartenschlager and T. J. Liang (2005). "Production of infectious hepatitis C virus in tissue culture from a cloned viral genome." Nat Med **11**(7): 791-796.

Wang, B., L. Zhao, M. Fish, C. Y. Logan and R. Nusse (2015). "Self-renewing diploid Axin2(+) cells fuel homeostatic renewal of the liver." Nature **524**(7564): 180-185.

Westbrook, R. H. and G. Dusheiko (2014). "Natural history of hepatitis C." J Hepatol **61**(1 Suppl): S58-68.

WHO. (2016). "Global health sector strategy on viral hepatitis 2016-2021." Retrieved 04.02.22 [Online on the internet], from https://www.who.int/publications/i/item/WHO-HIV-2016.06.

WHO. (2018). "Progress report on access to hepatitis C treatment: focus on overcoming barriers in low- and middle-income countries." Retrieved 04.02.22 [Online on the internet], from https://apps.who.int/iris/bitstream/handle/10665/260445/WHO-CDS-HIV-18.4-eng.pdf?sequence=1.

Yanagi, M., R. H. Purcell, S. U. Emerson and J. Bukh (1999). "Hepatitis C virus: an infectious molecular clone of a second major genotype (2a) and lack of viability of intertypic 1a and 2a chimeras." Virology **262**(1): 250-263.

Yaphe, S., N. Bozinoff, R. Kyle, S. Shivkumar, N. P. Pai and M. Klein (2012). "Incidence of acute hepatitis C virus infection among men who have sex with men with and without HIV infection: a systematic review." Sex Transm Infect **88**(7): 558-564.

Zahid, M. N., M. Turek, F. Xiao, V. L. Thi, M. Guerin, I. Fofana, P. Bachellier, J. Thompson, L. Delang, J. Neyts, D. Bankwitz, T. Pietschmann, M. Dreux, F. L. Cosset, F. Grunert, T. F. Baumert and M. B. Zeisel (2013). "The postbinding activity of scavenger receptor class B type I mediates initiation of hepatitis C virus infection and viral dissemination." Hepatology **57**(2): 492-504.

Zhang, J., G. Randall, A. Higginbottom, P. Monk, C. M. Rice and J. A. McKeating (2004). "CD81 is required for hepatitis C virus glycoprotein-mediated viral infection." J Virol **78**(3): 1448-1455.

8 List of abbreviations

apo	apolipoproteins
apoA-I	apolipoprotein A-I
apoB	apolipoprotein B
apoE	apolipoprotein E
aSCs	adult stem cells
BSA	bovine serum albumine
cDNA	complementary desoxyribonucleic acid
CLD	chronic liver disease
CRLM	colorectal liver metastases
DAA	direct acting antiviral
DALYs	disability-adjusted life years
DNAse	deoxyribonuclease
dsRNA	double stranded ribonucleic acid
ECM	extracellular matrix
EGF	epidermal growth factor
EGFR	epidermal growth factor receptor
EphA2	ephrin receptor A2
ESCs	embryonic stem cells
FBS	fetal bovine serum
FFU	focus forming units
FGF	fibroblast growth factor
FMO	fluorescence minus one
GAPDH	glyceraldehyde-3-phosphate dehydrogenase
HCC	hepatocellular carcinoma
HCV	hepatitis C virus
HCVcc	cell culture derived hepatitis C virus
HCVpp	hepatitis C virus pseudoparticles
HDL	high-density lipoprotein
HepOrgs	hepatocyte organoids
HFLCs	human fetal liver cells
HGF	hepatocyte growth factor
HIV	human immunodeficiency virus

HLCs	hepatocyte-like cells
HSPGs	heparan sulfate proteoglycans
IFN-α	interferon alpha
IL28B	interleukin-28B
iPSCs	induced pluripotent stem cells
IQR	interquartile range
IRF1	Interferon regulatory factor 1
IRF3	Interferon regulatory factor 3
ISGs	interferon stimulated genes
IU	international units
LDL	low-density lipoprotein
LDLR	low-density lipoprotein receptor
Lgr5	leucine rich repeat containing G protein-coupled receptor 5
LUT	look-up table
MFI	median fluorescence intensity
mRNA	messenger ribonucleic acid
MRP2	ATP binding cassette subfamily C member 2 (alternative: multidrug resistance-associated protein 2)
MSM	men who have sex with men
NANBH	non-A, non-B hepatitis
NPC1L1	Niemann-Pick C1–like 1
OSM	oncostatin m
OWB	organoid washing buffer
PBS	phosphate buffered saline
PHH	primary human hepatocytes
PRRs	pattern recognition receptors
PSCs	pluripotent stem cells
PWID	people who inject drugs
r.p.m.	revolutions per minute
RIG-1	retinoid acid inducible gene 1
RNA	ribonucleic acid
RSPO1	R-spondin 1
RT-qPCR	real time quantitative polymerase chain reaction
RTKs	receptor tyrosine kinases

SRB1	scavenger receptor class B member 1
STAT1	signal transducer and activator of transcription 1
TBK1	tank binding kinase 1
TCID50	tissue culture infectious dose 50
TGF	transforming growth factor
TLR3	toll-like-receptor 3
UN	United Nations
VLDL	very low density lipoprotein
vol	volume
WHO	World Health Organization
wt	weight

9 List of figures

10 List of tables

11 Danksagung

Zuletzt möchte ich mich noch bei all denen Bedanken, ohne deren Unterstützung ich diese Arbeit nie hätte vollbringen können.
Zunächst möchte ich mich herzlich bei Prof. Dr. Marcus Altfeld dafür bedanken, dass er mir die Möglichkeit gab an diesem spannenden Projekt zu arbeiten und ein Mitglied seiner Arbeitsgruppe zu werden. Ich bin dankbar für seine kontinuierliche Unterstützung und herausfordernden Ideen während des Projektes.
Ich bin der gesamten Arbeitsgruppe Virus Immunologie am LIV dankbar dafür, dass ich mit offenen Armen aufgenommen wurde. In den herausfordernden Zeiten einer globalen Pandemie habe ich den Team Spirit und die gegenseitige Unterstützung ebenso geschätzt, wie die hilfreichen Antworten auf meine Fragen oder Tipps zu meinem Projekt, wenn ich jemanden um Rat gefragt habe.
Insbesondere möchte ich mich bei Annika Niehrs, für die Unterstützung bei der Arbeit mit den Leber Organoiden sowie ihre stets hilfreichen Antworten auf meine unzähligen Fragen, bedanken. Heike Hildebrandt bin ich dankbar dafür, dass sie in herausfordernden Zeiten das Labor am Laufen gehalten hat und uns MD und PhD StudentInnen dazu inspiriert hat eine ordentlichere Version unserer selbst zu werden. Dem gesamten Liver Team bin ich dankbar für die gute Zusammenarbeit und inhaltliche sowie moralische Unterstützung.
Des weiteren bedanke ich mich bei Gabrielle Vieyres und Isabelle Reichert für das Überlassen den Viren für meine Experimente, sowie das Teilen ihrer virologischen Expertise mit mir.
Ebenso möchte ich mich bei der Hamburg School of Immunity and Infection (HSII) für ihre finanzielle und auch immaterielle Unterstützung bedanken, ohne welche diese Arbeit in dieser Form nicht möglich gewesen wäre.
Ich möchte mich zudem bei Prof. Dr. Maura Dandri und Prof. Dr. Julian Schulze zur Wiesch für ihre Unterstützung und hilfreichen Hinweise im Rahmen der Betreuungskommission des HSII Graduiertenkollegs bedanken.

Ich möchte mich ebenso bei allen Gewebespendern bedanken, ohne deren Gewebespenden es keine Arbeit mit Leber Organoiden geben würde und Prof. Dr. Karl Oldhafer für die Koordination und Organisation der Gewebespenden.

Zuletzt danke ich meinen Eltern, meiner Schwester und meinen Freunden für ihre fortwährende Unterstützung und ihren Glauben an mich. Katharina bin ich zutiefst dankbar für ihre stetige Ermutigung, konstruktiven Hinweise und emotionale Unterstützung. Euer Glaube an mich und eure Unterstützung bedeuten mir viel und waren elementar für die Entstehung dieser Arbeit.

12 Eidesstaatliche Versicherung

Ich versichere ausdrücklich, dass ich die Arbeit selbständig und ohne fremde Hilfe, insbesondere ohne entgeltliche Hilfe von Vermittlungs- und Beratungsdiensten, verfasst, andere als die von mir angegebenen Quellen und Hilfsmittel nicht benutzt und die aus den benutzten Werken wörtlich oder inhaltlich entnommenen Stellen einzeln nach Ausgabe (Auflage und Jahr des Erscheinens), Band und Seite des benutzten Werkes kenntlich gemacht habe. Das gilt insbesondere auch für alle Informationen aus Internetquellen.

Soweit beim Verfassen der Dissertation KI-basierte Tools („Chatbots“) verwendet wurden, versichere ich ausdrücklich, den daraus generierten Anteil deutlich kenntlich gemacht zu haben. Die „Stellungnahme des Präsidiums der Deutschen Forschungsgemeinschaft (DFG) zum Einfluss generativer Modelle für die Text- und Bilderstellung auf die Wissenschaften und das Förderhandeln der DFG“ aus September 2023 wurde dabei beachtet.
Ferner versichere ich, dass ich die Dissertation bisher nicht einem Fachvertreter an einer anderen Hochschule zur Überprüfung vorgelegt oder mich anderweitig um Zulassung zur Promotion beworben habe.
Ich erkläre mich damit einverstanden, dass meine Dissertation vom Dekanat der Medizinischen Fakultät mit einer gängigen Software zur Erkennung von Plagiaten überprüft werden kann.

_____ _____

Datum Unterschrift